Strål
säkerhets
myndigheten
Swedish Radiation Safety Authority

Authors: Laura Limer
Richard Kłos
George Shaw
Russell Walke

Research
2013:20

Terrestrial Biosphere Modelling of ^{14}C Research

Report number: 2013:20 ISSN: 2000-0456
Available at www.stralsakerhetsmyndigheten.se

SSM perspective

Background

The need to address radiological impacts from ^{14}C released to the biosphere has been recognized for some time. However, because of its role in biological processes and its ecological cycling, the standard methods employed to model long-term radionuclide transport and accumulation in the biosphere cannot be used satisfactorily for ^{14}C. In 2011, the Swedish Radiation Safety Authority (SSM) commissioned a study to develop a ^{14}C model of the soil-plant-atmosphere system that would provide an independently modelling capability in order to support the oncoming review of dose assessments associated with a license application for extension of a low- and intermediate-level radioactive waste repository and releases of radionuclides during normal operation of Nuclear Power Plants (NPPs). This study is comprised of a review of contemporary models, the development of a new conceptual model, SSPAM14C, and the application of SSPAM^{14}C to a set of experimental data, relating to the atmospheric exposure of cabbages.

Objectives

The purpose of this study is to evaluate, both qualitatively and quantitatively, the modelling of ^{14}C in the biosphere. In particular, this study is focused upon the soil-plant-atmosphere system. Consideration is given to the following aspects of ^{14}C in the biosphere:

- Releases from the geosphere into soils (cf. the scenarios for waste disposal), and also releases from aboveground sources (relevant for routine release from NPPs).
- An understanding and description of ^{14}C uptake processes in the soil – roots – canopy atmosphere and external atmosphere system.
- Spatio-temporal scales, including inter-annual processes and the necessary degree of complexity for long-term assessments.
- Development of a conceptual/mathematical model incorporating the key features derived from the review of a comprehensive model for ^{14}C transport and uptake in the soil – roots – canopy atmosphere and external atmosphere system including validation against experimental data.

Results

In this study a review of existing ^{14}C soil-plant-atmosphere models has been used to formulate a new model, SSPAM^{14}C. This model contains relatively detailed sub-models for the soil, plant and atmosphere systems making it, in principle, suited to modelling both long term and acute releases to the soil-atmosphere environment. The application of this model to a set of experimental data relating to a short term atmospheric release of ^{14}C-bearing gas has highlighted a number of areas requiring further development, as discussed above, both in terms of the model parameterisation, and also missing experimental data to further the empirical understanding of such systems and for model validation. Equivalent data are not yet available for assessing the performance of the model for the soil sub-system.

Need for further research

In the future consideration may be given as to whether or not the aboveground plant component need be discretised and whether the soil aspect of the model could be simplified. Further, there is an outstanding need for a comprehensive data set which permits validation of all aspects of the model.

Project information

Contact person SSM: Shulan Xu
Reference: SSM 2011/1200

Strål
säkerhets
myndigheten
Swedish Radiation Safety Authority

Authors: Laura Limer[1], Richard Kłos[2], George Shaw[3] and Russell Walke[4]
[1] Limer Scientific Consulting Ltd, UK, [2] Aleksandria Sciences Ltd, UK,
[3] University of Nottingham, UK, [4] Quintessa Limited, UK

2013:20

Terrestrial Biosphere Modelling of ^{14}C Research

Date: My 2013
Report number: 2013:20 **ISSN:** 2000-0456
Available at www.stralsakerhetsmyndigheten.se

This report concerns a study which has been conducted for the Swedish Radiation Safety Authority, SSM. The conclusions and viewpoints presented in the report are those of the author/authors and do not necessarily coincide with those of the SSM.

Summary

In this study a review of existing ^{14}C soil-plant-atmosphere models has been used to formulate a new model, SSPAM^{14}C. This model contains relatively detailed sub-models for the soil, plant and atmosphere systems making it, in principle, suited to modelling both long term and acute releases to the soil-atmosphere environment. The application of this model to a set of experimental data relating to a short term atmospheric release of ^{14}C-bearing gas has highlighted a number of areas requiring further development, both in terms of the model parameterisation, and also missing experimental data to further the empirical understanding of such systems and for model validation. Equivalent data are not yet available for assessing the performance of the model for the soil sub-system.

Content

1. Introduction

1.1 Background

Carbon is the "building block" of life, and is one of the most studied of all the elements. A component of the fourth most abundant atmospheric gas (carbon dioxide, CO_2), carbon is a key element in the biosphere and lithosphere. The global carbon cycle and the long term implications of continued ^{14}C discharges from the nuclear fuel cycle have been studied for several decades (Ekdahl et al., 1972; Killough, 1980). The need to address radiological impacts from disposal of radioactive waste containing ^{14}C has also been recognised for some time (Bush et al., 1984). However, because of its role in biological processes, and its ecological cycling, the standard methods employed to model radionuclide transport and accumulation in the biosphere cannot be used satisfactorily for ^{14}C.

Following the Swedish Nuclear Fuel and Waste Management Company's (SKB) SAR-08 assessment of the SFR low- and intermediate-level waste facility at Forsmark, the importance of ^{14}C in long-term dose assessments in Sweden has been re-emphasised (Thomson et al., 2008). ^{14}C has also been important elsewhere to the extent that the BIOPROTA programme[1] has carried out a qualitative review of dose assessment models (BIOPROTA, 2005) and has recently followed up with a quantitative model comparison (Limer et al., 2012; Norris et al., 2011).

Outcomes from the BIOPROTA studies indicate that the choice between dynamic and equilibrium assessment models is of particular interest, raising the issue as to whether dynamic models are useful and/or necessary in the context of radioactive waste disposal. One of the difficulties surrounding conceptual models for ^{14}C with respect to waste disposal assessments is the identification of conditions under which isotopic mixing and equilibrium may reasonably be assumed. Such system understanding needs to take account of the temporal and spatial scales of the assessment, including the nature of the release from the geosphere. However, a number of organisations, including the Swedish Radiation Safety Authority (SSM), have an interest in assessing shorter term release scenarios, where ^{14}C enters the surface ecosystem either from operational activities or as the result of an accident (e.g. Ciffroy et al., 2005; Le Dizès et al., 2012). ^{14}C models developed for long-term assessments may not have the appropriate spatio-temporal scope for application to shorter term release situations.

1.2 Aims and objectives

The purpose of this project is to evaluate, both qualitatively and quantitatively, the modelling of ^{14}C in the biosphere. In particular, this study is focussed upon the soil-plant-atmosphere system. Consideration is given to the following aspects of ^{14}C in the biosphere:

- Releases from the geosphere into soils (cf. the scenarios in SAR-08), and also releases from aboveground sources (relevant for routine release scenarios and accident consequence assessment). In both types of release the ^{14}C can enter the system either in dissolved form or as ^{14}C-labelled gas.
- An understanding and description of processes in the soil – roots – canopy atmosphere and external atmosphere system.
- Spatio-temporal scales, including inter-annual processes and the necessary degree of complexity for long-term assessments.
- Alternative modelling approaches (waste disposal, routine releases, accident consequence assessment, including representation of ^{14}C in the food chain).

[1] BIOPROTA is an international collaborative project aimed at addressing key uncertainties in long term assessments of contaminant releases into the environment arising from radioactive waste disposal, see http://www.bioprota.org/

- Development of a conceptual/mathematical model incorporating the key features derived from the review with implementation (in Ecolego[2]) of a comprehensive model for ^{14}C transport and uptake in the soil – roots – canopy atmosphere and external atmosphere system, including validation against experimental data. The aim is to develop a ^{14}C model that provides SSM with an independently developed assessment capability to match that developed by SKB for the next assessment of SFR, expected in 2013. It was anticipated that SKB's approach to representing ^{14}C in the biosphere would have evolved from that described by Avila & Pröhl (2008), although this is not the situation (SKB, 2010).

As long and short term releases are of interest to SSM, in this study a model has been developed based upon a considered review of models, and modelling techniques, not only from long-term assessment studies but also from assessments of shorter duration releases, i.e. those which express processes acting on an inter-annual timescale, rather that the annual average common to long-term assessments.

1.3 Report structure

This report is structured as follows. In Section 2, a literature review of existing contemporary models representing ^{14}C in the soil-plant-atmosphere system is given. Consideration has been given both to models used in the context of operational safety of accidental releases and also to those models used in safety assessments associated with the disposal of ^{14}C containing wastes, either for geological or near surface disposal. The details of the new model developed for SSM, SSPAM^{14}C (Swedish Soil-Plant-Atmosphere Model for ^{14}C), are given in Section 3. One of the aims of this project is to apply the model to existing experimental data. To this end, the details of an experiment performed by Imperial College (London) in the 1990s are given in Section 5. The application of SSPAM^{14}C to this data is discussed in Section 6. The final conclusions of this project and future directions for further research are discussed in Section 7.

Details of the parameterisation of SSPAM^{14}C are given in Appendix A. Additional experimental data from Imperial College are given in Appendix B. The determination of the source term for use in applying SSPAM^{14}C to a subset of the Imperial College data, as described in Section 6, are given in Appendix C.

[2] http://ecolego.facilia.se/

2 Review of existing contemporary models

2.1 Introduction

This section presents a review of the models used by a range of organisations to represent the behaviour of ^{14}C in the soil-plant-atmosphere system.

2.1.1 Types of models considered

The models used by the various organisations fall into two broad categories. One subset of the model considered have been developed to consider the potential implications of ^{14}C releases either through the routine operation of nuclear facilities, or following some form of incident (human or natural). The other subset of models have been developed to consider the implications of ^{14}C releases following the disposal of ^{14}C contaminated wastes, either in near surface or geological disposal facilities.

Operational and accidental release models

Small amounts of ^{14}C are generated during operation of all kinds of nuclear power plants (NPPs), due to capture of neutrons by nitrogen, carbon or oxygen, present as components of the fuel, graphite moderator, structural hardware, such as metal and concrete, or impurities within these materials (Limer and Thorne, 2011; NCRP, 1985). A fraction of the generated ^{14}C is released during normal operation of NPPs, mainly in two chemical forms; oxidised, i.e. carbon dioxide (CO_2), and reduced, which mostly is in the form of CH_4 (Walker and Otlet, 1999). Any $^{14}CH_4$ which is oxidised, either in the atmosphere, soil or water, is available for subsequent uptake and assimilation by plants as $^{14}CO_2$. ^{14}C in plants can then be ingested and transferred to animals and humans.

As well as NPP's, ^{14}C is licensed for use in radiopharmaceuticals and research, and may also enter the surface ecosystem as a result of an accidental release.

Releases from NPPs, routine or accidental, and from other facilities considered in this category, are not continuous because they relate to specific operations or incidents. Consequently, some released radionuclides do not reach equilibrium in the environment. For this reason, some models for routine and accidental atmospheric releases consider processes which might vary over a growing season and, in some instances, a degree of diurnal variation as well. The models considered as belonging to the operational and accidental release category are listed below:

- The UK Food Standards Agency models (STAR, PRISM and a sewage sludge model);
- POM14C, developed by Studsvik;
- N288.1, developed by the Canadian Standards Agency (CSA);
- OURSON, developed by Électricité de France (EdF);
- An unnamed model developed by the Korea Atomic Energy Research Institute (KAERI);
- An unnamed model developed by a number of Japanese organisations; and
- TOCATTA, currently in development by the Institut de Radioprotection et de Sûreté Nucléaire (IRSN).

Waste disposal models

The need to address radiological impacts from disposal of radioactive waste containing ^{14}C has been recognised for some time (e.g. Bush et al., 1984). Particular interest remains in improving the assessment of possible annual individual doses to members of hypothetical exposure groups arising from releases of ^{14}C to the biosphere from deep and shallow radioactive waste disposal facilities, e.g. the Swedish SFR facility (Thomson et al., 2008), the UK's surface LLW disposal facility (Limer et al., 2011a,b) and site-generic models for a variety of waste types, including ion exchange resins/process water (Magnusson et al., 2008) and graphite (Limer et al., 2010).

A number of models have been developed by and for organisations involved in the disposal or ^{14}C contaminated wastes. The following have been considered in this review:

- The enhanced RIMERS model, developed for the Nuclear Decommissioning Authority (NDA) Radioactive Waste Management Directorate (RWMD);
- The Avila and Pröhl (2008) model, developed for SKB and Posiva;
- AquaC_14, developed by Agence nationale pour la gestion des déchets radioactifs (Andra); and
- The model developed for the Low Level Waste Repository Ltd. (LLWR) as part of a 2011 Environmental Safety Case.

2.1.2 Review approach

The reviews focus on providing the following information for each model:

- The context, including the type of organisation for which it has been developed, their role, the type of ^{14}C source term to the biosphere that is represented, the associated timescales and endpoints of interest.
- The modelling approach, including whether and where specific-activity approaches, dynamic (time-dependent) and/or or equilibrium approaches are adopted. The components and processes that are represented explicitly and/or implicitly, including information on their associated timescales, where appropriate are discussed. The approach to including data in each model is also considered, be it generic or site/experiment specific.
- Further commentary.

2.1.3 Structure of the review

Each of the models reviewed is covered in the sub-sections below. Sections 2.2 to 0 cover models originally developed to assess the implications of operational and accidental discharges. Models developed in the context of waste disposal assessments are described in Sections 2.9 to 0. The conclusions of this review, and the implications for the development of a new model for SSM, are given in Section 2.13.

2.2 UK Food Standards Agency models

2.2.1 Context

The Food Standard Agency (FSA) is responsible for protecting the human food chain in the UK. The FSA has a role in supporting the environmental regulators in the UK in their authorisation of routine discharges of radionuclides from nuclear licensed sites and radiopharmaceuticals to the atmosphere. The FSA also has a role in protecting the human food chain in cases of accidental discharge of radionuclides to the atmosphere.

The FSA uses atmospheric dispersion models to calculate atmospheric concentrations following routine or accidental atmospheric releases. They use the PRISM code to calculate concentrations in foodstuffs resulting from radionuclides in the atmosphere. The FSA then uses habit data and standard dosimetric models to determine potential doses arising from ingestion of foodstuffs contaminated with radionuclides. ^{14}C is one of the radionuclides considered in PRISM.

In the early 1990s, the Ministry of Agriculture, Fisheries and Foods (MAFF, the predecessor of the FSA) developed the STAR code for assessing ^{14}C in the food chain (Smith et al., 1994). The parameterisation/ validation of the STAR code for a range of crop types was subsequently considered in conjunction with an experimental programme (Tucker and Shaw, 1997). The associated recommendations were considered in relation to the STAR code in Watkins et al. (1998).

The FSA also developed a model for the uptake of ^{14}C into the food chain following application of contaminated sewage sludge to farmland (Thorne et al., 2003a). The soil-plant model for sewage sludge draws on the STAR model.

The STAR model for ^{14}C was updated and incorporated into PRISM in 2005 (Maul et al., 2005). Similarly to the RIMERS model (Section 2.9), this process drew on the soil carbon model developed by Jenkinson and Rayner (1977), although it is subsequently abstracted to the structure of the STAR model for implementation into PRISM.

2.2.2 STAR: modelling approach

The STAR model adopts a compartment modelling approach and assumes that ^{14}C moves at the same rates and in the same way as stable C. The structure of the plant model is illustrated in Figure 1. There are two compartments representing plant carbon, one with a relatively short residence time (up to about a week) and another with slower turnover. The two compartments are justified with reference to studies that demonstrated distinct short and long-term components of retention.

The default parameters adopted in STAR are given in Table 1. Note that the STAR model is based on 1 kg of plant material and does not represent an individual plant or the plant biomass over a defined area. The potential effects of growth dilution are therefore not represented, although this was considered to be a reasonable and conservative approach. The parameterisation was reviewed in light of experimental work undertaken at Imperial College (Tucker and Shaw, 1997), but no changes were made (Watkins et al., 1998).

Figure 1: STAR conceptual model for plants for ^{14}C

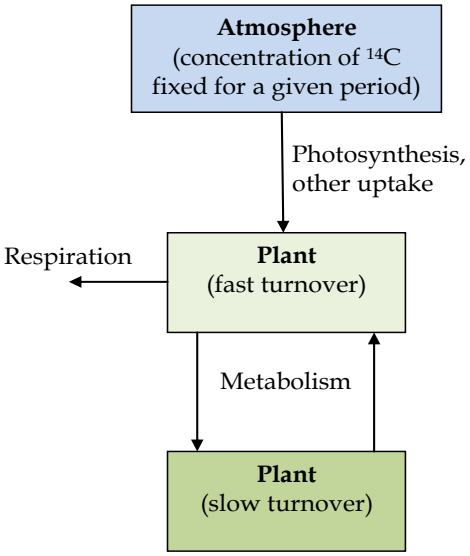

Table 1: Parameter values for the STAR ^{14}C model for plants

Parameter	Leafy Green Vegetables	Pasture	Potatoes	Leguminous Vegetables	Notes
Carbon concentration in the air, gC m^{-3}	0.16				Based on personal communication to the authors, recognised as being low but conservative
Total mass of the fast and slow plant compartments, kg WW	1	1	1	1	Such that the inventory of ^{14}C in the two compartments corresponds to the concentration in the crop, Bq kg^{-1}
Gross assimilation rate in daylight, gC d^{-1} kg^{-1} WW	4	4	10	10	Define the transfer rate from the atmosphere to the fast turnover compartment
Gross assimilation rate during dark hours as a fraction of daylight rate, -	0.01	0.01	0.01	0.01	
Fast compartment turnover rate during daylight, d^{-1}	6	6	6	6	
Fast compartment turnover rate during night, d^{-1}	6	6	6	6	
Efficiency of incorporation of initial synthates to long-term compartment, -	0.75	0.75	0.75	0.75	Defines fraction of loss from fast turnover compartment that goes to the slow component, the remainder is lost as respiration
Whole plant carbon turnover time during daylight, d^{-1}	0.013	0.013	0.013	0.013	Used to calculate the turnover rate in the slow compartment
Whole plant carbon turnover time during night, d^{-1}	0.013	0.013	0.013	0.013	
Mass of carbon in slow turnover compartment, g kg^{-1} WW	38	38	94	110	

2.2.3 PRISM: modelling approach

PRISM adopts a compartment structure and dynamically represents transfers of ^{14}C between the compartments on a probabilistic basis. The structure is illustrated in Figure 2. The Stored Energy compartment represents carbon in plant tissues stored in labile, generally small, molecules that can be metabolised in respiration to yield energy. These molecules comprise primary and secondary products of photosynthesis. The remaining plant compartments represent carbon in structural forms in plants, e.g. cellulose and lignin.

^{14}C from $^{14}CO_2$ in the atmosphere is taken up by the Stored Energy compartment according to the plant growth rate and an assimilation factor. For each period in the specification of the source term, a factor is employed to represent the fraction of the time that the plant will be photosynthesising. For ^{14}C in $^{14}CH_4$, the concentration of methane in the soil atmosphere and soil solution is taken to be the same as that in the atmosphere. Conversion rates to $^{14}CO_2$ are based on Thorne and MacKenzie (2005) and a specified fraction of this is taken to be taken up by the plants for photosynthesis.

$^{14}CO_2$ entering soil is initially present in the soil atmosphere, but it exchanges rapidly with bicarbonate in soil solution and is available for root uptake. However, when the source of $^{14}CO_2$ is from the atmosphere, these soil-mediated processes are of little importance compared with direct uptake from the atmosphere (this is different from the sewage sludge application context where there is more direct competition between root uptake and foliar uptake due to exhalation from soil to the sub-canopy atmosphere). ^{14}C in the soil water is assumed to be in equilibrium with the atmosphere, so no distinction is drawn between the direct uptake from the atmosphere and the much smaller uptake through roots; root uptake is assumed be a small but uncertain fraction of the total uptake.

The main carbon flux into and out of plants can be defined in terms of photosynthetic incorporation and respiratory loss, for which a growth-based model is used. $^{14}CO_2$ produced in respiration is taken to be released immediately to atmosphere (the CO_2 respiration transfer loss from Stored Energy in Figure 2). It is assumed that any transfers of ^{14}C from the plant or soil back to the atmosphere will be rapidly lost from the system.

Transfer from the plant Stored Energy to the structural components (leaves, grain/fruit, stem and roots) are dependent on the growth rate of those tissues.

The parameter values, and distributions, used by PRISM are given in Table 2.

Figure 2: Structure of the PRISM model for ^{14}C

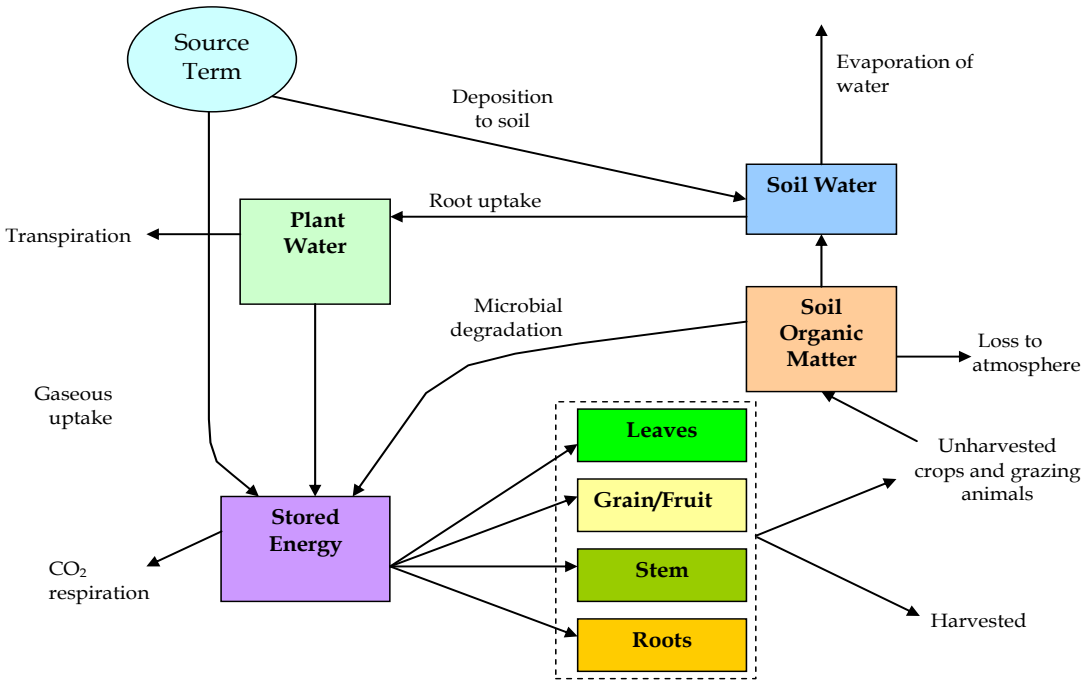

Table 2: Parameter values and distributions used by PRISM

Parameter	Comments
Concentration of carbon in the atmosphere, kg m^{-3}	Fixed value of 2E-4
Fraction of plant dry matter as carbon, -	Fixed value of 0.4 (based on glucose)
Mass of Stored Energy compartment expressed as a fraction of the total biomass Y, -	0.002 [0.001, 0.02] log-uniform, the best estimate is equates the Stored Energy with the fast turnover component in Smith et al. (1994)
Biomass production rate for plant part *i*, kg dw m^{-2} d^{-1}	Derived from PRISM growth curves - calculated by the code
Reciprocal of the plant assimilation factor	2 [1.67, 2.5] uniform. Based on observations that the carbon use efficiency (net primary productivity per unit of C assimilated by photosynthesis) is in the range 0.4 to 0.6 over a wide range of environmental conditions (Cannell and Thornley, 2000)
Deposition velocities (at full plant growth for C), m s^{-1}	CO_2: The deposition velocity for CO_2 is calculated from other model parameters
	CH_4: 2.7E-6 [1.3E-7, 7.5E-6] m s^{-1}, log uniform, assuming an average atmospheric CH_4 concentration and a methane metabolism rate of 0.3 [0.014, 0.84] mg m^{-2} d^{-1}, suitable for arable and pasture soils
	COS: 1E-3 m s^{-1} with a range of 1E-4 to 1E-2 m s^{-1}. The deposition velocity to the plant for COS only applies when photosynthesis is taking place and is modified by the fraction of plant growth.
Degradation rate of soil organic matter to soil water, d^{-1}	4E-3 [5E-5, 3E-2], triangular, best estimate based on the derivation in Appendix B of Maul et al. (2005) and range based on decomposition rate constants for soil components in Coleman and Jenkinson (2005)
Fraction of CO_2 respired from the soil that is recycled into photosynthesis, -	Around 0.06 [0.004, 0.3], lognormal. Derived from assumed photosynthetic rate of 3.6E-4 to 8.8E-4 kg [C] m-2 d-1 and assuming loss rate from below canopy to above canopy 2.9E-3 to 8.6E-2 kg [C] m-2 d-1 (5 minute to 10 second turnover)

2.2.4 Sewage Sludge: modelling approach

The structure of the FSA's model for sewage sludge is shown in Figure 3. It is similar to the PRISM model, whilst the differing source term means that:

- Additional compartments represent ^{14}C in sewage sludge that degrade to $^{14}CO_2$ in soil solution.
- A 'single-pass' model is used in which there is no return of ^{14}C to the soil from plants or animals.
- The soil atmosphere and below canopy atmosphere is explicitly represented to reflect the primary route of contamination for plants (in comparison to the atmospheric source term for PRISM).
- The fast and slow carbon pools within the plant reflect the STAR model and are analogous to the stored energy and structural components within the PRISM model.

The sewage sludge model adopts a deterministic approach, the parameter values are summarised in Table 3. The exchange rate between soil solution and soil atmosphere is set to being rapid in relation to other transfers, as is the case for the exchange rate between the below canopy and above canopy atmosphere.

Figure 3: Structure of the sewage sludge model for ^{14}C

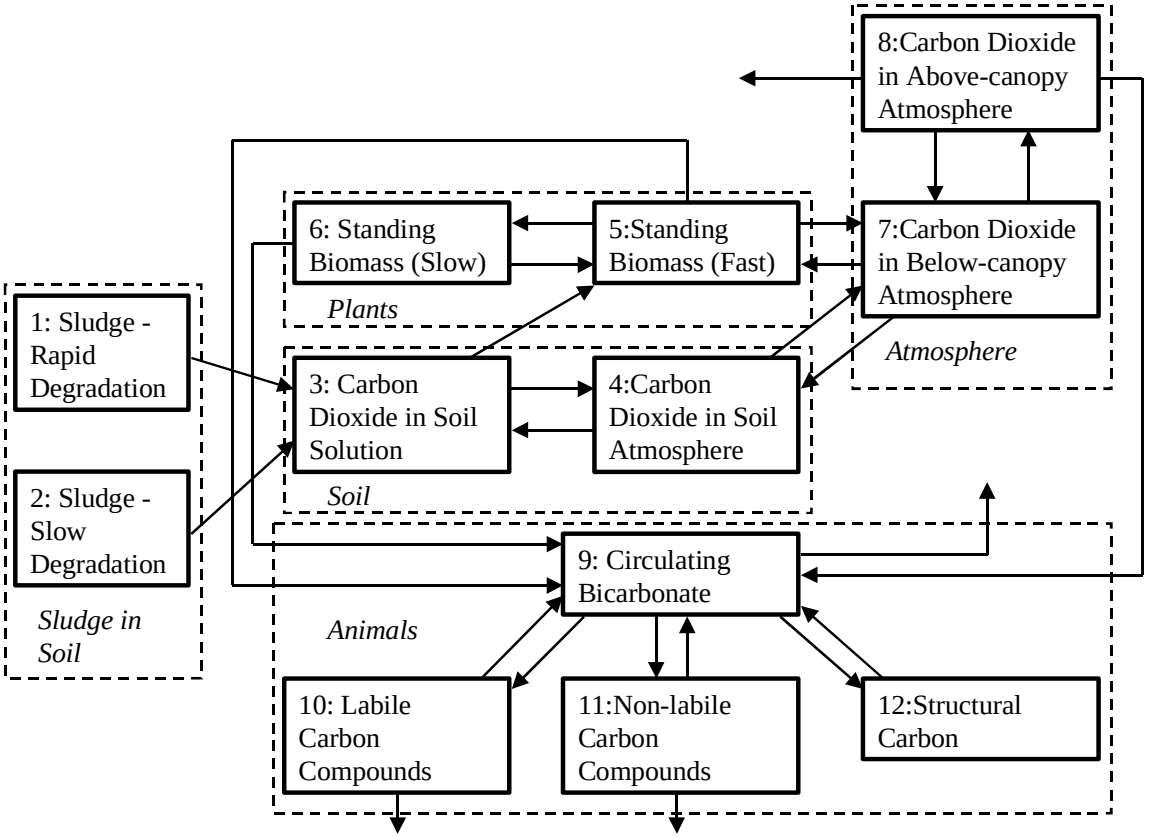

Table 3: Parameter values for the sewage sludge model

Parameter	Value	Comments
Fraction of the added activity associated with the rapid degradation component, -	0.5	Varied from 0 to 1 in sensitivity calculations
Amount of sludge or sludge product addition to agricultural land, kg m^{-2}	0.35	Varied from 0.1 to 1 kg m^{-2} in sensitivity calculations
Rapid degradation rate of sewage sludge within soil, y^{-1}	55	Varied from 25 to 85 y^{-1} in sensitivity calculations
Slow degradation rate of sewage sludge within soil, y^{-1}	1.1	Varied from 0.2 to 2 y^{-1} in sensitivity calculations
Concentration of carbon in the atmosphere, kg m^{-3}	$2\ 10^{-4}$	Based on 370 ppm CO_2 on a volumetric basis, density of air of 1.3 kg m^{-3} and a stoichiometric mass ratio of carbon in air of 12/28.8
Mass of carbon in plant canopy, kgC m^{-2}	$1\ 10^{-4}$	Based on plant canopy height of 0.5 m, whilst a height of 0.1 m is recognised as being appropriate for grazed pasture, this height reflects consideration of a hay field and some agricultural crops
Mass of carbon in above canopy atmosphere, kgC m^{-2}	$2\ 10^{-2}$	Based on a height of 100 m, although could be an order of magnitude greater or smaller
Mass of carbon in soil atmosphere, kgC m^{-2}	$1\ 10^{-4}$	Based on soil depth of 0.3 m, air filled porosity of 0.1 and enrichment of over an order of magnitude compared to the above soil atmosphere due to microbial respiration
Mass of carbon in soil solution, kgC m^{-2}	$2\ 10^{-4}$	Based on equilibration with the soil atmosphere
Exchange rates between soil atmosphere and soil solution	-	Based on a timescale of hours
Exchange rates between soil atmosphere, below canopy atmosphere and above canopy atmosphere	-	Based on a timescale of days or less
Loss rate from above canopy atmosphere, y^{-1}	$1\ 10^{6}$	Based on a height of 100 m and a wind speed of 5 m s^{-1}
Carbon assimilation rate by plants, kgC m^{-2} y^{-1}	0.2	Based on a fresh weight yield of 1 kg m^{-2} y^{-1}, a dry weight of 20% and allowance for the utilisation of assimilated carbon in respiration
Loss rate of carbon from plants due to respiration, kgC m^{-2} y^{-1}	0.12	Achieves net assimilation rate of 0.08 kgC m^{-2} y^{-1}, consistent with the above
Uptake of carbon from soil solution by plants, kgC m^{-2} y^{-1}	0.002	1% of uptake from below canopy atmosphere
Fraction of plant carbon in the fast pool, -	0.2%	Based on Thorne et al. (2003b)
Turnover rate of carbon in the fast plant compartment, d^{-1}	6	Taken from the STAR model (Smith et al., 1994)
Assimilation efficiency, -	0.4	Although a value of 0.75 was noted in the STAR model (Smith et al., 1994)

2.2.5 Commentary

The source term for the PRISM modelling of ^{14}C is an atmospheric concentration, therefore the canopy atmosphere is not represented in detail. In addition, with the primary route of uptake by plants being from the atmosphere, the various carbon pools in the soil are also not represented in detail.

The STAR model for ^{14}C was updated in light of experimental results (Tucker and Shaw, 1997, Watkins et al., 1998). The PRISM model for ^{14}C has been compared against the updated STAR model; however, no direct validation of the soil-plant model has been undertaken.

2.3 POM^{14}C model

2.3.1 Context

Studsvik is a supplier of nuclear analysis software and specialised services to the international nuclear industry, including fuel analysis software, waste treatment, decommissioning, engineering and services, and operating efficiency. Studsvik owns a number of decommissioned research reactors in Sweden, and waste processing facilities around the world.

In the 1990s in Sweden, the assessment of the impacts of ^{14}C released during routine operations at NPPs was assessed using transfer factors (Bergström et al., 1991), based on measured concentrations of ^{14}C in the air, vegetables and potatoes at Hinkley point (Kluczewski et al., 1986). In 2001, Studsvik developed a more process-oriented model, POM^{14}C (Aquilonius, 2001; Aquilonius and Hallberg, 2005). The reason for this development was both to test the former method and also to investigate whether site-specific parameter values would generate significant differences in the calculated plant ^{14}C concentrations.

2.3.2 Modelling approach

The processes and exposure pathways considered in POM^{14}C are shown in Figure 4.
In this model, a subset of the equations from the agricultural model DAISY (Hansen et al., 1993), are used to dynamically model the turnover of carbon in the crop. The specific activity of ^{14}C in the atmosphere at the location of concern (the source term) is then calculated using a straight-line Gaussian plume model. From this, a specific activity approach is used to determine the ^{14}C content of the crops at harvest. This is shown graphically in Figure 5.

In POM^{14}C, the carbon content in the plant at harvest is calculated based on the rate of photosynthesis, length of growing season, temperature and global radiation. As the values of the latter parameters vary during the growing season this is accounted for by using seasonal averages of several parameters, e.g. average temperature times number of days instead of the temperature sum, due to lack of time-dependent site specific data. It is assumed that all of the plant carbon is obtained through photosynthesis.
A number of parameters used in calculations with POM^{14}C are site-specific:

- atmospheric ^{14}C concentration, Bq m^{-3} (calculated using a Gaussian plume model);
- The length of the growing season, d;
- Global solar irradiation, W m^{-2}; and
- Mean temperature during the growing season, ^{o}C.

The generic parameters used in calculations using this model are given in Table 4, with crop dependent parameters given in Table 5.

Figure 4: Processes and exposure pathways for the POM^{14}C model (redrawn from Aquilonius and Hallberg, 2005)

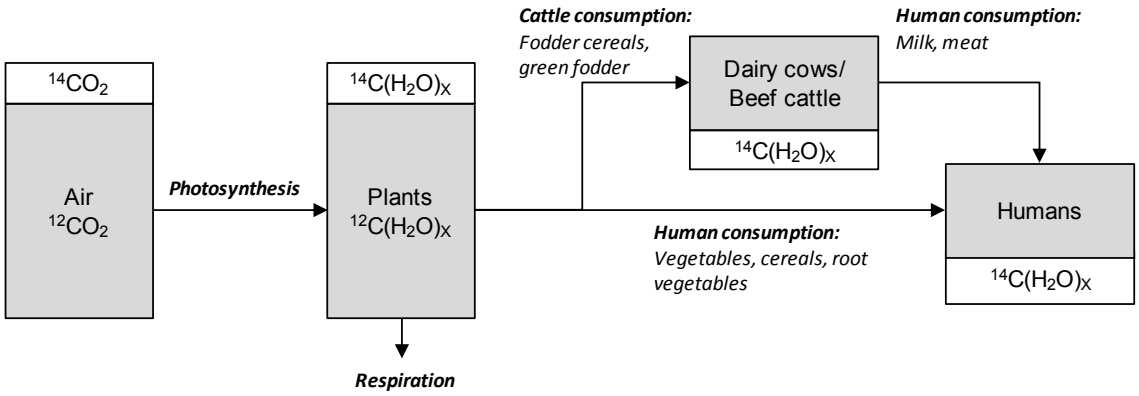

Figure 5: Detail of the calculation of ^{14}C concentration in plants in POM^{14}C (redrawn from Aquilonius and Hallberg, 2005)

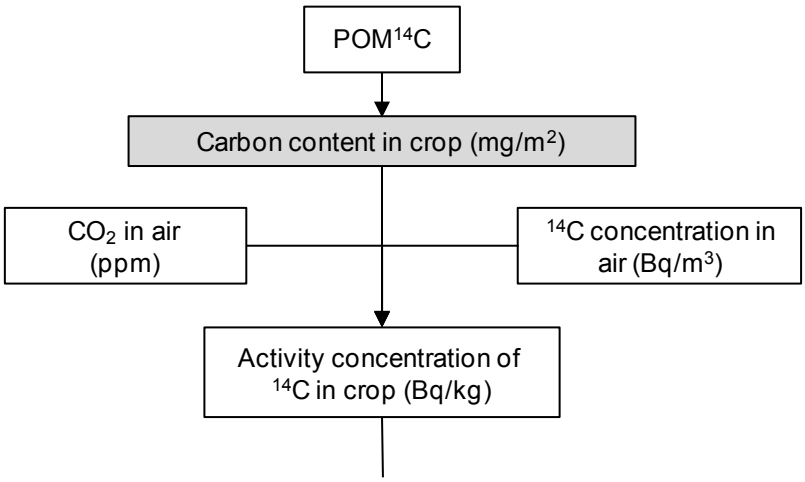

Table 4: Crop independent parameter values adopted in POM^{14}C

Parameter	Value	Notes / Reference
Stable C concentration in air, ppm	365	Keeling and Whorf (2001)
Extinction coefficient of crop canopy, -	0.4	Hansen et al. (1993)
Constant for plant absorbed global radiation, W m^{-2}	60	Hansen et al. (1993)
Unnamed constant used in the calculation of photosynthetically active radiation, -	0.48	Hansen et al. (1993)
Rate of photosynthesis, kg CO_2 m^{-2} day	0.072	Hansen et al. (1993)
Reflection coefficient, -	0.06	Hansen et al. (1993)

Table 5: Crop dependent parameter values adopted in POM^{14}C

Parameter	Value		Notes / References
	Winter wheat	Potatoes	
Specific green crop area, m^2 kg^{-1}	7	8.5	Hansen et al. (1993)
Accumulated top dry matter, kg m^{-2}	0.03	0.03	Hansen et al. (1993)
Canopy development parameter, Σ °C	450	1700	Hansen et al. (1993)
Total crop area damping parameter, Σ °C	600	200	Hansen et al. (1993)
Green crop area damping parameter, Σ °C	1000	500	Hansen et al. (1993)
Total crop index damping parameter, °C	1.25	1	Hansen et al. (1993)
Green crop index damping parameter, °C	1.8	0.3	Hansen et al. (1993)
Respiration rate, kg CO_2 kg^{-1} day	0.015 (t_1) 0.01 (t_2)	0.065 (t_1) 0.01 (t_2)	Hansen et al. (1993)

2.3.3 Commentary

Although this model was developed in 2001, and published in the peer-reviewed literature in 2005, at the time of its publication SSM accepted its use in safety assessment calculations by Studsvik without a thorough review. In 2010 SSM revisited this model, applying their review technique which had been developed during the iterative reviews of SKB's safety assessments relating to the disposal both of low- and intermediate-level radioactive wastes (LLW/ILW) and of high-level radioactive waste and spent nuclear fuel (HLW/SF); this review is reported in Xu et al. (2011). Through reproduction of one of the calculation cases presented in Aquilonius and Hallberg (2005), flaws in the quality assurance (QA), including missing parameter values and unclear model description, of the POM^{14}C model were found by SSM.

Notwithstanding the QA problems, Xu et al. (2011) found that, in principle, the POM^{14}C model can be applied reasonably well to predict the radioactivity level of ^{14}C in crops. However, it was questioned whether, given the assumption in the assessment presented in Aquilonius and Hallberg (2005) of calculating the C biomass at the end of the growing season, whether it was necessary to perform any calculations using POM^{14}C. Xu et al. (2011) argue that a transparent and robust dose assessment can be made by using literature values or measured data for the final yield and known ^{12}C concentrations in the crop. Then the ^{14}C content in the crops can be calculated from the average ^{12}C/^{14}C ratio in the atmosphere.

2.4 CSA N288.1 model

2.4.1 Context

The Canadian Standards Association (CSA) is a not-for-profit membership-based association serving business, industry, government and consumers in Canada and the global marketplace. The association develop standards that address real needs, such as enhancing public safety and health. In 1987, the CSA published guidelines and a methodology for calculating derived release limits for routine releases of radionuclides to air and surface water from nuclear facilities. The guidelines, and associated models, are known as N288.1. Following significant scientific advances that have been made in dosimetry and in the understanding of radionuclide behaviour in the environment since the mid-1980s, there was agreement within the Canadian nuclear industry that the models and data used in N288.1 needed revising. This process began in 2000, with the most recent edition of the guideline published in 2008 (CSA, 2008).
The model covers releases to the atmosphere and to surface water (both freshwater and marine water). It does not address releases to groundwater, although transfers from other media to groundwater wells and ponds are considered. The methods specified in N288.1 are designed for routine, continuous, low-level emissions. They also apply to periodic, short-term releases (see Clause 8.2 of CSA, 2008), provided that

1. The releases are controlled and associated with normal operations;
2. The release rate is roughly the same from event to event;
3. For atmospheric releases, the total release duration exceeds approximately 400 hours in the year; for aquatic releases, at least one or two releases occur in each month of the year; and
4. The releases occur randomly over time.

Where the requirement of Item (4) is not met but the releases are known to occur at a particular time of day or year, N288.1 applies only if the air (water) concentrations are calculated using the meteorological (hydrological) data in effect for that time.

2.4.2 Modelling approach

Figure 6 shows the part of the N288.1 model in which the contamination of soil and plants are calculated. The atmosphere is regarded as a single layer, which is subject to the effects of wind.
Although many of the inter-compartment transfers of ^{14}C are modelled using the same trace element partitioning concepts as for other radionuclides, there are some transfers for which an alternative approach is adopted for ^{14}C (highlighted red in Figure 6). The N288.1 model includes two different specific-activity models for ^{14}C uptake by plants: (i) from the atmosphere and (ii) from irrigation water.

Plant uptake of gaseous ^{14}C from the soil is disregarded for ^{14}C, as it is considered that, provided the air ^{14}C concentrations are relatively uniform from year to year, that the specific activity of CO_2 emitted from the soil will be the same as that in the air (highlighted blue in Figure 6). Thus, for all scenarios other than an irrigation scenario, the concentration of ^{14}C in plants is derived directly from the aboveground atmospheric concentration using a specific activity approach (red arrow in Figure 6). For the irrigation scenario the water is assumed to reach the soil, and a fractional amount of the ^{14}C reaching the soil is assumed to be volatilised and thus become available for plant uptake via photosynthesis. As the soil ^{14}C concentration is not used for to derive ^{14}C concentrations in plants, it is not modelled in any great detail. The parameters used in this model are given in Table 6.

Figure 6: Soil-plant contamination components of N288.1 (adapted from CSA, 2008)

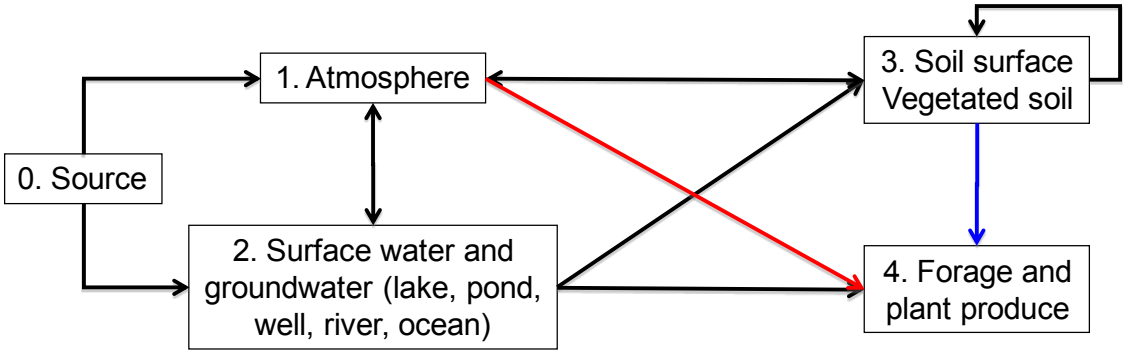

Table 6: Parameters values adopted in the N288.1 model

Description	Value	Notes / Reference
Surface roughness length, m	0.4	
Soil depth, m	0.2	In cultivated soils, the top 20-30 cm are mixed annually or seasonally. In uncultivated soils the flora and fauna that lead to most food chain exposures interact with soil depths on the order of tens of cm.
Soil dry bulk density, kg d.w. m^{-2}	Sand: 1500 Loam: 1300 Clay: 1400 Organic: 400	Dependent on soil type.
Carbon content of dry plant tissue, g C kg^{-1} plant d.w.	500	Although the typical dry plant tissue carbon content is typically 45%, the slightly conservative value of 50% is adopted (Zach and Sheppard, 1992).
Air CO_2 concentration, ppm	375	CSA (2008)
Carbon content of air, g m^{-3}	0.2	CSA (2008)
Fraction of carbon in plants derived from the air, -	1	Amiro et al. (1991)
Carbon content of pore water, g L^{-1}	1.2E-3	Lindsay (1979)

2.4.3 Commentary

In the N288.1 model the ^{14}C can enter the soil-plant system either via the atmosphere or via contaminated irrigation water. However, irrespective of the source of the ^{14}C, the plant uptake is always assumed to occur via photosynthesis. This is achieved using a specific activity model. As the sole source is the atmosphere, the ^{14}C concentration in the soil is not modelled in great detail.

2.5 OURSON model

2.5.1 Context

EdF Group is one of the largest energy producers in Europe, with much of the electricity they produce coming from NPPs, although they also run a number of wind farms and also supply gas. With respect to the nuclear side of their business, EdF are concerned with both the safe operation of their existing NPPs and also with potential new reactors. EdF must demonstrate to their regulator (the French Nuclear Safety Authority, ASN) that they understand and are able to assess the potential impacts associated with routine releases of radionuclides from operating NPPs.

For this reason, EdF has developed a model called OURSON (acronym for "Tool for Environmental and Health Risk Assessment") in order to assess the potential impacts associated with routine radionuclide releases to freshwater (Ciffroy et al., 2005). In particular, the model was developed to consider: (1) the many potential exposure pathways as identified through a review of literature; (2) when possible, dynamic transfer processes; and (3) seasonality in growing cycles of crops and agricultural practices. OURSON has been implemented such that it can be used for both deterministic and probabilistic calculations. One of the radionuclides considered in the OURSON model is ^{14}C, which is introduced to the soil-plant system via irrigation water. The important concepts for ^{14}C in the context of human dose estimation, and the important features that need to be embedded into such a ^{14}C river model are discussed in Sheppard et al. (2006a). The parameterisation of such a model is discussed in Sheppard et al. (2006b).

2.5.2 Modelling approach

A schematic of the ^{14}C model is shown in Figure 7. The original formulation of the soil-plant model for ^{14}C dealt exclusively with contaminated irrigation water as the source. The model has subsequently also been applied to scenarios which consider ^{14}C-labelled gas being released to the soil from a sub-surface waste repository as indicated in Figure 7 (Limer et al., 2012; Norris et al., 2011; Mobbs et al., 2012). In the model, fluxes of ^{14}C and stable C are modelled separately. The parameters used in OURSON are given in Table 7.

It is assumed that the plants absorb C as CO_2 during photosynthesis, and that all other sources of C are negligible in comparison. Plant growth is modelled dynamically, with a specific activity model to determine the ^{14}C concentration in plants so that isotopic dilution is accounted for.

The model accounts for the fact that the air in the plant canopy is a mixture of air from the soil pore space and the free atmosphere, so the plant ^{14}C specific activity is implicitly based on a mixture of the two sources. Sheppard et al. (2006a) note that modelling the mixing of soil and atmospheric free air in the plant canopy is not a simple matter and that simplifications are often made (e.g. Amiro et al., 1991; Sheppard et al., 1991). For this reason, in the OURSON model it is conservatively assumed that the CO_2 in the plant canopy is dominated by CO_2 released from the soil; the contribution from the above canopy atmosphere is implicitly accounted for by use of a canopy dilution factor (Table 7). This means that the plant specific activity is related to the specific activity of the CO_2 volatilized from the soil. This entails calculation of the activity concentration of labile ^{14}C in the soil, the volatilization rate of that ^{14}C, and the flux density of stable C emitted from the soil.

There is evidence (Sheppard et al., 1991; Sheppard and Evenden, 1996a,b) that ^{14}C in soil can be partitioned between labile and relatively recalcitrant forms, where the recalcitrant forms may be inorganic (carbonate minerals) or organic (insoluble humic substances). For this reason a portion of the ^{14}C which enters the soil is assumed to be fixed in a recalcitrant form, and is lost from there either by decay/degradation or re-mineralisation to inorganic carbon.

The amount of labile ^{14}C in the soil at any time depends on the balance of ^{14}C entering the soil in contaminated irrigation water, and that lost through fixation to a recalcitrant form, via leaching or as a result of volatilisation to the plant canopy atmosphere.

Figure 7: Schematic of the OURSON soil-plant model for ^{14}C (Mobbs et al., 2012)

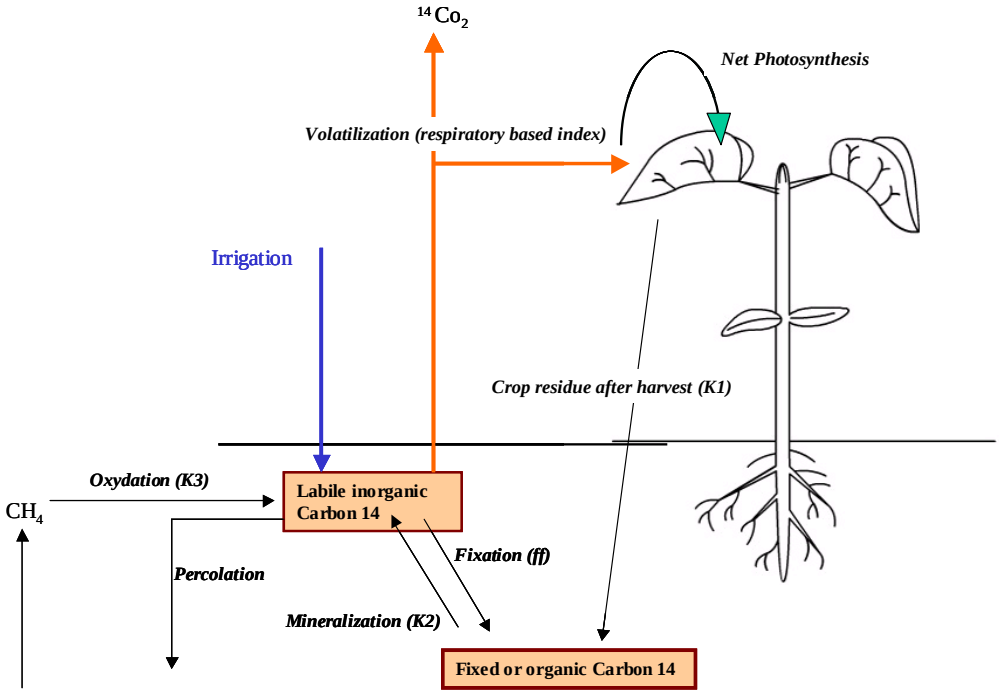

Although soil volatilisation rates of ^{14}C and stable C will vary seasonally, being more active in summer rather than winter, as the underlying processes are most the same these volatilisation rates will likely be similarly affected. The stable C volatilisation rate is related to the crop yield, concentration of stable C in the plant and the ratios of total and harvested shoot and root biomass. The ^{14}C volatilisation rate, meanwhile, is computed as being correlated to the soil ^{14}C concentration in labile materials.

The specific activity of the plant canopy atmosphere is then determined by multiplying the ratio of volatilised ^{14}C and volatilised ^{12}C by the degree of dilution of the canopy atmosphere with that of the free air above the plants. For dense canopies, such dilution can be disregarded, though for more open canopy structures, the dilution could be as much as an order of magnitude (see Table 7 and also Sheppard et al., 2006b). Although not given explicit representation in the mathematical model, the concept of field size is implicit in the conceptual model in the definition of the canopy dilution factor, with the value approaching unity for large areas and decreasing for smaller fields, sparse or tall crops (Sheppard et al., 2006b).

Within the plant, isotopic dilution as a result of plant growth is accounted for explicitly. The ^{14}C content of the plant at any time is then determined by summing the concentration of existing plant tissues (accounting for the plants relative growth rate) with input from new growth, which is assumed to have the specific activity of the atmosphere at that time.

2.5.3 Commentary

Although this model was initially developed to represent releases of ^{14}C into freshwater, and the subsequent application of that water to crops via irrigation, the model has been shown to be readily adapted to consider the release of ^{14}C-labelled gas to the soil. This model allows for the retention of ^{14}C in the soil in recalcitrant material, and also for the isotopic dilution of ^{14}C in the plant as a result of growth.

Table 7: Parameters values adopted in the OURSON model

Description	Value	Notes / Reference
Loss of ^{14}C from soil as a result of volatilisation, d^{-1}	0.04	There is uncertainty in this value, with the potential to vary by orders of magnitude. A log-normal distribution is recommended, with a GSD of 3.2; 0.04 is the GM.
Soil solid/ liquid partition coefficient, L kg^{-1}	3 (soils low or devoid of carbonates) 40 (soils with carbonates)	These values are the GM of distributions. The recommended GSD for both is 2.3.
Fraction of ^{14}C which is fixed in recalcitrant form, -	0 (no evidence of carbonate material, or if soil pH < 8) 0.02 (potential for carbonate minerals to be present)	
Canopy dilution factor, -	1 (conservative value, upper limit) 0.2-0.3 (for typical irrigated field sizes, 100-1000 m in length) 0.1 (for land areas the size of a garden, 10 m length; lower limit)	The fraction of C that the plants fix which comes from the soil as opposed to the free atmosphere. Relatively high values might be expected to come from crops with a dense canopy.
Stable C content of plants, g C kg^{-1} d.w.	500	

2.6 KAERI model

2.6.1 Context

The KAERI was established in the 1959. Their mission is to find a wide range of uses for nuclear energy (e.g. treatment of certain cancers). As with many organisations involved in the nuclear industry, one of the radionuclides of interest to KAERI is ^{14}C. In 2008 they published a paper which describes a model that was developed to calculate plant ^{14}C concentrations resulting from atmospheric releases of ^{14}C, including a test of the model using experimental data in which rice was exposed to $^{14}CO_2$ for short periods of time at different growth stages (Keum et al., 2008).

2.6.2 Modelling approach

A schematic of the model is given in Figure 8. The carbon in the plant is assumed to have been acquired through photosynthetic uptake, i.e. any root uptake is disregarded. Thus the source of ^{14}C for the plant is $^{14}CO_2$ in the atmosphere. Both plant compartments can lose C, and thus ^{14}C, via respiration. In addition to photosynthesis, the plant ears can gain ^{14}C as a result of the translocation from other parts of the plant. Plant growth is modelled in three distinct phases:

- growth of the plant body only;
- growth of ears only, with the plant body mass at equilibrium; and
- both plant body and ears at maximum biomass (i.e. no further growth).

Unlike some of the other models considered in this review, the ^{14}C content is not calculated by simply assuming that the ratio $^{14}C/^{12}C$ in the plant is always equal to that of the atmosphere. In this kinetic model, the ^{14}C content of both plant compartments are described by differential equations in which there is a balance of an input of new ^{14}C through the growth of the plant, and also translocation for the plant ears, versus losses from respiration of existing plant tissue, dilution due to plant growth, and in the case of the plant body losses due to translocation.

The parameters of the model are given in Table 8.

2.6.3 Commentary

This model was later noted by Tani et al. (2011) as being one of a number of dynamic compartment models used to estimate the specific activity of ^{14}C in crops following atmospheric releases of ^{14}C, with a temporally changing concentration. The other models to which Tani et al. refer to were also developed in the context of the atmospheric exposure of rice (Andoh and Amano, 2003; Karashi et al., 2008; Takahashi et al., 2008).

Figure 8: Schematic of the conceptual model for ^{14}C uptake from the atmosphere to rice developed by KAERI (redrawn from Keum et al., 2008)

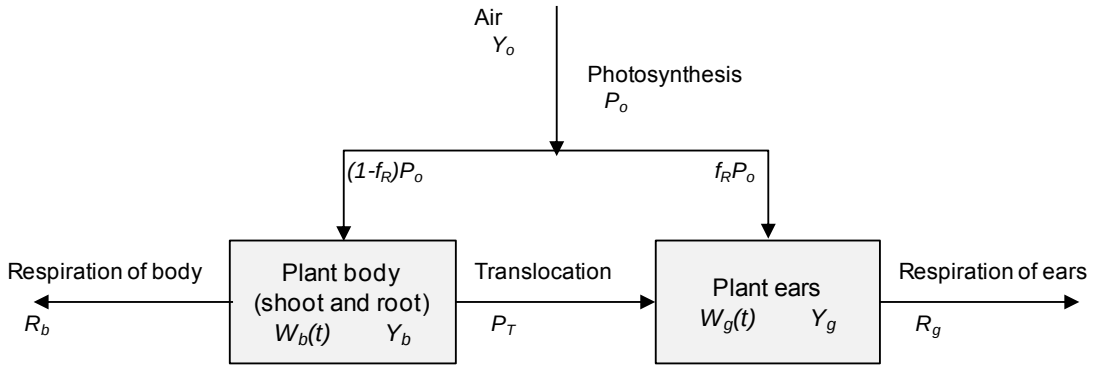

Table 8: Parameters values adopted in the model developed by KAERI

Parameter	Value	Notes / Reference
Dry weight of plant body (shoot & root) at fully developed stage, kg d.w. m^{-2}	2.19	This value includes the dry weight of the root, which was assumed to be 18% of the dry weight of the whole plant
Dry weight of ears at fully developed stage, kg d.w. m^{-2}	1.3	-
Ratio of respiration rate to photosynthesis rate of plant body, -	0.3	Range of 0.1 to 0.5 suggested
Ratio of respiration rate to photosynthesis rate of ears, -	0.4	Range of 0.1 to 0.6 suggested
Contribution of translocation to total ears maturity, -	0.2	Range of 0.1 to 0.3 suggested
Ratio of photosynthesis rate of ears to total photosynthesis rate of plant, -	0.5	Range of 0.2 to 0.8 suggested
Carbon content of dry body, g C kg^{-1} d.w.	420	-
Carbon content of dry ears, g C kg^{-1} d.w.	460	-
Time period from transplanting to flowering, d	81	Keum et al. (2008) note that, in the associated experiment, the transplanting date was 22 May, flowering date near August 11, and the ears reached maturity near 25 September
Time period from flowering to maturity of ears, d	45	
Time period from maturity of ears to harvest, d	19	Harvest time was 13 October.

2.7 Japanese Model

2.7.1 Context

In 2011 scientists from a number of organisations in Japan published a paper discussing the development of a dynamic model for the transfer of ^{14}C to rice plants following an atmospheric release (Tani et al., 2011). The model was developed to form part of the assessment of the potential impacts associated with radionuclide discharges associated with the spent nuclear fuel processing plant currently undergoing test operations at Rokkasho, Japan; the research was funded by the Aomori Prefectural Government. The model was tested against some laboratory data from experiments conducted using growth chambers at the Closed Ecology Experiment Facilities (CEEF) at the Institute for Environmental Sciences, Japan; the experimental facility is described in Tako et al. (1997, 2001).

2.7.2 Modelling approach

This model discretises the plant into three compartments. The plant body is considered as comprising immobile and mobile C in shoots, whilst C in the ears is represented separately. Earlier experimental evidence indicates that the redistribution of C from the shoot to the roots is negligible (Okano et al., 1983), as is the transfer of C from roots to other organs (Okawa et al., 2002); for this reason roots are not included in this model (Figure 9). ^{14}C enters the mobile carbon and ear compartments via photosynthesis, and is lost from them as a result of respiration. It is assumed that there is no isotopic fractionation in the plant, so that C, and thus ^{14}C, can be redistributed in equal portions from the mobile C in the plant shoots to both the immobile C and plant ears.

Many of the parameter values used in the model have been based on the experimental observations; the model parameters are given in Table 9.

2.7.3 Commentary

In the analysis presented by Tani et al. (2011), they argue that their results imply that the model can be used for estimating the specific activity of ^{14}C in the edible part of rice plants exposed to atmospheric ^{14}C with temporally changing specific radioactivity. However, some of the key parameters, in particular the net C gain in the plant components, were specific to the experimental conditions. The experimental results reproduced in the paper were based on constant temperature conditions. Tani et al. (2011) suggest that for application of the model to the estimation of specific activity of ^{14}C in rice plants grown in actual fields, data on growth curves of the plants in the fields and the temperature dependence of respiration rate constants should be incorporated into the model.

Figure 9: Schematic of the conceptual model developed by the Japanese

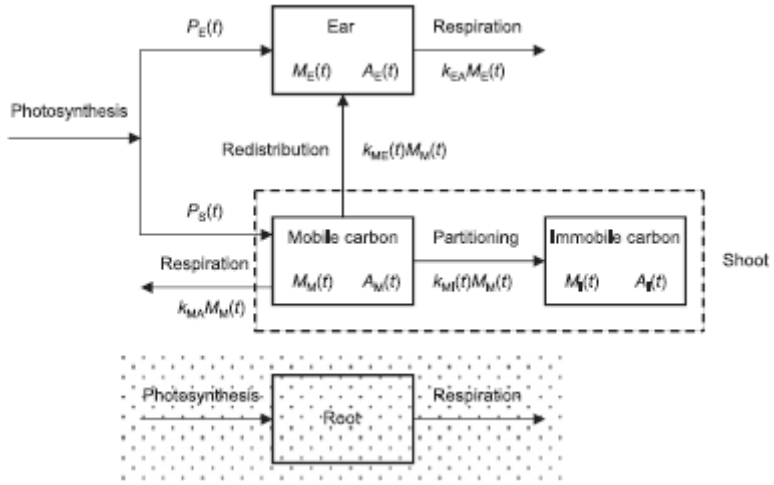

Table 9: Parameters values adopted in the model reported in Tani et al. (2011)

Parameter	Value	Notes / Reference
Dry weight of plant shoot, g plant^{-1}	-	Values based on observations of the different stages of the experiment, and thus plant growth.
Dry weight of plant ear, g plant^{-1}	-	
C content of plant shoot, g C g^{-1} d.w.	-	
C content of plant shoot, g C g^{-1} d.w.	-	
Four constants used to fit the logistic growth curves associated with the plant shoot and ear C mass	-	Values determined by fitting logistic growth curves to the measured changes in the C mass of the plant shoot and ear.
Ratio of the redistribution rate of C from the shoot to ear to the rate of gross C gain in the ear, -	0.4	It has been reported that about 0-40% of the total carbohydrates in matured rice grain are supplied from the carbohydrates accumulated in the shoot (Cock and Yoshida, 1972; Murthy, 1976; Yoshida, 1981).
Transfer of C (and ^{14}C) from ear to atmosphere, d^{-1}	-	Values generated by fitting model to experimental data.
Transfer of C (and ^{14}C) from mobile shoot C to atmosphere, d^{-1}	-	
Transfer of C (and ^{14}C) from mobile to immobile C in plant shoot, d^{-1}	-	

2.8 TOCATTA Model

2.8.1 Context

IRSN is the French Institute for Radiological Protection and Nuclear Safety and is the nation's public service expert in nuclear and radiation risks, providing assessments and conducting research to meet the needs of public authorities. The TOCATTA model is currently under development by IRSN (Le Dizès et al., 2012), with the aim to be able to estimate ^{14}C (and ^{3}H) transfers in terrestrial ecosystems exposed to atmospheric ^{14}C (and ^{3}H) releases from nuclear facilities either as part of normal operating or as a result of an accident. The TOCATTA model sits within a wider modelling framework at IRSN, SYMBIOSE, which considers the transport and fate of a wide range of radionuclides in the environment arising from such atmospheric release situations. Integration within the SYMBIOSE framework means that the TOCATTA models need to be relatively simple (Aulagnier et al., 2012; Le Dizès et al., 2011).

2.8.2 Modelling approach

It is assumed that the isotopic ratio of ^{14}C and carbon in the vegetation is in isotopic equilibrium with that of the canopy atmosphere at each time step. The biomass of the plant (i.e. stable carbon content) at any given time can be derived using either time-dependent predefined growth curves or experimental data. The reference parameter values are given in Table 10.

Table 10: Parameters values adopted in the TOCATTA model

Parameter	Value	Notes / Reference
Concentration of stable C in the atmosphere, g C m^{-3}	0.2	
Canopy dilution factor, -	0.3	Based upon OURSON (see Sheppard et al., 2006b)
Stable carbon content of dry plant matter, mol kg^{-1} dw	40.8	Garnier-Laplace (1998)
Fraction of dry matter in grass, kg kg^{-1} dw	0.1	IAEA (1994)
Fraction of plant dry matter growth lost as C to the soil through the process of root exudation	0.03	Jouven et al. (2006a,b)
Ratio of decomposable and resistant plant material	1.44	Jenkinson et al. (1992); Parshotam et al. (2001)
Soil volatilisation rate, d^{-1}	0.04	Sheppard et al. (2006b)
Soil partition coefficient, L kg^{-1}	6.7	Roussel-Debet (2001)
Stable carbon flux that falls to ground as litter, kg m^{-2} d^{-1}	0.1	Van Veen and Paul (1981)
Minimum dry biomass after a cut,and maximum dry biomass of grass, kg m^{-2}	-	Site specific, based on empirical data
Rate of volatilisation from soil, d^{-1}	0.04	Sheppard et al. (2006b)
Decomposition rate for soil organic DPM compartment, d^{-1}	0.027	Jenkinson et al. (1987, 1992); Xu et al. (2011b)
Decomposition rate for soil organic RPM compartment, d^{-1}	8.0E-4	Jenkinson et al. (1987, 1992); Xu et al. (2011b)
Decomposition rate for soil organic BIO compartment, d^{-1}	1.8E-3	Jenkinson et al. (1987, 1992); Xu et al. (2011b)
Decomposition rate for soil organic HUM compartment, d^{-1}	5.4E-5	Jenkinson et al. (1987, 1992); Xu et al. (2011b)

2.8.3 Commentary

TOCATTA was recently applied to ^{14}C concentrations measured *in situ* on a grassland ecosystem located 2 km downwind of the AREVA NC La Hague nuclear fuel recycling plant between 2006 and 2009. In this test of the model, some weaknesses in the simple model were identified. As it currently stands, TOCATTA is not sufficiently accurate to be able to reproduce either the month-to-month or day-to-day variability seen in the measured grass ^{14}C activities arising from the releases from the fuel recycling plant, and has results which are independent of whether or not the release occurs in the day or night. IRSN therefore intend to further develop TOCATTA so that it can take into account the variation in plant carbon uptake throughout a 24 hour period. A pasture simulation model called PASIM (Reido et al., 1998; Vuichard et al., 2007) is to be used to inform this development of TOCATTA. Two papers discussing the TOCATTA model parameterization for ^{14}C and a test of TOCATTA, and PASIM, against measurements performed at the La Hague nuclear fuel recycling plant have recently been published (Aulagnier et al., 2012; Le Dizès et al., 2012).

2.9 Enhanced RIMERS model

2.9.1 Context

The NDA RWMD is responsible for developing the safety case for geological disposal of the UK's higher activity radioactive wastes. The geological disposal process in the UK is current at the stage of identifying potential locations, so the context for the safety case developed by NDA RWMD is currently site-generic. NDA RWMD is interested in both gaseous and liquid releases of ^{14}C to the biosphere from a geological disposal facility, the timescales of which cover tens to tens of thousands of years (limited only by the

half-life of ^{14}C). ^{14}C is of primary interest in scenarios where there is potential for ^{14}C labelled methane to reach the biosphere. An enhanced version of the RIMERS model is used, which is formulated primarily to address releases of gaseous ^{14}C to the soil zone, although the model is also suitably structured for calculating the radiological implications of releases to the atmosphere.

The RIMERS model was developed by UK Nirex Limited (Nirex). In 2005, Nirex undertook a review of their modelling of gases derived from radioactive waste, including their representation in the biosphere (Thorne and MacKenzie, 2005; Thorne, 2005). The review included a full description of the RIMERS model and comparison against the representation of ^{14}C in an FSA model developed to represent ^{14}C in the food chain following application to farmland in sewage sludge. The review led to the development of the 'enhanced RIMERS' model, which is currently used by NDA RWMD.

2.9.2 Modelling approach

The enhanced RIMERS model adopts a compartment structure and dynamically represents transfers of ^{14}C between the compartments on a deterministic basis. The structure is illustrated in Figure 10.
The model assumes that the ^{14}C behaves in the soil-plant system in the same way as stable carbon, such that compartment sizes and transfer rates between compartments are based on consideration of stable carbon. Compartment volumes and transfer rates between compartments are expressed in terms of the equivalent volume of CO_2 at standard temperature and pressure (m^3 and $m^3\ day^{-1}$, respectively), assuming a density of gaseous CO_2 of 1.9647 kg m^{-3}. The resulting compartment sizes are given in Table 11, whilst the transfer fluxes and resulting rates are given in Table 12.

2.9.3 Commentary

The soil model for both the original and enhanced RIMERS models is primarily based on Jenkinson and Rayner (1977), which provides a model of the turnover of soil organic matter based on long-term cropping and manuring experiments at the Rothamsted research centre in the UK. A single set of reference parameter values is defined, based on a pasture system, although a range of alternative values is used in sensitivity studies. The original Jenkinson and Rayner (1977) model provides good agreement with measurements from long-term experiments.

A single compartment is used to represent plant carbon, whilst five compartments are used to represent organic carbon in the soil, including decomposable and resistant plant material, microbial biomass, physically and chemically stabilised organic matter. The model was enhanced to provide explicit representation of carbon in soil solution, soil atmosphere and the below canopy atmosphere.

Figure 10: Structure of the Enhanced RIMERS model

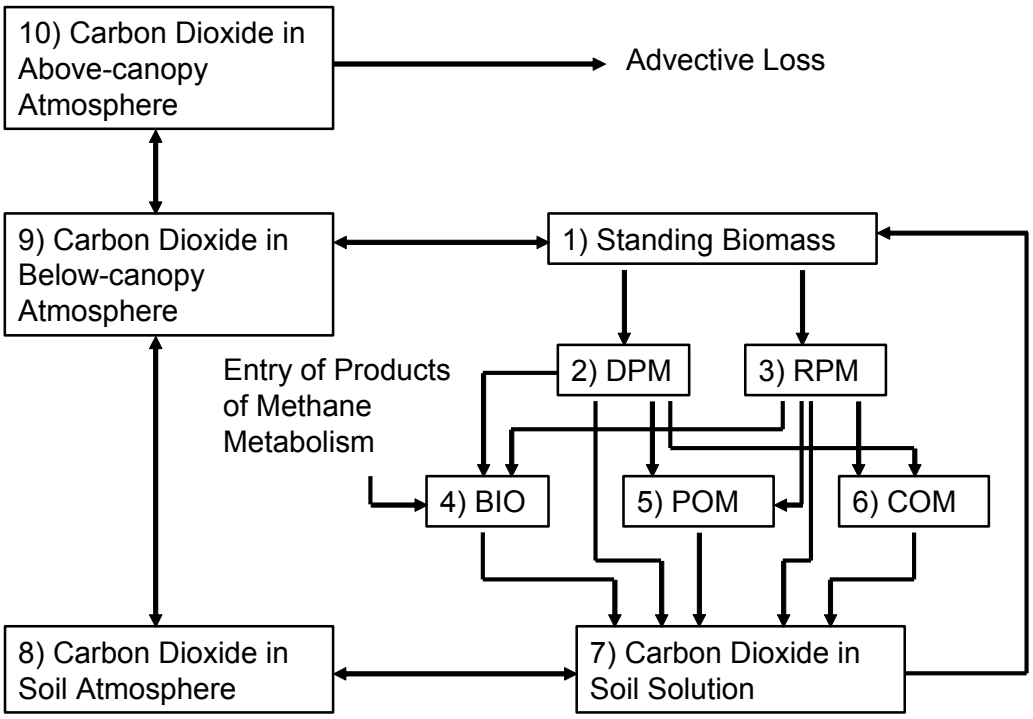

Note: DPM is decomposable plant material, RPM is resistant plant material, BIO is microbial biomass, POM is physically stabilised organic matter, COM is chemically stabilised organic matter.

Table 11: Compartment size for the Enhanced RIMERS model (Thorne, 2005)

Name	Volume (m^3)	Mass (kgC)	Notes
Standing biomass (1)	$7.467\ 10^{-2}$	$4.0\ 10^{-2}$	Based on 1 kg m^{-2} fresh weight, dry to fresh weight ratio of 0.1 and composition of cellulose.
DPM (2)	$1.867\ 10^{-3}$	$1.0\ 10^{-3}$	From Jenkinson and Rayner (1977) long term pasture plot experiments.
RPM (3)	$8.773\ 10^{-2}$	$4.7\ 10^{-2}$	
BIO (4)	$5.227\ 10^{-2}$	$2.8\ 10^{-2}$	
POM (5)	$2.109\ 10^{0}$	$1.13\ 10^{0}$	
COM (6)	$2.277\ 10^{0}$	$1.22\ 10^{0}$	
Soil solution (7)	$3.733\ 10^{-4}$	$2.0\ 10^{-4}$	Based on equilibrium between soil solution and soil gas and CO_2 in soil gas to be enriched based on Stolp (1977).
Soil atmosphere (8)	$1.867\ 10^{-4}$	$1.0\ 10^{-4}$	
Below-canopy atmosphere (9)	$1.650\ 10^{-4}$	$8.84\ 10^{-5}$	Canopy height taken to be 0.5 m and mixing height 5 m above. Assumes same CO_2 concentration below and above.
Above-canopy atmosphere (10)	$1.650\ 10^{-3}$	$8.84\ 10^{-4}$	

Table 12: Transfer fluxes and rates for the Enhanced RIMERS model (Thorne, 2005)

Transfer		Flux (m^3 d^{-1})	Rate (d^{-1})	Notes
From	**To**			
Biomass	Below-canopy atmosphere	$2.044\ 10^{-4}$	$2.74\ 10^{-3}$	Set equal to the growth rate
Biomass	DPM	$1.71\ 10^{-4}$	$2.29\ 10^{-3}$	Based on Jenkinson and Rayner (1977)
Biomass	RPM	$3.33\ 10^{-5}$	$4.46\ 10^{-4}$	
DPM	BIO	$1.30\ 10^{-5}$	$6.96\ 10^{-3}$	
DPM	POM	$2.14\ 10^{-5}$	$1.15\ 10^{-2}$	
DPM	COM	$5.99\ 10^{-7}$	$3.21\ 10^{-4}$	
DPM	Soil solution	$1.36\ 10^{-4}$	$7.28\ 10^{-2}$	
RPM	BIO	$2.53\ 10^{-6}$	$2.88\ 10^{-5}$	
RPM	POM	$4.16\ 10^{-6}$	$4.74\ 10^{-5}$	
RPM	COM	$1.17\ 10^{-7}$	$1.33\ 10^{-6}$	
RPM	Soil solution	$2.65\ 10^{-5}$	$3.02\ 10^{-4}$	
BIO	Soil solution	$1.55\ 10^{-5}$	$2.97\ 10^{-2}$	
POM	Soil solution	$2.56\ 10^{-5}$	$1.21\ 10^{-5}$	
COM	Soil solution	$7.16\ 10^{-7}$	$3.14\ 10^{-7}$	
Soil solution	Biomass	$8.80\ 10^{-6}$	$2.36\ 10^{-2}$	Assumed that plants obtain 1 to 5% of C direct from soil, remainder is from below canopy atmosphere
Below-canopy atmosphere	Biomass	$4.00\ 10^{-4}$	$2.42\ 10^{+0}$	
Soil solution	Soil atmosphere	$3.733\ 10^{0}$	$1.00\ 10^{+4}$	Balance because uptake by plant is small. Relatively rapid exchange
Soil atmosphere	Soil solution	$3.733\ 10^{0}$	$2.00\ 10^{+4}$	
Soil atmosphere	Below-canopy atmosphere	$1.867\ 10^{-3}$	$1.00\ 10^{+1}$	Balance. Arbitrary
Below-canopy atmosphere	Soil atmosphere	$1.867\ 10^{-3}$	$1.13\ 10^{+1}$	
Below-canopy atmosphere	Above-canopy atmosphere	$1.63\ 10^{-2}$	$9.88\ 10^{+1}$	Slight difference reflects uptake by plants. Arbitrary
Above-canopy atmosphere	Below-canopy atmosphere	$1.65\ 10^{-2}$	$1.00\ 10^{+1}$	
Above-canopy atmosphere	Global atmosphere	$4.52\ 10^{-1}$	$2.74\ 10^{+2}$	Represents moderate degree of dispersion in open air

2.10 Avila and Pröhl (2008)

2.10.1 Context

SKB, of Sweden, and Posiva Öy, of Finland, are two waste management organisations which both have active programs relating to the development of site specific safety cases for the geological disposal of spent fuel and HLW, and also the disposal of LLW and ILW. These organisations report to their regulators, SSM and STUK respectively. One of the key radionuclides in the safety cases of both organisations is ^{14}C. For that reason, SKB and Posiva jointly commissioned the development of a specific model for ^{14}C in the biosphere for use in their assessments of human exposures from potential underground releases of ^{14}C. This model is described in Avila and Pröhl (2008)[3]. This report describes a set of simplified models for considering the potential impacts to humans of releases of ^{14}C to both terrestrial and aquatic ecosystems. The models can be used to assess both continuous and pulse-like ^{14}C releases (to soil in terrestrial ecosystems or bottom sediment in aquatic ecosystems), and can be applied to various ecosystems: forests, agricultural land, sea basins and lakes. The exposure pathways considered are the ingestion of contaminated food and water, and also the inhalation of contaminated air.

2.10.2 Modelling approach

This model adopts the specific activity approach to determining the ^{14}C concentration in all biota. The primary assumption of the terrestrial model is that all ^{14}C that is input to the system, either contained within irrigation water or an atmospheric release, will be immediately released to an atmospheric mixing layer where it can be assimilated by plants via photosynthesis (Figure 11).
The incorporation of ^{14}C into the plant via photosynthesis can then be estimated by calculating the excess $^{14}C/^{12}C$ ratio (specific activity) at equilibrium. This is dependent upon a number of factors:

- the fraction of ^{14}C released to the mixing layer that occurs in a period when photosynthesis can take place (-);
- the mixing height (m);
- the wind speed at the vegetation height (m y^{-1});
- the air exchange rate in the mixing layer (y^{-1});
- the stable C content in the air (kg C m^{-3}); and
- the net primary production in the ecosystem (kg C m^{-2} y^{-1}).

The wind speed at the vegetation height is based upon a scaling of the assumed wind velocity at 10 m above the ground, assuming an exponential wind profile and a vegetation-specific roughness length (z_d, m) (Seinfeld, 1986). The roughness length is defined as the height at which the wind speed becomes zero when the wind profile above the canopy is extrapolated.

The air exchange rate in the mixing layer is then obtained by dividing the wind speed at the vegetation height by the 'fetch' of the affected area. Under the assumption that the release area is circular, the fetch is defined as the square root of the area divided by π.

The reference parameters used by model for an agricultural ecosystem are given in Table 13.

[3] This report is also available as Posiva Working report 2007-107.

Figure 11: Schematic of the SKB model (adapted from Avila and Pröhl [2008])

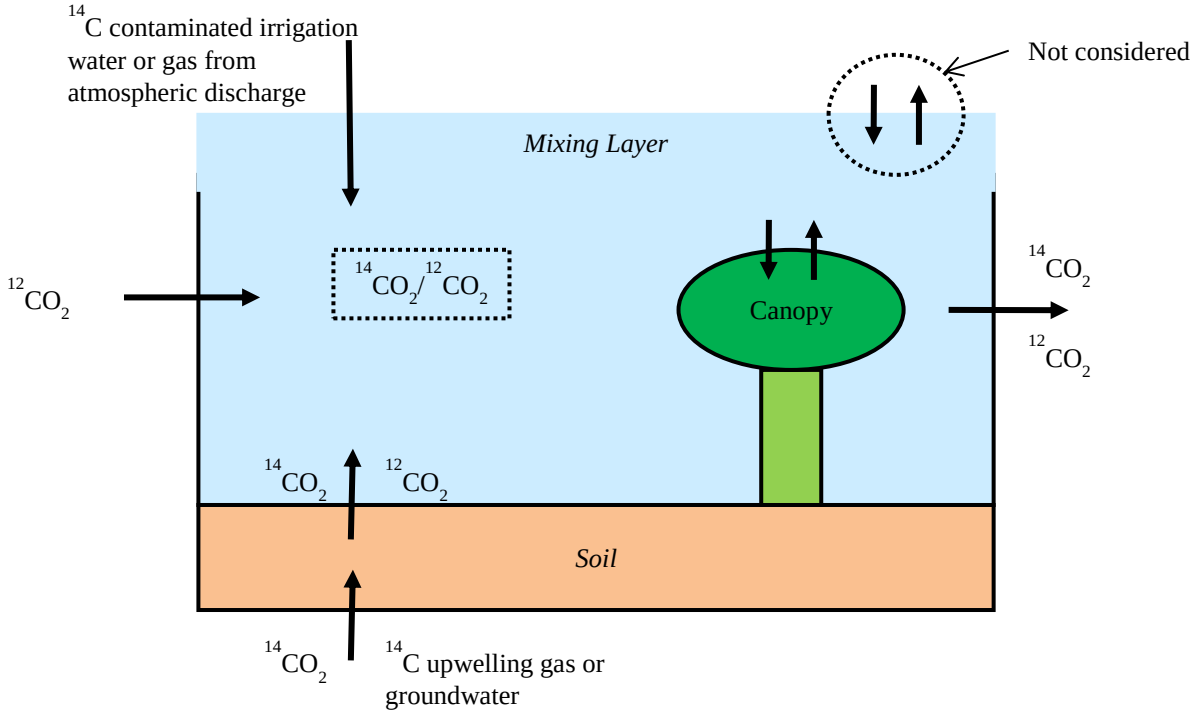

Table 13: Parameter values adopted in the Avila and Pröhl model for ^{14}C

Description	Value	Notes / Reference
Effective release fraction, -	1	It is conservatively assumed that all of the ^{14}C is released during periods when it can be assimilated into the plant by photosynthesis.
Vegetation height of agricultural lands, m	1	Value for farmland given in Seinfield (1986) and Mayall (2003).
Height of the mixing layer, m	10	Height for agricultural lands
Area, m^2	-	Situation specific value required
Wind velocity 10 m above the Earth's surface, m s^{-1}	5	The value of 5 m s^{-1} is the default value typically adopted for Pasquill Category D conditions (e.g. CSA, 2008). It is fairly typical as an annual average value for northern Europe (Troen and Lundtag Petersen, 1991).
Roughness length for agricultural lands, m	0.25	Value for farmland given in Seinfield (1986) and Mayall (2003).
Net primary productivity for agricultural lands, g C m^{-2} y^{-1}	120	Value given for agricultural lands in the Forsmark area in Lindborg (2005).
Net primary productivity for vegetation, g C m^{-2} y^{-1}	98	Obtained by multiplying the yields of vegetables (g f.w. m^{-2} y^{-1}) as reported in Bergström and Barkefors (2004) by the carbon content of the vegetables (0.049 g C g^{-1} f.w.).

2.10.3 Commentary

This model was used in the SFR 1 SAR-08 and KBS-3H safety assessments to calculate the ^{14}C doses associated with the disposal of spent fuel. A sensitivity analysis reported in Avila and Pröhl (2008) determined that, independent of the nature of the release, the parameter with the most influence on the calculated plant ^{14}C concentrations, and thus human doses, was the wind speed. This parameter defines the removal of ^{14}C from the mixing layer. However, concern has been raised about the relative thickness

of the mixing zone, as compared to the non-turbulent zone (Kłos & Shaw, 2008). For an agricultural setting the thickness of the layer without turbulence is 0.25 m (roughness length, Table 13), so that the mixing zone thickness will be nearly 40 times that of the non-turbulent layer.

2.11 AquaC_14

2.11.1 Context

One of the aims of Andra is to develop a safe long-term solution for radioactive waste for which there is no current disposal route; this remit includes long-term surface storage as interim solutions while final disposal systems are being studied. Within this remit, Andra works to ensure it has the capability to model the behaviour of radionuclides in the biosphere that represent both trace elements and also more specialised elements that either are essential elements (e.g. ^{3}H, ^{14}C) or exhibit redox sensitive behaviour (e.g. ^{79}Se, ^{238}U).

The Andra ^{14}C model was originally developed by Penfold and Watkins (1998) and transcribed into the general radionuclide biosphere transfer model, Aquabios (Albrecht and Miquel, 2010). Some minor modifications to the model were performed by van Hecke (2001), at which juncture the ^{14}C aspect of the model was made stand alone, and is now known as AquaC_14. In light of discussions within the BIOPROTA ^{14}C working group, a detailed analysis of AquaC_14 was performed in 2010, and the mathematical model updated slightly (Albrecht, 2010).

2.11.2 Modelling approach

^{14}C is assumed to enter the biosphere either as contaminated water, which can be in the form of irrigation water or upwelling groundwater, or as contaminated gas, which could come from an underground or surface repository or be released from some operational site, either as part of a routine discharge or an accident.

For an irrigation scenario, the ^{14}C concentration in the soil is modelled in the same manner as any trace element, using a K_d approach to calculate the retention of ^{14}C in the soil. The input term comprises a portion of ^{14}C which reaches the soil directly following irrigation, and a portion of ^{14}C which reaches the soil indirectly having previously been intercepted by the leaves, or leached from the leaves. The output considers losses through leaching, evapotranspiration and volatilisation,

The uptake of ^{14}C into plants is modelled using a specific activity approach, assuming three environmental sources: interception and translocation, root uptake and photosynthesis (Figure 12). To estimate the contamination via incorporation of $^{14}CO_2$ during photosynthesis requires information on the volume concentration in the canopy of plants, which itself depends on the concentration of ^{14}C in the soil, the soil density and the rate of volatilisation of $^{14}CO_2$ from the soil. A geometric factor related to the wind direction, the wind speed and the 'fetch' must also be taken into account. The latter allows the field size to be represented, such that the larger the field the smaller the fetch and the less diluted the $^{14}CO_2$ in the atmosphere is assumed to be.

The parameters used in this model are given in Table 14.

2.11.3 Commentary

As with some of the other models considered in this review, e.g. the OURSON and Avila and Pröhl (2008) models (see Sections 2.5 and 2.10), AquaC_14 includes the size of the field of concern in calculating the atmospheric ^{14}C concentration. However, one particular feature of this model is that what is termed "fetch" is defined as the inverse of the width of the field, and as such has units of m^{-1}. In other models fetch is given units of length (i.e. m).

Figure 12: Schematic of the AquaC_14 model (adapted from Marschner, 1995)

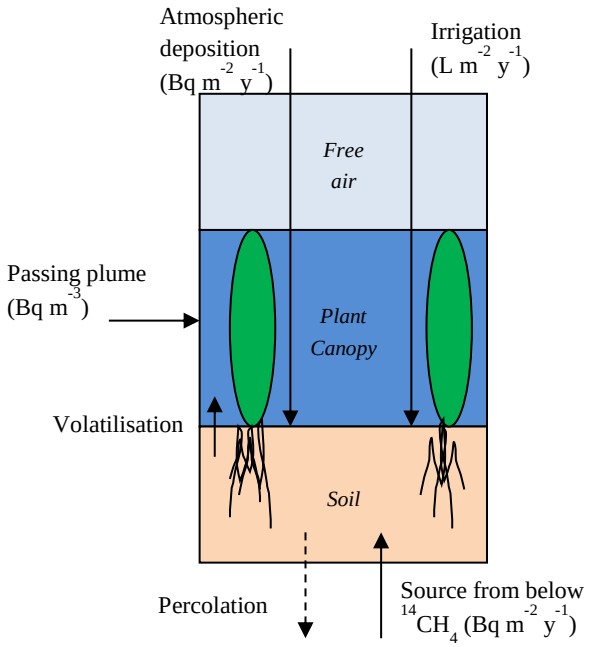

Table 14: Parameters values adopted in AquaC_14

Parameter	Value	Notes / Reference
Thickness of soil layer, m	0.25	
Soil porosity, -	0.5	
Soil water content, -	0.5	
Soil distribution coefficient, $m^3\ kg^{-1}$	0.0095	
Coefficient to scale irrigation needs	1	A crop specific scaling factor of water uptake by plants
Average irrigation need for all four plants, $L\ m^{-2}\ y^{-1}$	-	Site specific value used
Evapotranspiration, $L\ m^{-2}\ y^{-1}$	-	Site specific value used
Average precipitation, $L\ m^{-2}\ y^{-1}$	-	Site specific value used

Parameter	Value	Notes / Reference
Fetch, m^{-1}	0.01	Inverse of the width of the field (100 m), with three supplemental calculations with fetch (width) = 0.1 (1m), 0.001 (1,000m), and 0.0001 (10,000m)
Wind velocity in canopy, m s^{-1}	2	This is the average wind speed at the canopy height, and is taken from the RESRAD model for a non-coastal site (Penfold and Watkins, 1998). A range of 1 to 4 m s^{-1} is given for uncertainty calculations.
Activity concentration in contaminated aquifer irrigation water, Bq L^{-1}	-	Scenario specific value
Fraction of irrigation water reaching the soil, -	0.8	
Upward flux of $^{14}CH_4$ into the soil column, Bq m^{-2} y^{-1}	1	
Degree of transformation of methane to CO_2, -	0.11	Le Mer and Roger (2001).
Fraction of plant carbon coming from the air, -	0.98	
Fraction of plant carbon coming from the soil via root uptake, -	0.02	
Soil degassing, y^{-1}	14.6	
Wash-off from leaves, y^{-1}	3000	
Translocation factor, y^{-1}	1.8	
Evaporation losses of leaves, y^{-1}	6000	
Stable C content of crops, kg C kg^{-1} d.w.	Leafy: 0.325 Root: 0.5 Fruit: 0.415 Cereal: 0.7	These data are based upon values reported in Baes et al. (1984) and Pinner and Maple (1987), converted from fresh to dry weights.
Stable C content of the air, kg m^{-3}	1.7E-04	
Stable C content of soil, kg C kg^{-1} d.w.	0.029	

2.12 LLWR model for ^{14}C

2.12.1 Context

This model was developed for post-closure assessment of a near-surface disposal facility for low level radioactive waste in the UK. The source term is a relatively homogenous release of ^{14}C labelled gases, $^{14}CH_4$ and $^{14}CO_2$, through a cap and into overlying soil. The model covers the behaviour of ^{14}C in an agricultural soil-plant and animal system, together with subsequent exposure calculations for humans. The model builds on experience gained through a quantitative model inter-comparison exercise undertaken within the BIOPROTA framework (Limer et al., 2012; Norris et al., 2011). That comparison exercise emphasised the importance of the representation of vertical and horizontal air exchanges within the plant canopy and any losses to the wider atmosphere. A new model for ^{14}C, hereafter referred to as the Thorne-Limer model, was therefore developed for an Environmental Safety Case (ESC) supporting the LLWR that was submitted to regulators in May 2011. The model is described in Limer et al. (2011a,b).

2.12.2 Modelling approach

The reference model assumes that 100% of the methane reaching the soil is oxidised to carbon dioxide, which is conservative for the soil-plant pathway. The vertical structure of the soil-plant model is shown in Figure 13. The model includes three layers and distinguishes the base of the model from the soil surface:

- The region $[0, z_1]$ corresponds to soil solution plus soil atmosphere. The height of this compartment corresponds to the thickness of the soil plus subsoil of the cap.
- The height of the second layer $[z_2]$ is chosen to be equal to the height where turbulent mixing in the plant canopy commences, and thus is plant-type specific. This height is characterised by the zero displacement height (z_d) at which the wind speed is taken to fall to zero. The zero

displacement height is related to the height of the crop canopy by factors of three quarters and two thirds for dense and moderate canopy densities, respectively, based on Allen et al. (1998) and Mölder (1997). The value for a moderate canopy density was used in the assessment, as it was considered appropriate for the nature of the vegetation that might be grown upon the cap over the waste at the facility.

- Layer 3 [z_2, z_3] extends beyond the top of the plant canopy; the height of z_3 is fixed for all plant types to ensure that there is a minimum of a 10 m thickness of free air that overlies the canopy. Air exchanges can occur between the layers and a horizontal flow of air can occur both within and above the canopy, but not within the soil zone.

Figure 13: Vertical structure of the representation of soil/atmosphere within the LLWR model

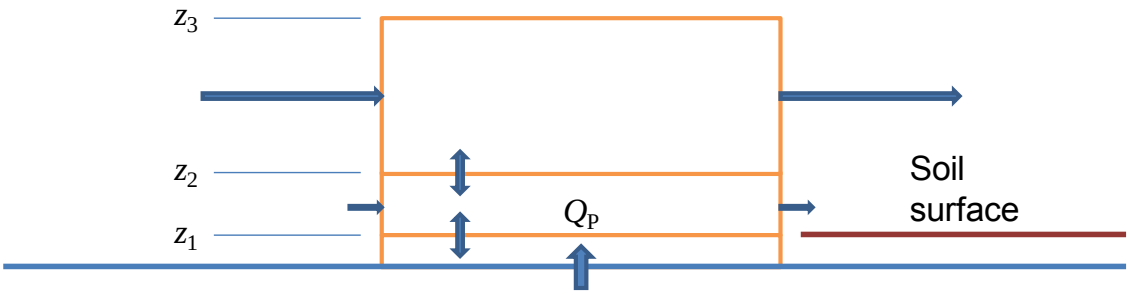

Transport vertically in and through the canopy is treated as a diffusion-like process. Below the zero displacement height it is characterised by the diffusion coefficient in air. Above the zero displacement height the diffusion coefficient is modified by the von Karman's constant and the friction velocity, which depends on the wind speed away from the surface and the surface roughness length[4], which is in turn related to the height of the plant canopy (the roughness elements).

Above the zero displacement height [z_2, z_3] air flows horizontally and is characterised by the wind speed at 10 m, which is adjusted to the height of the mid-point of the layer by consideration of the friction velocity.

The concentration of ^{14}C in soil solution (Bq m^{-3}) is taken to be the same as that in the soil atmosphere (Bq m^{-3}). The concentration of carbon dioxide in the soil atmosphere is assumed to be enriched in comparison to the above ground atmosphere by a factor of between 30 and 60. All plant carbon is assumed to be derived from photosynthetic uptake from the atmosphere. The fraction of plant carbon derived from the two above-ground atmospheric layers is determined by light intensity, which is related to the leaf area index (LAI).

Parameter values adopted for the reference calculations are shown in Table 15 and Table 16.

[4] The zero displacement height, and roughness length are not the same entity. These, and other factors associated with the modelling of near surface turbulence are discussed further in Foken (2008).

Table 15: Crop-independent parameter values adopted in the LLWR model for ^{14}C

Parameter	Value	Notes / Reference
Wind speed at 10 m, m s^{-1}	5	Clarke (1979)
Diffusion coefficient in air, m^2 s^{-1}	1.4 10^{-5}	Lide (2006). Described as a reasonable value
Von Karman's constant, -	0.4	Zhang et al. (2008). Described as a reasonable value
Friction velocity, m s^{-1}	0.2	Value assumed for an agricultural surface (Clarke, 1979). Described as a reasonable value for a closed canopy. For a more open canopy, this can be significantly increased
Soil thickness, m	0.6	Sum of the thickness of the soil and drainage layer of the cap
Height of top of turbulent mixing atmospheric compartment, m	12	Chosen to ensure that it includes the 10 m reference height
Integral of photosynthesis, -	1	To ensure 100% of plant profile account for in photosynthetic uptake
Ratio of the coefficient of nitrogen allocation to the extinction coefficient for diffuse light	0.4	Anten (1997)

Table 16: Crop-dependent parameter values adopted in the LLWR model for ^{14}C

Parameter	Crop Specific Value				
	Potatoes and Root Vegetables	Green Vegetables	Garden Fruit	Cattle and Goat Pasture	Sheep Pasture
Above ground plant height [1], m	0.40	0.40	0.55	0.20	0.02
Leaf Area Index [2], -	3.62			1.71	
Extinction coefficient for diffuse light [3], -	0.85			0.4	

[1] Based on a canopy height data in Allen et al. (1998).

[2] Based on data in Scurlock et al. (2001). Cropland values are assumed for the plants consumed directly by humans, and a grassland value is assumed for pasture.

[3] Based upon the ranges observed for broadleaf species and grassed by Monsi and Saeki (1953). The mid-point of each range is the recommended value.

2.12.3 Commentary

The LLWR model builds on the experience gained through the BIOPROTA forum by explicitly representing a diffusive layer within the plant canopy. Whilst plants can still obtain some of their carbon from air that is flowing horizontally, it would seem that the diffusive layer dominates ^{14}C uptake, which practically removes the impact of field size on calculated concentrations in plant tissues.

The LLWR model does not include any retention of ^{14}C in soil carbon pools beyond soil solution nor does it include the return of organic matter containing ^{14}C to the soil. This is justified with reference to studies with the enhanced RIMERS model (Thorne, 2006), in which it was shown that a single-pass model is appropriate to representing the flow of ^{14}C labelled carbon dioxide through the plant canopy and its uptake in photosynthesis for long-term releases to the soil, for which the continuing source term would dominate.

It is acknowledged that this model has a conceptually cautious assumption that ^{14}C migration in the lower part of the plant canopy was only by molecular diffusion. LLWR is currently undertaking a study to examine this, and other key technical and conceptual issues that influence the estimated radiological

impact from ^{14}C bearing gas (Sumerling, 2012). That study has shown that resistance analogue models, employed in plant canopy studies, are equivalent to the representation in Thorne-Limer model, if the lower canopy compartment is conceived as a zone in which dispersive transport takes place driven by variations in turbulent flow in the upper canopy. Test calculations have led to significant reductions in the calculated estimates of the potential impact of any releases.

2.13 Discussion of the contemporary models

2.13.1 General observations

The models for ^{14}C considered in this review represent a range of levels of detail, reflecting both the ^{14}C source terms considered and also when they were developed. General observations are given in Table 17. The following points relating to specific models are highlighted:

- The LLWR model provides the most physically based representation of exchange rates between the soil atmosphere, below canopy atmosphere and above canopy atmosphere.
- The enhanced RIMERS model provides the most detailed representation of soil carbon pools, based on the Jenkinson and Rayner (1977) model, which developed into the RothC model (Coleman and Jenkinson, 2005). Whilst a single-pass model may be appropriate to represent soil carbon for long-term releases, it is not necessarily appropriate for shorter term releases for which the subsequent retention and release for the soil may be of interest.
- Both the model developed by KAERI and PRISM consider respiration explicitly as a loss mechanism of ^{14}C from the plant.
- A number of the models (the model developed by KAERI, OURSON, and PRISM) dynamically model plant growth, and thus explicitly account for isotopic dilution in the plant tissues due to growth.

Table 17: General observation from qualitative model review

Aspect of Model	Operational Models	Waste Disposal Models
Time steps	Often sub-annual	Equilibrium conditions or annual average assumed
Source	Gas from aboveground Irrigation water Short-term, episodic	Gas from belowground Upwelling water Irrigation water Long-term
Soil	Not always explicitly modeled. One or multiple compartments.	
Plant	Often multiple compartments Dynamic plant growth Isotopic dilution due to new growth	Typically a single compartment Static plant biomass No isotopic dilution
Atmosphere	Sometimes multiple compartments	
Plant ^{14}C concentration	Specific activity approach (photosynthesis)	Specific activity approach (photosynthesis) Sometimes root uptake

2.13.2 Other issues

Temporal resolution

With respect to operational or accidental releases, the temporal resolution of a model needs to be smaller than the time frame of the release, particularly if it is possible that the release can occur over time period when plants are not photosynthesising. It was considered that not explicitly representing diurnal processes in TOCATTA meant that it was not able to satisfactorily recreate the observed plant ^{14}C concentrations in the vicinity of the Le Hague fuel reprocessing plant (Aulagnier et al., 2012; Le Dizès et al., 2012).

If a single model is to be used for operational and post-closure safety assessments, then a balance needs to be given to the detail of the processes considered, as that can have implications of the temporal resolution of the model implementation. Resolution to half a day would enable diurnal changes in plant behaviour to be captured, whilst minimising the number of time steps, and thus computation, required for a medium to long-term simulation.

Model validation

The Tucker and Shaw (1997) data provide a potential basis for validating models for ^{14}C. Although other datasets, such as that collected by IRSN, may be available, it is considered that this data provide the most complete set of information for testing soil-plant-atmosphere models for ^{14}C at the present time. It is also acknowledged that the NDA RWMD is currently undertaking an experimental programme relating to soil-plant-atmosphere exchanges of ^{14}C, and that the data may become available in the future.

2.14 Theory of what the plant "sees" in terms of ^{14}C uptake

Irrespective of the source term, a specific activity approach is used to determine the plant ^{14}C concentration. In a specific activity approach it is assumed that the ^{14}C reaches equilibrium in some components of the system in the same proportions with stable carbon. The movement of ^{14}C and stable carbon is then treated dynamically between some model compartments, and not others.

$$^{14}C_{plant} = {}^{14}C_{plant\_environment}\left(\frac{^{stable}C_{plant}}{^{stable}C_{plant\_environment}}\right) \qquad \text{(Equation 1)}$$

Typically the soil, if explicitly represented, and atmospheric compartments are modelled dynamically. In instances where the source term is ^{14}C-labelled gas, consideration needs to be given as to whether the gas is CO_2 or CH_4. Whereas CO_2 is readily available for plant uptake (via photosynthesis), CH_4 needs to be oxidized to CO_2 before it is available to the plants (e.g. Le Mer and Roger, 2001). The degree of oxidation will depend upon the soil microbial population present. Any $^{14}CH_4$ which is oxidized, either in the atmosphere, soil or water, is available for subsequent uptake and assimilation by plants as $^{14}CO_2$. ^{14}C in plants can then be ingested and transferred to animals and humans. Where multiple plant compartments are used then consideration must be given to which compartments are ingested by animals and humans, as these compartments may differ in both stable and ^{14}C concentrations.

Although there is some limited evidence to suggest that up to a few percent of a plants carbon might result from direct uptake by roots (Sheppard et al. 1991; Vourinen et al. 1989), it is generally considered that photosynthesis is the dominant, if not only, means by which plants obtain carbon. The models considered in this review consistently assume that over 95% of ^{14}C enters the plant as a result of photosynthesis.

Given this, it is necessary to consider the profile of photosynthesis through the plant canopy as well as that of the profile of $^{14}CO_2$. There is an argument that the profile of the uptake of carbon is dependent upon the canopy density and the penetration of light through the canopy (Figure 14; Monsi and Saeki

2005). Further, as indicated in Figure 14, it is possible that the greater plant mass of photosynthetic issue is found in the upper part of the plant canopy, particularly for a broadleaf plant (Figure 14a).
For a release of ^{14}C from an aboveground source it might be argued that the profile of ^{14}C in the plant canopy atmosphere would decrease towards the bottom of the plant. Particularly in the instance of a broadleaf plant, this may be a similar pattern as the plant biomass. However, the profile of ^{14}C in the plant canopy following a release from belowground may not follow the same pattern as the plant biomass. In this instance, it would be reasonable to argue that the ^{14}C concentration in the canopy air would decrease towards the top of the plant canopy, i.e. potentially behave in an inverse manner to the plant biomass. The implications of assumptions with respect to the plant biomass distribution and the $^{14}CO_2$ distribution in the plant canopy profile in a model that considers the plant and atmosphere each as multiple compartments are discussed below in some scoping calculations.

2.14.1 Exploration of some plant uptake assumptions

In this exploration of model assumptions, for simplicity, it is assumed that 100% of the plant C (and thus ^{14}C) comes from photosynthesis. Consider a two-compartment aboveground plant and two-compartment atmosphere model. The plant is 1 m high. Using the broadleaf and grass photosynthetic tissue distributions shown in Figure 14, three theoretical plant biomass distributions are shown in Figure 15. Consider three possible atmospheric ^{14}C specific activity profiles: (a) equal specific activity in both compartments, (b) lower compartment has a specific activity twice that of the upper compartment ("below-ground release"), and (c) lower compartment has a specific activity half that of the upper compartment ("atmospheric release"); these are given in Table 18. Combining the plant biomass distributions and the atmospheric specific activities, the resulting plant ^{14}C concentrations are shown in Figure 16. This demonstrates that assuming an equal uptake through a homogenous plant structure could provide a conservative estimate of plant ^{14}C concentration or potentially underestimate it, for both release scenarios. Specifically, for a below-ground release, assuming equal uptake through a homogeneous structure would potentially overestimate the ^{14}C specific activity in broad leaved plants, whilst underestimating the ^{14}C specific activity in grass like plants; the opposite holds for atmospheric releases.

Table 18: Specific activity of atmospheric compartments (Bq kg^{-1} C)

Model variable		Atmosphere assumption		
		Equal	"Below" release	"Atmospheric" release
Assumed total atmospheric ^{14}C concentration (Bq m^{-3})		1	1	1
Assumed stable C concentration of atmosphere (kg m^{-3})		2.00E-04	2.00E-04	2.00E-04
Calculated atmospheric concentration in compartment (Bq m^{-3})	Upper (0.33 m)	1	0.6	1.5
	Lower (0.67 m)	1	1.2	0.75
Calculated specific activity of atmosphere (Bq kg^{-1} C)	Upper (0.33 m)	5000	3000	7500
	Lower (0.67 m)	5000	6000	3750

Figure 14: Productive structure of some plant communities. The dashed thick line shows the relative light intensity (*I*, %). (A) Broadleaf type: *Chenopodium album var. centrorubrum*-consociation, measured on 28 June 1949. (B) Grass type: *Pennisetum japonicum*-consociation (with fruits), measured on 28 September 1949. F = Fresh weight of the photosynthetic tissue in g per 50x50 cm^2. C = fresh weight of the non-photosynthetic tissue in g per the same area. SN = stem number in 50x50 cm^2. [Reproduced from Monsi and Saeki (2005).]

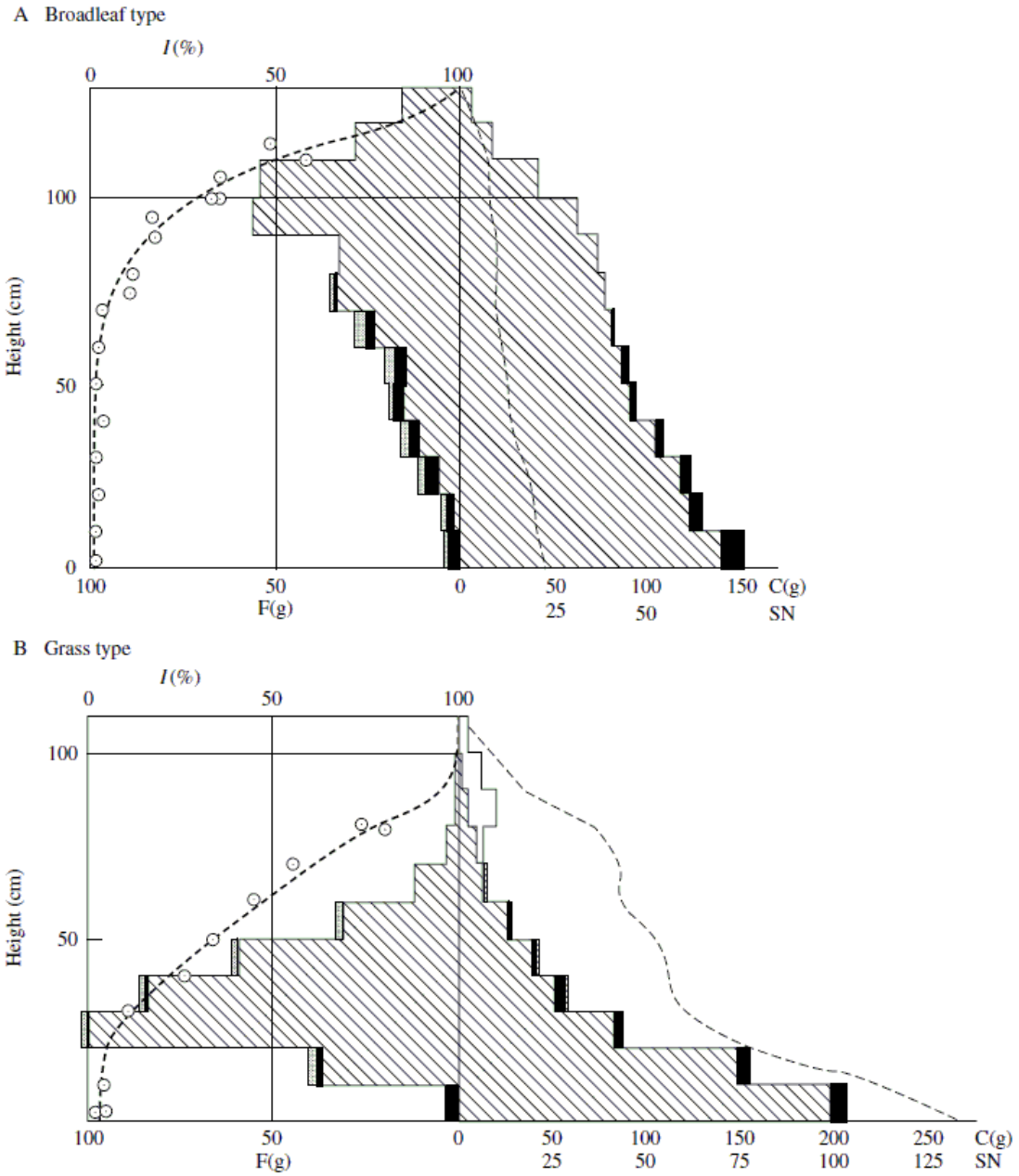

Figure 15: Theoretical plant biomass distribution

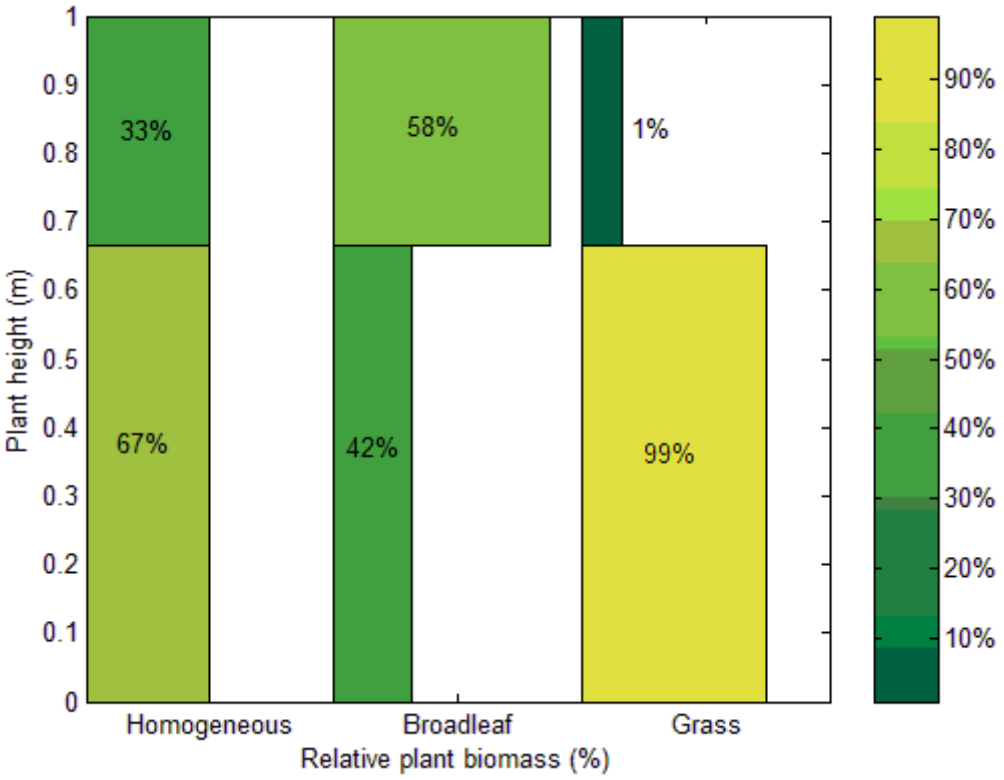

Figure 16: Calculated plant specific activities (Bq kg^{-1} C). The white is the calculated ^{14}C specific activity in the lower plant compartment. The black is the calculated ^{14}C specific activity in the upper plant compartment. H – Homogeneous; B – Broadleaf; G – Grass.

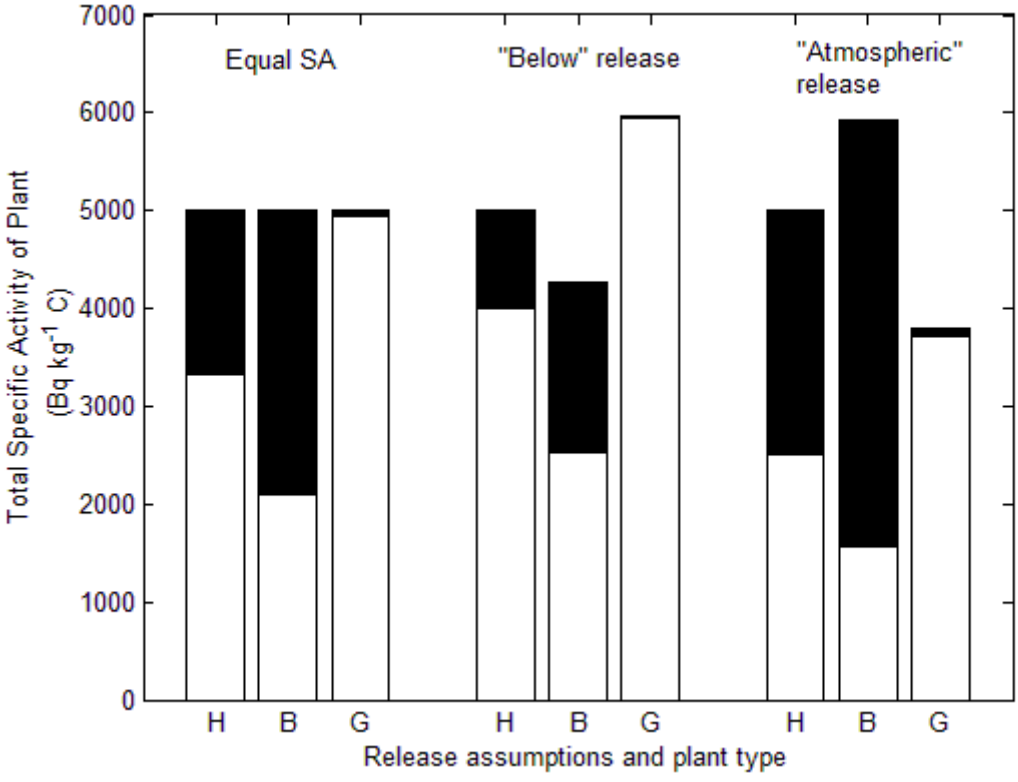

3 Model development

3.1 Requirements of SSM

The review of ^{14}C models in the previous section forms the basis for the derivation of the new compartment based model for SSM – SSPAM^{14}C (Swedish Soil-Plant-Atmosphere Model for ^{14}C). SSM has responsibility for assessing the safety associated with releases of radionuclides to the surface environment following the disposal of radioactive waste, operational releases of radionuclides and incidents or accidents leading to acute releases of radionuclides.

If SSM were to use a single model for the assessment of all these release scenarios then the model must be able to accept a variety of source terms (i.e. gaseous and liquid discharges from above- and below-ground), and also to consider processes within the ecosystem on a range of time-scales. Therefore, the aim in developing a new model for ^{14}C for SSM is that it will be as broadly based and as flexible as possible. Many of the models described above have specific intent – whether for short timescale releases to atmosphere or to scenarios associated with releases from geological or near-surface radioactive waste disposal facilities.

The conceptual and mathematical model descriptions are given in Sections 3.2 and 3.3. In order to provide some initial testing of SSPAM^{14}C, the model is applied to data from a series of experimental measurements carried out by Tucker & Shaw (1997), to test the ability of the model to reproduce experimental results for the uptake of atmospheric $^{14}CO_2$ in crops, specifically cabbages in this case. This model testing is described in Section 6.

3.2 Conceptual model for SSPAM^{14}C

The overall structure of the model, with interactions, is illustrated in Figure 17. The compartments through which the source terms interact with the model are also indicated. There are eleven structural elements (compartments) comprising reservoirs for ^{14}C in the model and these are divided into three sub-models – atmosphere, plant and soil. There is also a sink compartment into which losses from the modelled system are transferred; these include losses from harvesting plant material and ^{14}C in the atmosphere that transfers (by air movement) out of the area of interest.

The components of the sub-models are based on the models reviewed in the previous section with revised interpretations in the light of the interaction matrix set out here. As the model has been developed for application to long and shorter-term releases of ^{14}C, in this initial model development SSPAM^{14}C has the maximum number of compartments for each sub-model as have been used in any of the models reviewed in the preceding section. For example, the Enhanced RIMERS model, with its detailed and well-documented soil sub-model was particularly useful in developing the SSPAM^{14}C soil sub-model. The plant has been separated into many compartments, reflecting those models developed for shorter-term releases, such as PRISM and the model developed by KAERI.

The compartments form the leading diagonal of an interaction matrix (Figure 14); the interactions define the structure and processes in the model. The processes considered in this model are summarised in Table 19.

The compartments used in each of the sub-models are summarised in Section 0. The translation of the transfer processes between the compartments into the mathematical model is given in Section 3.3. Some of the parameter values are given in Section 3.3, though the full parameterisation in given in Appendix A.

Figure 17: Overall Conceptual Model for SSPAM^{14}C.

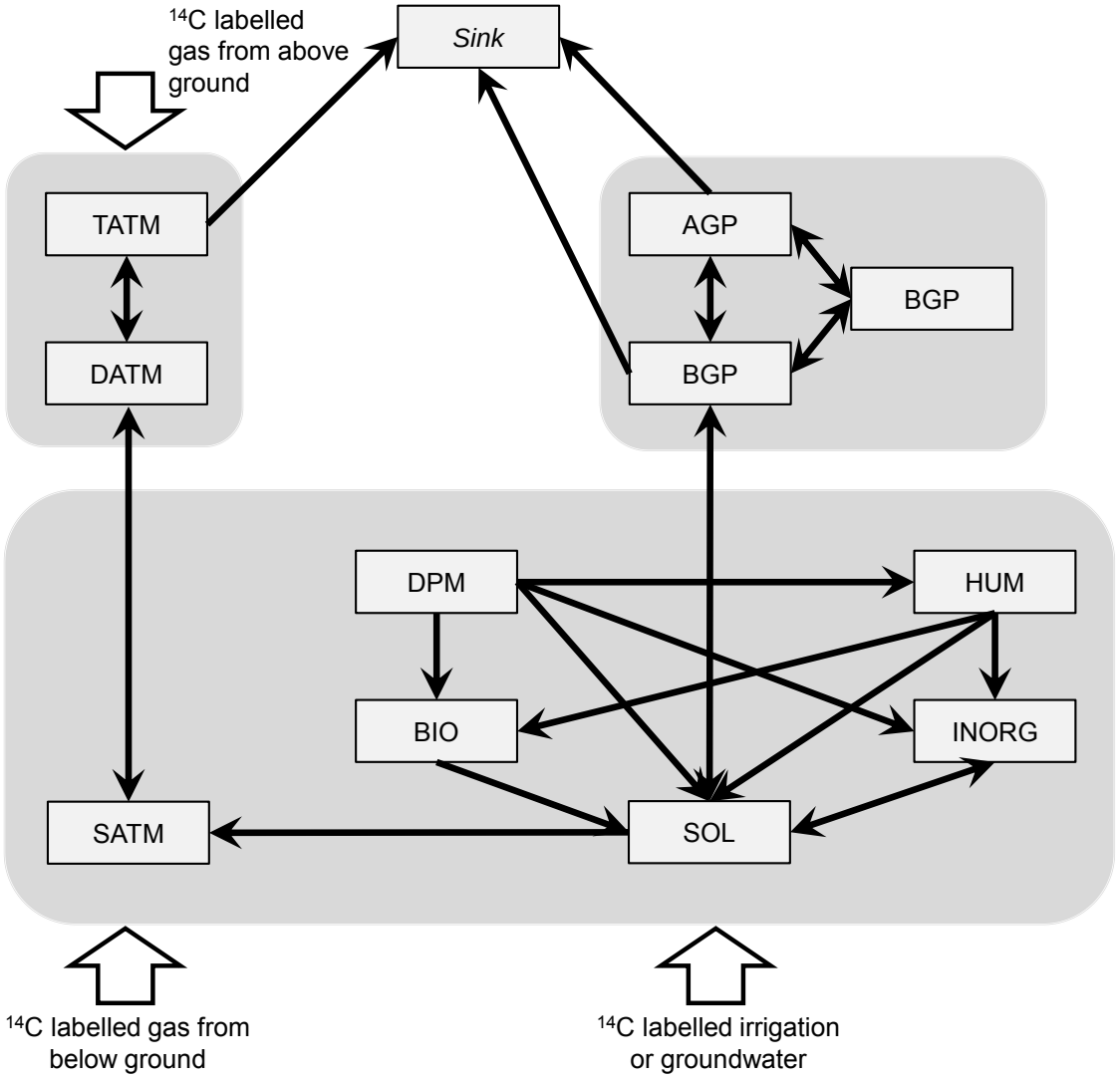

There are eleven compartments (plus a downstream sink) comprising three distinct sub-models: atmosphere (TATM, DATM), plant (AGP, BGP, FRUIT) and soil (SATM, SOL, INORG, BIO, DPM and HUM). See text for details.

Figure 18: The SSPAM^{14}C transfer matrix in Ecolego[5]. Leading diagonal elements are the structural components of the model. Off-diagonal elements represent the transfer coefficients described by Equation 1. The first row defines potential sources into the model.

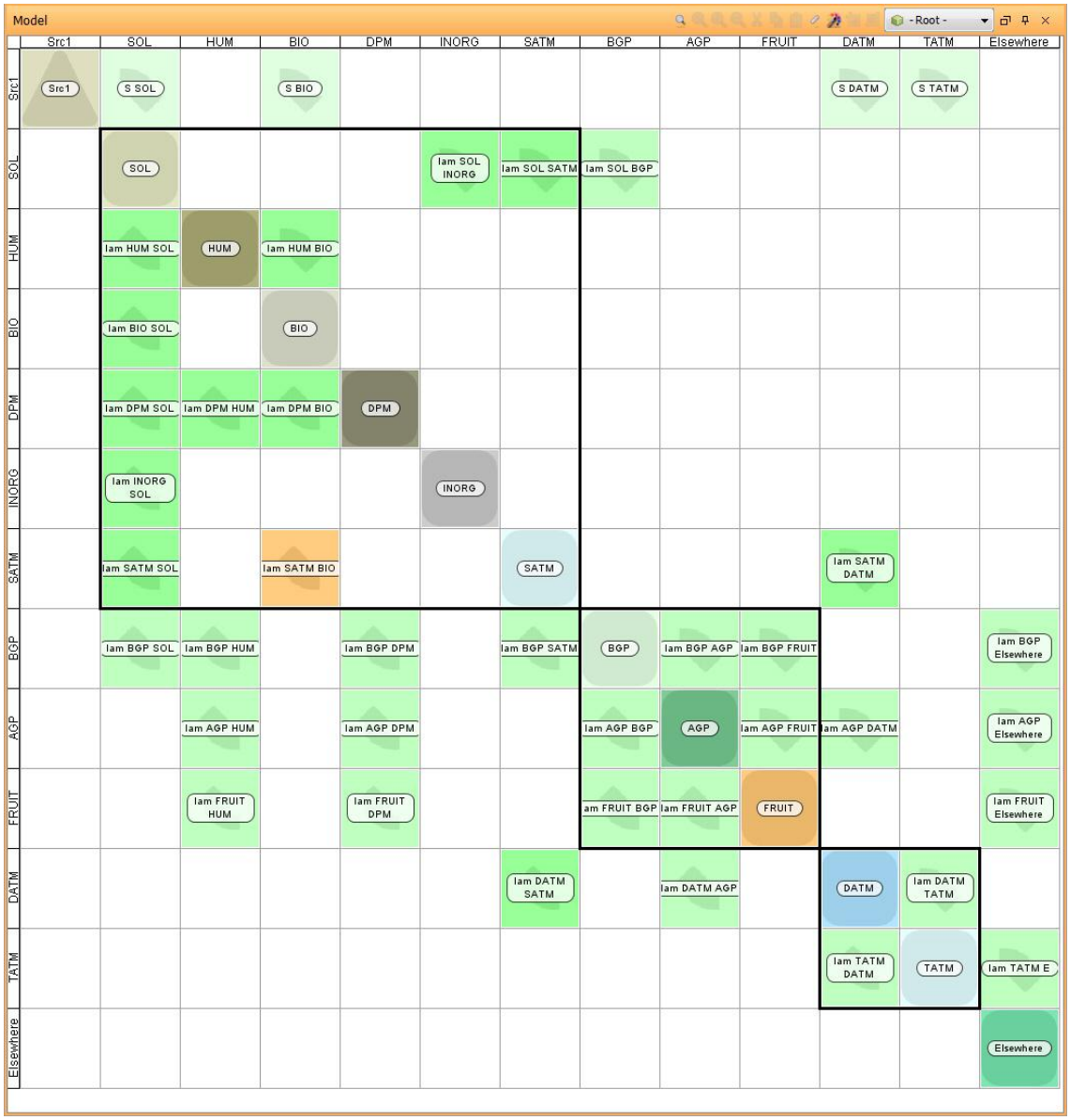

[5] Facilia (2011)

Table 19: Processes considered in SSPAM^{14}C

Process	Description	Compartments involved
Atmospheric exchange	Exchange of air, and C, between atmospheric compartments, and loss from the system. Includes air entering soil from aboveground.	DATM → TATM DATM → SATM TATM → DATM TATM → Sink
Cropping loss	Loss of plant material from the system.	AGP → Sink BGP → Sink FRUIT → Sink
Decomposition	Decay of plant and soil material.	AGP → DPM AGP → HUM BGP → DPM BGP → HUM FRUIT → DPM FRUIT → HUM DPM → HUM DPM → BIO DPM → SOL HUM → BIO HUM → SOL BIO → SOL
Degassing / volatilisation	Release of gaseous ^{14}C from the soil to the aboveground atmosphere.	SATM → DATM SOL → SATM
Dissolution		INORG → SOL SATM → SOL
Foliar uptake &/or photosynthesis	Uptake of C by the plant.	DATM → AGP
Respiration	Loss of C by the plant as a result of respiration.	AGP → DATM BGP → SATM
Root exudation	Loss of C from roots in a dissolved form.	BGP → SOL
Root uptake	Uptake of C from the soil by plant roots.	SOL → BGP
Sorption		INORG → SOL
Translocation	Movement of C within the plant. *	AGP → BGP AGP → FRUIT BGP → FRUIT *BGP → AGP* *FRUIT → AGP* *FRUIT → BGP*

* Translocation of C is thought to only occur between the AGP and the BGP or FRUIT, and between BGP and FRUIT in root crops (G. Shaw, personal communication)

3.2.1 Sub-model descriptions

Atmosphere sub-model

- TATM – turbulent atmospheric mixing layer
- DATM – Diffusive atmospheric mixing layer

The two compartments are the *Turbulent ATMosphere* (*TATM*), characterised by high advective flows leading to rapid turbulent mixing. It corresponds both to the above-canopy atmosphere considered in some of the reviewed models and also accounts for the space between crops where there is sparse coverage. There is a body of more quiescent air around and within the canopy – this is the *Diffusively controlled ATMosphere* (*DATM*) where carbon fluxes are controlled by concentration gradients rather than pressure differences.

Plant sub-model

- AGP – above ground plant
- BGP – below ground plant
- FRUIT – produce of the plant

There are many ways in which the plant could be sub-divided. For convenience a distinction is made between the *Above Ground Plant* (*AGP*) and the *Below Ground Plant* (*BGP*). *AGP* comprises primarily the leaves and those surfaces active in photosynthesis, respiration and evapotranspiration, but also includes the stem. In the soil, *BGP* relates essentially to the roots.

A distinction is made between the *FRUIT* and the other parts of the plant. The *FRUIT* is the edible tissue which the plant produces during the growing season (as well as growth in the AGP and BGP) which can be either borne on the AGP tissue – such as grain or beans – or it can be part of the BGP, such as potato tubers. In this regard, SSPAM^{14}C has some similarities with the KAERI and Japanese models (see Sections 2.6 and 0).

Soil sub-model

- SATM – soil atmosphere
- SOL – soil solution
- INORG – inorganic material
- BIO – microbial biomass
- HUM – humus
- DPM – decomposable plant matter

While the discretisation of the atmosphere and plant sub-models is fairly straightforward, the soil sub-model differs from the descriptions in the literature reviewed above. The choice was made to maintain clearly defined domains within the soil as structural elements.

SSPAM^{14}C's soil sub-model is derived from the RothC model (Coleman and Jenkinson, 2005). This model evolved from a model developed for an agricultural soil in the 1970s, using empirical data from extensive field experiments at Rothamsted, UK (Jenkinson and Rayner, 1977). It is the older model which was used as the basis for the soil sub-model of Enhanced RIMERS model (Thorne, 2005). There are some notable differences between SSPAM^{14}C's soil sub-model, RothC and Enhanced RIMERS, which are described in Table 20.

Table 20: Comparison of the soil sub-model of SSPAM^{14}C and the models from which it is derived

Component	Enhanced RIMERS	RothC	SSPAM^{14}C
Soil atmosphere	Individual compartment	Not considered explicitly, though exists as an implicit sink	Individual compartment (SATM)
Soil solution	Individual compartment	Not considered	Individual compartment (SOL)
Microbial biomass	Individual compartment	Individual compartment	Individual compartment (BIO)
Decomposable plant material	Individual compartment	Individual compartment	Individual compartment (DPM)
Resistant plant material	Individual compartment	Individual compartment	Not considered
Physically and chemically bound organic matter	Two separate compartments	Single compartment, known as humified organic matter.	Individual compartment, known as humus (HUM)
Inorganic material	Not considered	Not considered	Individual compartment (INORG)

3.3 Mathematical model

The description below gives details of the implementation of this prototype model. The parameterisation is a balance between that used in other models and expert opinion as to what processes need inclusion. Future developments will be implemented during the 2013 work programme.

The mathematical model uses a first order linear approximation to represent inter-compartmental transfers:

$$\frac{d\mathbf{N}}{dt} = \mathbf{S} + (\mathbf{\Lambda} - \lambda_0 \mathbf{I})\mathbf{N} \qquad \text{(Equation 2)}$$

The source term is **S** (Bq y^{-1}) and the radioactive decay constant λ_0 (y^{-1}); the latter is applied to the ^{14}C in each model compartment via its multiplication with the identity matrix **I** (-). The inventory of ^{14}C in the compartments is **N** (Bq). The detailed set of interactions is encoded in the transfer matrix $\mathbf{\Lambda}$ (y^{-1}), the individual elements, λ (y^{-1}), of which are calculated as:

$$\lambda_{ij} = C_{ij} / M_i \qquad \text{(Equation 3)}$$

where M_i is the mass of carbon in the compartment (kg C), and C_{ij} represents the mass transfers of carbon between the compartments (kg C y^{-1}). It is therefore assumed that the ^{14}C content of the compartments is well mixed in the total mass of carbon. This means that the total mass of carbon and the carbon transfer rates can be used for the purpose of deriving the ^{14}C fractional transfer rates. Thus the model depends on the parameterisation of two quantities:

1. The mass of carbon in the compartment, and
2. The mass of carbon transferred to other compartments per unit time.

However, while the masses involved are readily quantifiable, the available literature does not always allow for the transfers to be calculated. Instead, it is often the case that only a value for the absolute transfer rate is available. The following parameterisation makes such situations clear.

The model has been implemented using the Facilia Ecolego model development tool (Facilia, 2011) and Figure 18 shows the non-zero interactions in the model for which numerical values are required. The remainder of this section gives the definition of the transfer coefficients for each non-zero element of the transfer matrix in turn.

This section gives details of the derivation of the transfer coefficients in the model using the parameters listed in 0. One difficulty encountered in translating the literature models into a form which could be used here was the lack of clarity in the parameterisation of some processes. Care is taken here to identify parameters clearly so that the model is constructed as a set of expressions which can be readily manipulated and converted for use with sampled data, as and when required. The model description therefore emphasises the relationship between parameters, which can then be used with appropriate databases to represent a number of different scenarios.

3.3.1 Transfers within and from the atmosphere sub-model

The model domain comprises a volume $A_f \left(l_{TATM} + l_{DATM} + l\right)$ (m^3) given the area of land is $A_f = 10^4$ m^2, the thickness of the soil is l = 0.3 m, the turbulent atmosphere layer thickness is l_{TATM} = 5.0 m and the diffusive atmosphere layer thickness is l_{DATM} = 0.5 m. These values are taken from the Enhanced RIMERS parameterisation (see Table 11 and Thorne, 2005) for the above canopy atmosphere and below canopy atmosphere respectively. These values are applied as a first approximation and, in particular, the thickness of the diffusive layer may be seen to be too large. The values are justified for the present usage in that the aims are to i) provide a numerical intercomparison with the Enhanced RIMERS model and ii) provide a basic database which is open to revision in the context of the interpretation of experimental results in Section 6.

This defines the volumes of the model's physical domains (Figure 19).

Figure 19: Schematic of the atmosphere sub-model of SSPAM^{14}C

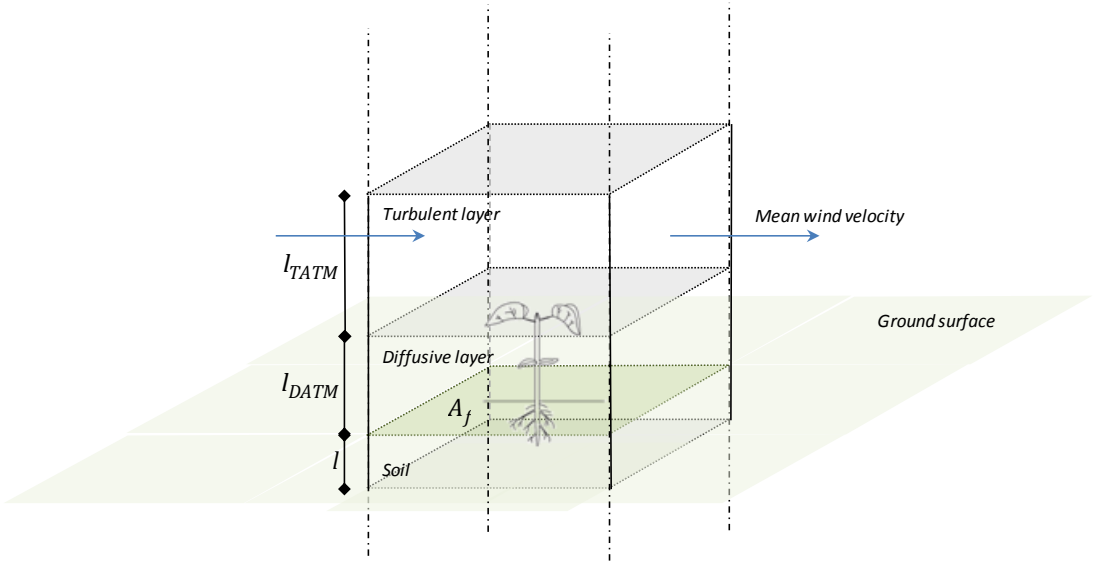

The mass carbon in the atmospheric compartments (M_{TATM} and M_{DATM}, kg C) is derived from the atmospheric concentration of CO_2, $m_{C,ATM}$ (kg CO_2 m^{-3}), with C = 12 amu, O_2 = 32 amu, so that:

$$M_{TATM} = f_{TATM} \cdot m_{C,ATM} \cdot l_{TATM} \cdot A_f$$
$$M_{DATM} = f_{DATM} \cdot m_{C,ATM} \cdot l_{DATM} \cdot A_f \qquad \text{(Equation 4)}$$

Here the f_i are enhancement factors of the concentration of carbon in each atmosphere layer; the values for these are obtained by a comparison of stable carbon dioxide concentrations in the soil atmosphere with stable carbon dioxide concentrations in the above-ground atmosphere (Thorne, 2005). For most purposes f_i can be set to 1 for TATM and DATM. Given the widely accepted dominance of photosynthesis as a means of C uptake in plants, the following transfer requires careful parameterisation:

$$\lambda_{\substack{DATM \\ AGP}} = (1 - f_{ru}) \cdot \frac{\dot{m}_{phot} \cdot A_f}{M_{DATM}} \qquad \text{(Equation 5)}$$

Here $\dot{m}_{phot}$ is the growth rate of the crop (kg C m^{-2} y^{-1}). Thorne (2005) quotes a value equivalent to 0.2 kg C m^{-2} y^{-1}. The fractional uptake of carbon through the plant roots is f_{ru}, this is assumed to be 1% of the total growth rate. The transfer rate is therefore calculated to be $\lambda_{\substack{DATM \\ AGP}} = 2.03 \times 10^3$ y^{-1}.

Thorne (2005) discusses the exchange between below canopy atmosphere (equivalent to DATM here) and soil atmosphere. A rate constant is used to describe the transfer to DATM from SATM:

$$\lambda_{\substack{SATM \\ DATM}} = \kappa_{\substack{SATM \\ DATM}} \qquad \text{(Equation 6)}$$

According to Thorne (2005) the rate "*was taken to be 1×10^4 y^{-1} as internal exchange processes in soil are expected to occur on timescales of no more than hours"*. Equilibrium with the DATM compartment is assumed so that the transfer from DATM to SATM is given as:

$$\lambda_{\substack{DATM \\ SATM}} = \frac{M_{SATM}}{M_{DATM}} \cdot \lambda_{\substack{SATM \\ DATM}} = (\varepsilon - \theta) \cdot f_{SATM} \cdot \frac{l}{l_{DATM}} \cdot \kappa_{\substack{SATM \\ DATM}} \qquad \text{(Equation 7)}$$

The enhancement factor for SATM is $f_{SATM} = 20$ (Thorne, 2005) and the gas filled pore space in the soil is calculated from the porosity (ε, -) and the volumetric moisture content (θ, -) (see Appendix A for values), so that $\lambda_{\substack{DATM \\ SATM}} = 6 \times 10^3$ y^{-1}.

A similar procedure is used to evaluate the exchange between the turbulent and diffusive layers:

$$\lambda_{\substack{DATM \\ TATM}} = \kappa_{\substack{DATM \\ TATM}} \qquad \text{(Equation 8)}$$

As the expected process of exchange between the diffusive and turbulent atmosphere compartments is expected to occur on timescales of days or less, Thorne (2005) notes a rate of $\kappa_{\substack{DATM \\ TATM}} = 10^3$ y^{-1}. The return process, in equilibrium, may be written as:

$$\lambda_{\substack{TATM \\ DATM}} = f_{DATM} \cdot \frac{l_{DATM}}{l_{TATM}} \cdot \kappa_{\substack{DATM \\ TATM}} \qquad \text{(Equation 9)}$$

Thus $\lambda_{\substack{TATM \\ DATM}} = 100$ y^{-1}. Thorne notes that these processes "*are not well constrained"* in this interpretation and this is certainly the case. The interpretation of the experimental data provides for an improved parameterisation in Section 6.

The final transfer from the atmosphere sub-model concerns the turbulent flux through the TATM compartment. This is represented as:

$$\lambda_{\substack{TATM \\ E}} = n_{spy} \cdot \frac{v_{wind}}{\sqrt{A_f}} \qquad \text{(Equation 10)}$$

The mean wind speed, v_{wind}, is assumed to be 5 m s^{-1} (Thorne, 2005) and the conversion to m y^{-1} is made using the number of seconds per year, n_{spy}.[6]

3.3.2 Transfers within and from the plant sub-model

In many ways the multi-compartment plant has proved the least amenable to a raw parameterisation. The generic values adopted here were used to establish that the new model could function correctly in the context set by the Enhanced RIMERS model. It is only with the application to the modelling of the experimental data of Tucker & Shaw (1997) that a clearer understanding of the processes involved, particularly concerning ^{14}C within the plant, has been possible. These matters are pursued in Section 6. In this section a rudimentary generic crop is derived based on the Enhanced RIMERS model.

The masses of carbon in the three plant compartments (M_i, i = AGP, BGP and FRUIT; kg C) are derived from the total above and below ground standing biomass m_{SB} (kg fw m^{-2}) with the fractional mass in each of the compartments:

$$M_i = f_i \cdot m_{SB} \cdot A_f \qquad \text{(Equation 11)}$$

A biomass of 1 kg fw m^{-2} is assumed and the fractions in AGP and BGP are, respectively taken to be 0.49 and 0.5, with $f_{FRUIT} = 1 - f_{AGP} - f_{BGP}$[7].

The fractional carbon content of plant tissue (f_{pC}) is based on the stoichiometric formula for starch and cellulose $(C_6H_{10}O_5)_n$, so that

$$Zf_{pC} = \frac{6 \times 12}{10 + 5 \times 16 + 6 \times 12} \approx 0.444 \qquad \text{(Equation 12)}$$

The fresh weight to dry weight ratio is assumed to be $Z = 5$.

Many of the modelled carbon transfers within and from crops are not process-based and so use transfer rates based on consideration of overall turnover rates. The carbon loss from roots by exudation is included but set to a very low value of $\kappa_{exd} = 10^{-3}$ y^{-1} (i.e. it is represented as a minor C transfer process[8]). In this prototype model, plant senescence[9] is modelled as a once per year process[10], $\kappa_{plantdeath} = 1$ y^{-1} but it is the internal translocation factors that are missing. However, because the crop is homogeneous in most other models, the assumption is made that the translocation rates are zero with the exception of the AGP $\rightarrow$ BGP transfer, i.e. a fraction of carbon taken in through the leaves is transferred to the root system. The nine transfers between components of the plant sub-model are written as:

$$\lambda_{ij} = \kappa_{ij} \qquad i, j = AGP, BGP, FRUIT \qquad i \neq j \qquad \text{(Equation 13)}$$

[6] It is noted that assuming a radial geometry is slightly more conservative and would better reflect a uniform wind rose.

[7] These values are used for the test calculations and are approximate values for potatoes. They are not universally appropriate and such parameters are open to revision in respect of specific instances; in the experiment described in Section 5, the characteristics of the crop are part of the measured dataset.

[8] Further work planned in 2013 will investigate further the necessity for such a transfer to be included in the model.

[9] Cropping is considered in the transfer defined in Equation 19.

[10] The validity of this assumption is to be considered further in the continuing model development program.

The values of these internal translocation (y^{-1}) are given in the following matrix, assuming the order AGP, BGP and FRUIT for both the rows and the columns:

$$\boldsymbol{\kappa}_{\mathbf{transloc}} = \begin{bmatrix} 0 & 0.2 & 0 \\ 0 & 0 & 0 \\ 0 & 0 & 0 \end{bmatrix} \qquad \text{(Equation 14)}$$

This means that only $\kappa_{\substack{AGP \\ BGP}}$ has a non-zero value in this prototype model configuration.[11]

The root exudation transfer is modelled as:

$$\lambda_{\substack{BGP \\ SOL}} = \kappa_{exd} \qquad \text{(Equation 15)}$$

The respiration rates from foliage, and from roots, are calculated as:

$$\lambda_{\substack{AGP \\ DATM}} = \frac{\dot{m}_{resp} \cdot A_f}{M_{AGP}} \qquad \text{(Equation 16)}$$

$$\lambda_{\substack{BGP \\ SATM}} = (1 - f_{BIO}) \cdot \frac{\dot{m}_{resp} \cdot A_f}{M_{BGP}} \qquad \text{(Equation 17)}$$

where f_{BIO} = 0.54 is the maximum fraction of the total soil respiration coming from the microbial biomass (Löfgren, 2008). Here the Thorne (2005) value of $\dot{m}_{resp}$ = 0.12 kg C m^{-2} y^{-1} is assumed.

Plant death transfers the carbon content of the plant to the components of the soil model. The destination of the material released is determined by the partitioning coefficients derived by Jenkinson and Rayner in their model of organic matter turnover in the pasture (Jenkinson and Rayner, 1977). This was the formalism used by Thorne (2005). Using the partitioning coefficient p_{DPM} = 0.837 for the transfer to decomposable plant matter (and p_{HUM} (= 1 - p_{DPM}) direct to humus). Transfers from the plant components are therefore:

$$\begin{aligned} \lambda_{\substack{AGP \\ DPM}} &= \lambda_{\substack{BGP \\ DPM}} = \lambda_{\substack{FRUIT \\ DPM}} = p_{DPM} \cdot (1 - f_{\text{export}}) \cdot \kappa_{plantdeath} \\ \lambda_{\substack{AGP \\ HUM}} &= \lambda_{\substack{BGP \\ HUM}} = \lambda_{\substack{FRUIT \\ HUM}} = p_{HUM} \cdot (1 - f_{\text{export}}) \cdot \kappa_{plantdeath} \end{aligned} \qquad \text{(Equation 18)}$$

Only three transfers from the plant system remain which correspond to the export of material out of the system:

$$\lambda_{\substack{AGP \\ E}} = \lambda_{\substack{BGP \\ E}} = \lambda_{\substack{FRUIT \\ E}} = f_{\text{export}} \cdot \kappa_{plantdeath} \qquad \text{(Equation 19)}$$

In the prototype model used in this study, this export of plant material from the system as a result of cropping is set to zero.

[11] The value is based on expert opinion (G Shaw, personal communication).

3.3.3 Transfers within and from the soil sub-model

The soil sub-model described below is derived from the material discussed in Section 2. For this first implementation of SSPAM^{14}C, the goal is to have both functionality and flexibility while retaining links to the most relevant features of the other models. Unavoidably there are some differences of interpretation as to what soil compartments to include, and the dynamics of the interactions between them. It is anticipated that these will be resolved in the developments of SSPAM^{14}C following this initial phase. The determinant of acceptability is the degree to which the model is able to reproduce features of the results from the test datasets discussed in Section 5. The overall aim is to create a simplified, physically based model.

The carbon content of the various soil components is assumed to be as follows:

- $m_{C,BIO}$ = 0.065 kg C m^{-2};
- $m_{C,DPM}$ = 0.464 kg C m^{-2};
- $m_{C,HUM}$ = 0.203 kg C m^{-2}; and
- $m_{C,INORG}$ = 1125 kg C m^{-2}.

These values use the area concentration of carbon in the soil layer (assumed to be 0.3 m thick). Whilst an area concentration in used for the solid compartments, a volumetric carbon concentration is used for the SOL and SATM compartments (kg C m^{-3}):

$$m_{C,SATM} = f_{SATM} \cdot m_{C,ATM} \qquad \text{(Equation 20)}$$

where f_{SATM} = 20 is the soil atmosphere enhancement factor (Thorne, 2005), relative to the background atmospheric concentration defined in Section 0. Thorne (2005) also suggests that the carbon concentration in soil solution is given by:

$$m_{C,SOL} = \frac{\varepsilon - \theta}{\theta} \cdot m_{C,SATM} \qquad \text{(Equation 21)}$$

Allowing for the air-filled and water filled porosity in the soil, with SATM and SOL have volumes (m^3) defined by:

$$\begin{aligned} V_{SATM} &= (\varepsilon - \theta) \cdot l \cdot A_f \\ V_{SOL} &= \theta \cdot l \cdot A_f \end{aligned} \qquad \text{(Equation 22)}$$

Masses of carbon in the soil sub-model (kg C) are therefore given by:

$$\begin{aligned} M_i &= m_{C,i} \cdot A_f \qquad i = BIO, DPM, HUM, INORG \\ M_i &= m_{C,i} \cdot l \cdot A_f \qquad i = SATM, SOL \end{aligned} \qquad \text{(Equation 23)}$$

Thorne (2005) employed the Jenkinson & Rayner (1977) model for the turnover of organic materials in soils. In that model, the overall rate of loss from each of the BIO, DPM, HUM, and SOL were derived and reinterpreted by Thorne (2005). The overall loss rates (y^{-1}) assumed in this prototype model are:

$$\kappa_{BIO} = 0.108 \qquad \kappa_{DPM} = 33.4 \qquad \kappa_{HUM} = 0.134 \qquad \kappa_{SOL} = 0.409 \qquad \text{(Equation 24)}$$

Jenkinson and Rayner (1977) and Thorne (2005) employed a system of partitioning to direct the fluxes to different parts of the system. These are reinterpreted here in Figure 20, based on the Jenkinson & Rayner (1977) model.

The decay of plant material is partitioned according to $p_{DPM} + p_{HUM} = 1$, with p_{DPM} = 0.837 and p_{HUM} = 0.163. These transfers are already implemented, as previously described in Equation 18.

Losses from DPM are given by:

$$\lambda_{\substack{DPM \\ BIO}} = p_{BIO} \cdot \kappa_{DPM} \qquad \lambda_{\substack{DPM \\ SOL}} = p_{SOL} \cdot \kappa_{DPM} \qquad \lambda_{\substack{DPM \\ HUM}} = p_{slow} \cdot \kappa_{DPM} \qquad \text{(Equation 25)}$$

For which p_{BIO} = 0.0076, p_{SOL} = 0.1285 and:

$$p_{slow} + p_{BIO} + p_{SOL} = 1 \qquad \text{(Equation 26)}$$

Figure 20: Partitioning factors in the revised interpretation of the Jenkinson and Rayner (1977) soil model. The factors are shown relative to the loss rates quoted in Equation 23. The absolute values for the transfer rates are given in the main text below.

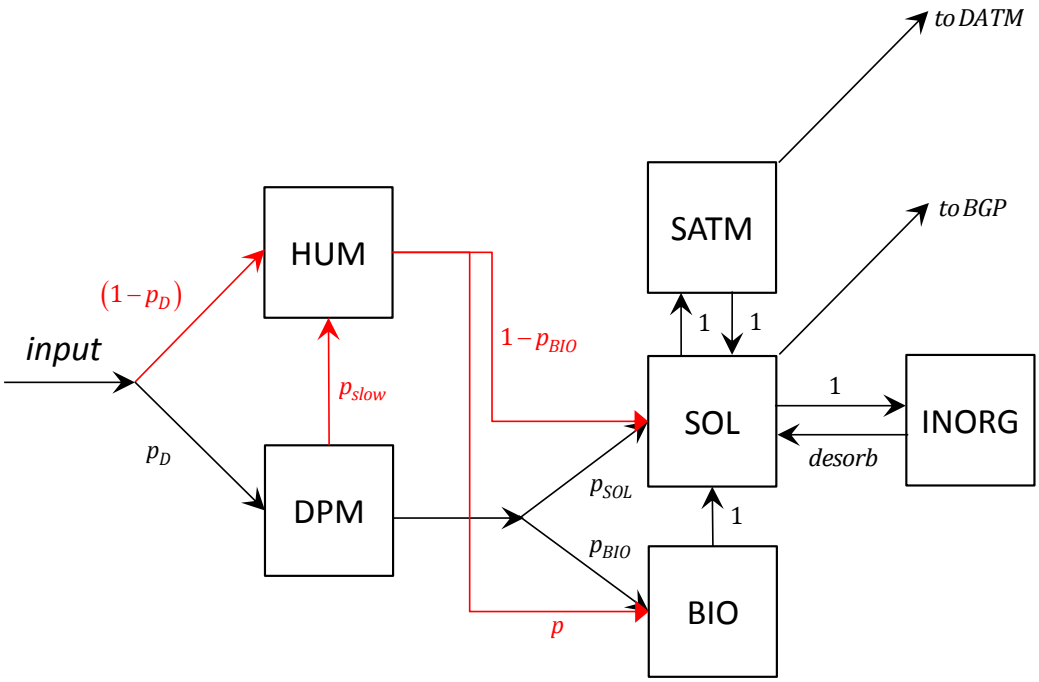

Losses from HUM are similarly

$$\lambda_{\substack{HUM \\ BIO}} = p_{BIO} \cdot \kappa_{HUM} \qquad \lambda_{\substack{HUM \\ SOL}} = (1 - p_{BIO}) \cdot \kappa_{HUM} \qquad \text{(Equation 27)}$$

Consistent with Jenkinson and Rayner (1977) and Thorne (2005), it is assumed that no material is returned to either the DPM or HUM compartments. The microbial biomass only interacts with the soil solution, so that:

$$\lambda_{\substack{BIO \\ SOL}} = \kappa_{BIO} \qquad \text{(Equation 28)}$$

There is no transfer from the soil atmosphere to the microbial biomass.

As well as the interaction with the BGP, as described in the plant sub-model, the soil solution exchanges with the soil atmosphere, as represented by:

$$\lambda_{\substack{SOL \\ SATM}} = \lambda_{\substack{SATM \\ SOL}} = \kappa_{\substack{SATM \\ SOL}} \qquad \text{(Equation 29)}$$

With a rate of $\kappa_{\substack{SATM \\ SOL}} = 10^4$ y^{-1} as specified by Thorne (2005) for equilibrium between SOL and SATM, where the rate is expected to proceed on the timescale of *no more than hours*.[12]

The remaining exchange requiring definition is the sorption/desorption of carbon onto/from the inorganic material in the compartment:

$$\lambda_{\substack{SOL \\ INORG}} = \kappa_s$$

$$\lambda_{\substack{INORG \\ SOL}} = \frac{\theta \cdot \kappa_s}{(1-\varepsilon)\cdot(1-\varphi_{BIO}-\varphi_{DPM}-\varphi_{HUM})\cdot k_d \cdot \rho_{inorg}} \qquad \text{(Equation 30)}$$

In practice the values adopted for the sorption rate $\kappa_s = 10$ y^{-1} and the $k_d = 0.1$ m^3 kg^{-1} were determined from the comparison of the results from an implementation of Enhanced RIMERS using the rate coefficients in Thorne (2005) with those obtained using the prototype SSPAM^{14}C model and varying κ_s and k_d (see Section 1).

The volume correction term in Equation 30 assumes that the fractional volumes of the solid material in the soil are:

$$\phi_{BIO} + \phi_{DPM} + \phi_{HUM} < 1 \qquad \text{(Equation 31)}$$

where the arbitrary assumption is made that $\phi_{BIO} = 0.1$, $\phi_{DPM} = 0.2$ and $\phi_{HUM} = 0.3$.

3.3.4 Summary of mathematical model

The mathematical formulae used to define the various transfers between compartments have been described in the preceding text. Below is a summary of the overall ^{14}C dynamics of each of the model compartments.

$$\frac{dN_{TATM}}{dt} = S_{Atmos} + \lambda_{\substack{DATM \\ TATM}} N_{DATM} - \left(\lambda_{\substack{TATM \\ DATM}} + \lambda_{\substack{TATM \\ E}} + \lambda_{14C} \right) N_{TATM} \qquad \text{(Equation 32)}$$

$$\frac{dN_{DATM}}{dt} = \lambda_{\substack{TATM \\ DATM}} N_{TATM} + \lambda_{\substack{SATM \\ DATM}} N_{SATM} - \left(\lambda_{\substack{DATM \\ TATM}} + \lambda_{\substack{DATM \\ SATM}} + \lambda_{\substack{DATM \\ AGP}} + \lambda_{14C} \right) N_{DATM} \qquad \text{(Equation 33)}$$

$$\frac{dN_{AGP}}{dt} = \lambda_{\substack{DATM \\ AGP}} N_{DATM} - \left(\lambda_{\substack{AGP \\ BGP}} + \lambda_{\substack{AGP \\ FRUIT}} + \lambda_{\substack{AGP \\ DPM}} + \lambda_{\substack{AGP \\ HUM}} + \lambda_{\substack{AGP \\ E}} + \lambda_{14C} \right) N_{AGP} \qquad \text{(Equation 34)}$$

[12] Note that this transfer is in addition that of the decomposition of the soil solution (κ_{SOL} – see equation 24).

$$\frac{dN_{BGP}}{dt} = \lambda_{\underset{BGP}{AGP}} N_{AGP} + \lambda_{\underset{BGP}{SOL}} N_{SOL} - \left(\lambda_{\underset{FRUIT}{BGP}} + \lambda_{\underset{DPM}{BGP}} + \lambda_{\underset{HUM}{BGP}} + \lambda_{\underset{E}{BGP}} + \lambda_{14C} \right) N_{BGP} \quad \text{(Equation 35)}$$

$$\frac{dN_{FRUIT}}{dt} = \lambda_{\underset{FRUIT}{AGP}} N_{AGP} + \lambda_{\underset{FRUIT}{BGP}} N_{BGP} - \left(\lambda_{\underset{DPM}{FRUIT}} + \lambda_{\underset{HUM}{FRUIT}} + \lambda_{\underset{E}{FRUIT}} + \lambda_{14C} \right) N_{FRUIT} \quad \text{(Equation 36)}$$

$$\frac{dN_{DPM}}{dt} = \lambda_{\underset{DPM}{AGP}} N_{AGP} + \lambda_{\underset{DPM}{BPG}} N_{BGP} + \lambda_{\underset{DPM}{FRUIT}} N_{FRUIT} - \left(\lambda_{\underset{HUM}{DPM}} + \lambda_{\underset{BIO}{DPM}} + \lambda_{\underset{SOL}{DPM}} + \lambda_{\underset{INORG}{DPM}} + \lambda_{\underset{E}{DPM}} + \lambda_{14C} \right) N_{DPM} \quad \text{(Equation 37)}$$

$$\frac{dN_{HUM}}{dt} = \lambda_{\underset{HUM}{AGP}} N_{AGP} + \lambda_{\underset{HUM}{BPG}} N_{BGP} + \lambda_{\underset{HUM}{FRUIT}} N_{FRUIT} - \left(\lambda_{\underset{BIO}{HUM}} + \lambda_{\underset{SOL}{HUM}} + \lambda_{\underset{INORG}{HUM}} + \lambda_{\underset{E}{HUM}} + \lambda_{14C} \right) N_{HUM} \quad \text{(Equation 38)}$$

$$\frac{dN_{BIO}}{dt} = \lambda_{\underset{BIO}{DPM}} N_{DPM} + \lambda_{\underset{BIO}{HUM}} N_{HUM} - \left(\lambda_{\underset{SOL}{BIO}} + \lambda_{14C} \right) N_{BIO} \quad \text{(Equation 39)}$$

$$\frac{dN_{INORG}}{dt} = \lambda_{\underset{INORG}{DPM}} N_{DPM} + \lambda_{\underset{INORG}{HUM}} N_{HUM} + \lambda_{\underset{INORG}{SOL}} N_{SOL} - \left(\lambda_{\underset{SOL}{INORG}} + \lambda_{14C} \right) N_{INORG} \quad \text{(Equation 40)}$$

$$\frac{dN_{SOL}}{dt} = \lambda_{\underset{SOL}{BGP}} N_{BGP} + \lambda_{\underset{SOL}{DPM}} N_{DPM} + \lambda_{\underset{SOL}{HUM}} N_{HUM} + \lambda_{\underset{SOL}{INORG}} N_{INORG} + \lambda_{\underset{SOL}{SATM}} N_{SATM} - \left(\lambda_{\underset{BGP}{SOL}} + \lambda_{\underset{INORG}{SOL}} + \lambda_{\underset{SATM}{SOL}} + \lambda_{14C} \right) N_{SOL} \quad \text{(Equation 41)}$$

$$\frac{dN_{SATM}}{dt} = S_{UpwellGas} + \lambda_{\underset{SATM}{DATM}} N_{DATM} + \lambda_{\underset{SATM}{SOL}} N_{SOL} - \left(\lambda_{\underset{DATM}{SATM}} + \lambda_{\underset{SOL}{SATM}} + \lambda_{14C} \right) N_{SATM} \quad \text{(Equation 42)}$$

$$\frac{dN_{E}}{dt} = \lambda_{\underset{E}{TATM}} N_{TATM} + \lambda_{\underset{E}{AGP}} N_{AGP} + \lambda_{\underset{E}{BGP}} N_{BGP} + \lambda_{\underset{E}{FRUIT}} N_{FRUIT} \quad \text{(Equation 43)}$$

4 Comparison of SSPAM^{14}C with enhanced RIMERS

In order to verify the correct working of the SSPAM^{14}C model, a version of the Enhanced RIMERS model has been run to produce ^{14}C inventories in each of the model compartments for a chronic release of 1 Bq y^{-1} to soil solution. The values of the transfer rates are taken from Thorne (2005) and these are shown in matrix form in 0. The integration was performed by a set of Fortran routines taken from Press et al. (1992). The results were used to assess the overall performance of the Ecolego implementation of SSPAM^{14}C, checking the general model dynamics, and to optimise some parameters in the detailed soil sub-model. Because of the different structures in the soil the results were not expected to be identical. In dose assessment modelling it is, in any case, the content of the plant that matters. For the purpose of comparison with the Enhanced RIMERS model, the fruit compartment is neglected.

Figure 21 shows results for the atmosphere and plant compartments and the soil compartments separately. Of primary importance is that the models should agree on the uptake by plants. The plots show that the compartment inventories approach equilibrium from 10^{-2} y to 100 years. The above ground plant (AGP) is in close agreement with the standing biomass of Enhanced-RIMERS after about 1 y. It is the AGP which is directly involved in the uptake of carbon from the atmosphere. The BGP plant parallels the AGP throughout the time period but at a much lower level so that the total plant inventory is well represented by the AGP inventory. For the purposes of comparison, there is no FRUIT inventory as indicated by Equation 14.

There are, however, discrepancies – for example the results for TATM are lower than those for the Above Canopy Atmosphere (ACA) but by a factor of less than 1.7 over the long term. This implies that the SSPAM^{14}C model retains more activity in the soil. By the end of the simulation the DATM compartment is equal to the Below Canopy Atmosphere (BCA) compartment. At earlier times, again the results for DATM are lower. From Figure 21(a), it is clear that the SSPAM^{14}C inventory for the SATM compartment is higher than that calculated with the Enhanced RIMERS model; the ratio is a factor of around four.

Comparing the overall loss from the two models, is overall agreement after 100 years, although SSPAM^{14}C retains more of the ^{14}C on earlier timescales.

Turning to the soil model in Figure 21(b), the agreement between the two models is rather less than for the plant and atmosphere compartments. The dynamics show reasonably close similarities, however, and the ratio between the compartments is less than a factor of ten in all cases except for DPM.

The reason for the large discrepancy in the DPM (decomposable plant material) compartment is that in Enhanced RIMERS there are losses from this plant matter compartment to two more recalcitrant (physically and chemically bound) organic matter pools, whereas in SSPAM^{14}C losses are sent to an inorganic carbon pool. The role of the COM and POM compartments in the original Jenkinson and Rayner (1977) model was to help fit the model to observations. Conceptually it makes no sense to transfer directly from the DPM compartment to the INORG compartment in SSPAM^{14}C, although the loss from DPM to the HUM compartment is logical. Loss from DPM potentially could be higher but, for now, the value is adopted though it is clear that there is a lack of understanding of the processes in soil at the level of detail required.

Within SSPAM^{14}C, transfers to and from the INORG compartment are modelled with a sorption rate and a k_d. The best fit of the SSPAM^{14}C INORG compartment to the POM and COM compartments is shown in Figure 22, for κ_s = 10 y^{-1} and k_d = 0.1 m^3 kg^{-1}.

Thus, there are reasonable fits for the key parameters. The remainder of this report deals with the application of the model to experimental data. There are some revisions required to the parameterisation of the model in order to best match the experimental results.

Figure 21: Comparison of Enhanced RIMERS and SSPAM^{14}C

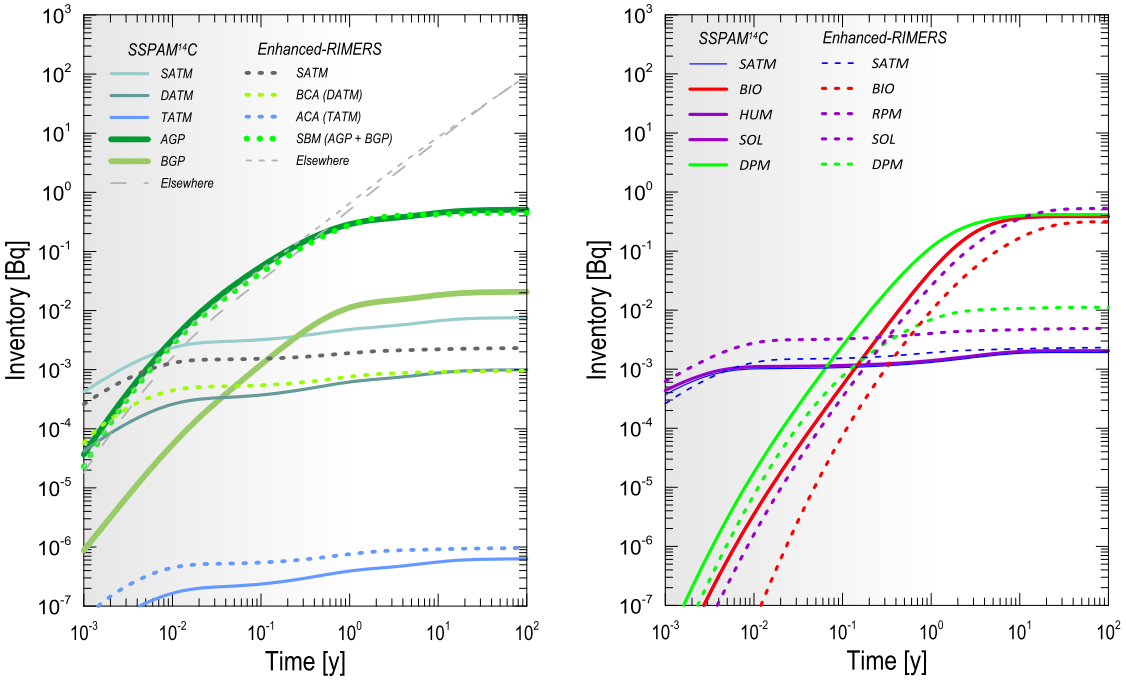

(a) Atmosphere and plant compartments

(b) Soil compartments

Figure 22: Comparison of Enhanced RIMERS compartments and COM and POM with the SSPAM^{14}C INORG compartment. Values are for parameter k_s = 10 y^{-1} and k_d = 0.1 m^3 kg^{-1} which give the nearest approach to the inventory in combined POM + COM possible with the simplified SSPAM^{14}C model.

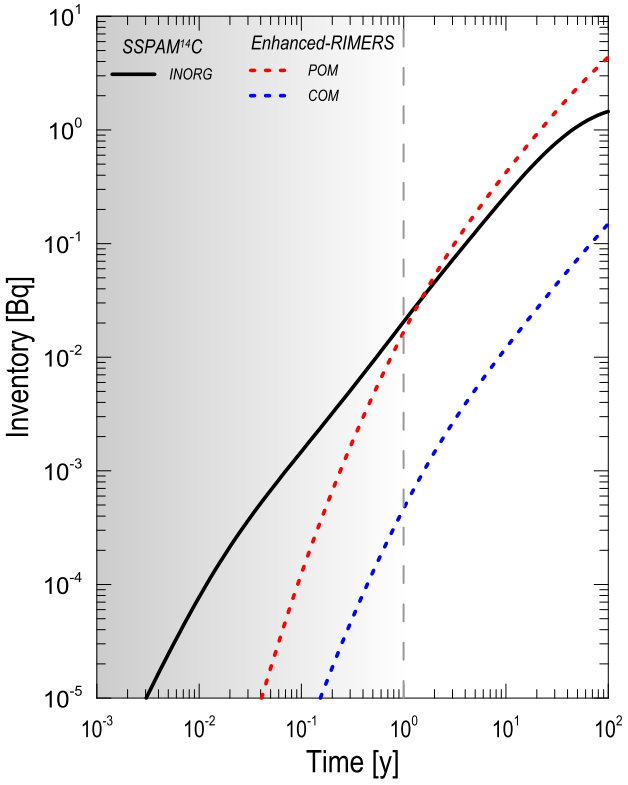

5 Review of experimental data from Imperial College

5.1 Background

In the 1990's, MAFF engaged Imperial College to study the assimilation of ^{14}C by three different crops, and the subsequent dynamics of the ^{14}C fixed within those crops. The primary objective of the study was to provide high quality time-dependent data on the assimilation and re-translocation of ^{14}C, supplied to crops as $^{14}CO_2$ gas, in order to verify the applicability of the crop component of MAFF's STAR C14 model (see Section 2.2.2 for an overview of the model)[13]. The experiments performed by Imperial College, and the results, are summarised in this section. A full description of the experiments is provided by Tucker (1998) and Tucker and Shaw (1997) and the following description is based on these documents.

5.2 Experimental setup

5.2.1 Crop production

In this experiment three crops were studied:

- Cabbage (Brassica oleracea)
- Broad beans (Vicia faba)
- Potatoes (Solanum tuberosum cv. Romano).

The application of the model, SSPAM^{14}C, in this current study is focussed upon the cabbage data from the Imperial College experiments (see Section 6), so the remainder of this section primarily focuses upon the setup, and results associated with this crop only. The reason for this is that the cabbage is the simplest crop system, with only AGP and BGP components involved. The general details about the experimental setup apply equally to all three crops; the more detailed aspects of the setup and results associated with the bean and potato crops are given in Appendix B.

The three crops were grown in the walled garden at Silwood Park (Berkshire, UK) and transported to a specially designed wind tunnel for experimentation, when required. For each of the three crops, one hundred 40 x 40 x 40 cm 'shrub tubs' were used, each one filled with peat-based compost. January King cabbages were sown at a rate of six seeds per tub on 14th July 1994. On germination the plants were thinned to four plants per pot. During periods of dry weather the pots were watered as required so that the soil did not completely dry out at any stage. In the few days prior to each experiment extra care was taken to ensure the plants did not suffer from water stress.

5.2.2 Canopy construction

The crop was exposed to $^{14}CO_2$ in a wind tunnel. This was to allow the exposure to take place under as close to realistic boundary layer conditions as possible, while providing adequate containment for the $^{14}CO_2$ (Figure 23). The wind tunnel had the capacity to accommodate thirty tubs. Twenty of these tubs constituted the 'fetch' of the canopy and facilitated the build up of the turbulent boundary layer. The remaining ten tubs provided the experimental material enabling a maximum of forty plants to be sampled for each exposure.

Before each exposure, thirty tubs were transported to the wind tunnel. The height of the crop was measured and adjusted so that the lip of the wind tunnel was level with the zero plane displacement of the crop when the pots were loaded. This was not possible when the plants became too large. The twenty pots which constituted the fetch were clearly labelled and re-used for each exposure. The ten experimental

[13] Prior to the experiments performed by Imperial College the parameterisation of STAR C14 was based upon literature reviews (Smith et al., 1994). As noted in Section 2.2.2, the parameterisation of the model was not altered in light of the results from these experiments (Watkins et al., 1998).

pots were labelled with identification numbers for each plant. The canopy was illuminated with a bank of six 450 W agricultural lights set to a sixteen hour photoperiod. Whenever possible, plants were transported 48 hrs before the start of the exposure to allow them to 'acclimatise' to the wind tunnel conditions.

Figure 23: Plan layout of the wind tunnel (from Tucker, 1998)

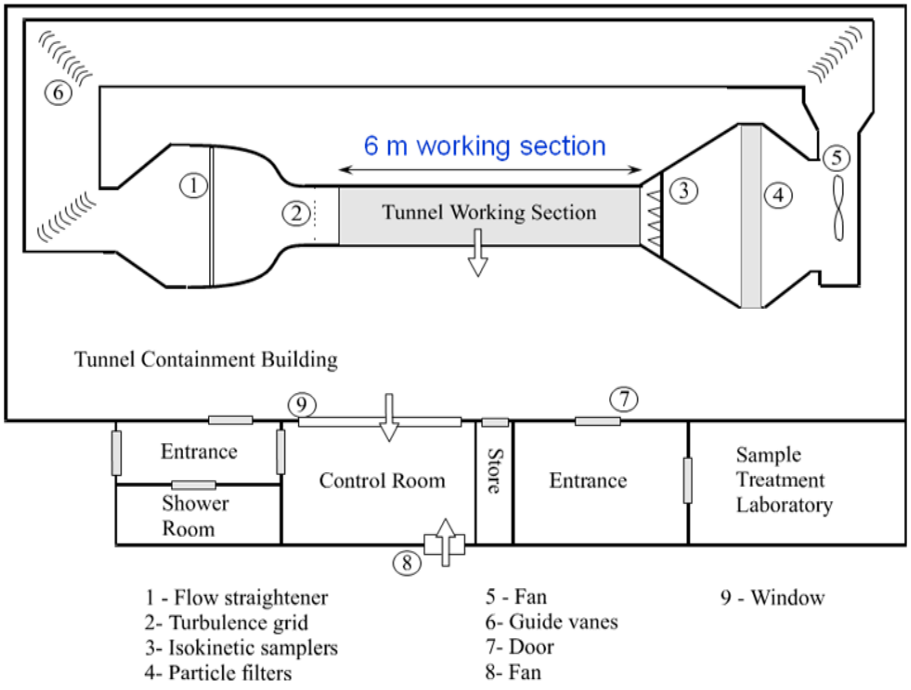

5.2.3 Gas injection

With the wind tunnel sealed and running at a wind speed of 1 m s^{-1}, $^{14}CO_2$ was injected from a cylinder at 10.30 am each time to minimise differences in uptake caused by diurnal rhythms of stomatal conductance. Immediately after injection a CO_2 purging system was activated and the exposure of the crop was allowed to continue for 10 hours before sampling the plants. This meant that the cabbages were exposed to exponentially declining $^{14}CO_2$ concentrations in the wind tunnel airstream, as shown in Figure 24. The integrated air concentrations of $^{14}CO_2$ during each crop exposure are shown in Table 21; the integration time is 600 minutes. The total (non-radioactive) CO_2 concentrations within the wind tunnel were measured during selected experiments using an infra-red gas analyser (IRGA): these data were subsequently used to calculate specific activities of ^{14}C:^{12}C during crop exposures to $^{14}CO_2$.

Table 21: Integrated ^{14}C air concentrations

Cabbage	C1	C2	C3	C4	C5
IAC (MBq m^{-3} min)	7.4	6.0	6.4	6.41	10.6

5.2.4 Exposure and sampling codes

The sampling schedules for the cabbage crop are given in Table 22. The exposure code consists of a letter and number. Here C is used to identify the crop (cabbage) and the number denotes whether it was the first exposure replicate, second exposure replicate etc.

Each harvest is identified by the exposure code and a harvest number e.g. C3H3 refers to the third harvest taken from the third cabbage exposure replicate.

Figure 24: ^{14}C air concentration above the cabbage crop during five experiments

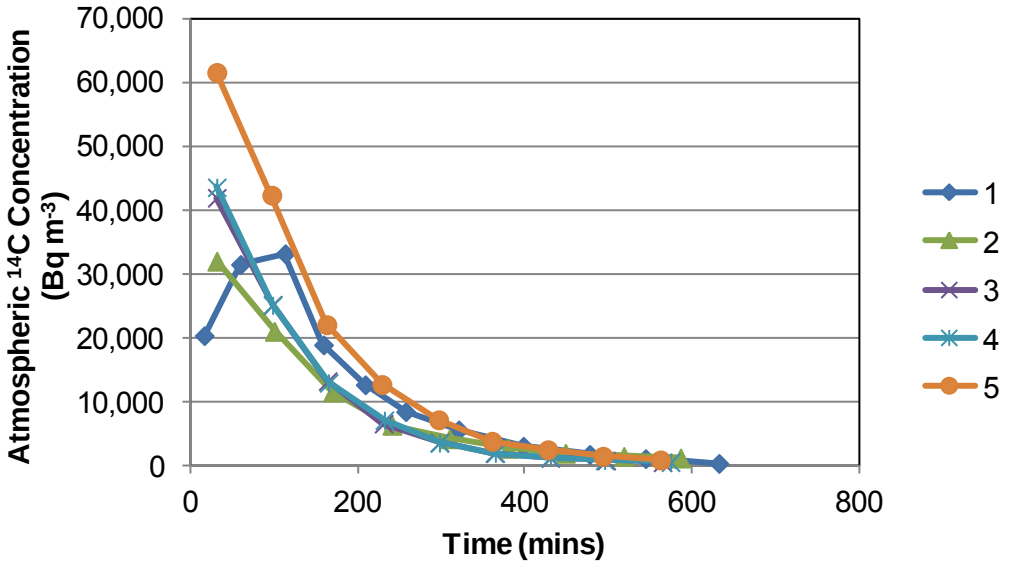

Note: The exposures were replicated when the plants were 33 days olds (1), 50 days old (2), 70 days old (3), 84 days old (4) and 114 days old (5).

Table 22: Cabbage sampling schedule (crop ages and times from exposure in days)

	Exposure Replicate									
	C1		C2		C3		C4		C5	
Harvest	Age	T	Age	T	Age	T	Age	T	Age	T
H1	33	0	50	0	70	0	84	0	114	0
H2	37	4	52	2	72	2	86	2	117	3
H3	41	8	58	8	76	6	90	6	119	5
H4	51	18	69	19	85	15	98	14	121	7
H5	75	42	96	46	98	28	112	28	125	11
H6	125	92	125	75	128	57	127	43	127	13

5.3 Experiment results

This section provides details of the experimental results for the cabbage crop.

5.3.1 Net assimilation rates

Table 23 shows two sets of estimates for net assimilation rates for $^{12}C + {}^{14}C$ expressed in g C kg wwt^{-1} d^{-1} for cabbages; these assimilation rates are presented here in the same units used in STAR C-14. The averaging time used in making these estimates was 24 hours, as assumed in STAR C14: the estimated C assimilation rates presented in the tables would be slightly greater if only the photoperiod were used as an averaging period. The results from IRGA measurements of stable carbon in the wind tunnel suggested that the stable CO_2 concentration of the wind tunnel atmosphere was higher than ambient. Therefore the average ^{14}C:^{12}C specific activity and assimilation rate were calculated using both the ambient ^{12}C

concentration (0.16 g C m^{-3}) and the measured ^{12}C concentration of 0.24 g C m^{-3}. These data show a greater rate of incorporation of ^{14}C in the cabbages exposed at an early stage of development than those exposed later. This can be explained by a greater photosynthetic rate per unit mass in younger plant tissues, probably due to a general reduction in photosynthetic activity of plant tissue with age as well as increased self-shading as the cabbage canopy grew denser towards the end of the experiment.

The experimental estimates of carbon assimilation rates are lower than, though similar to, the default value of 4 g C kg wwt^{-1} d^{-1} used by STAR C-14. However, given the relatively low light levels within the wind tunnel (equivalent to a cloudy day) the STAR C-14 default carbon assimilation rate would appear to be approximately correct, if slightly conservative.

Table 23: Comparison of cabbage experiments: C1 to C5

Cabbage Experiment	C1	C2	C3	C4	C5
Assimilation Rate (g C kg wwt^{-1} d^{-1}) (0.16 g C m^{-3})	1.64 ± 0.63	1.44 ± 0.68	0.82 ± 0.3	1.38 ± 1.01	0.82 ± 0.64
Assimilation Rate g C kg wwt^{-1} d^{-1} (0.24 g C m^{-3})	2.46 ± 0.95	2.16 ± 1.01	1.24 ± 0.45	2.07 ± 1.51	1.23 ± 0.96
Transfer Factor* at Harvest 5 ($x10^{-4}$)	1.91	2.13	3.88	4.35	8.75
CoV† Inventory Measurement (%)	31	127	87	62	85
Dilution Factor‡	0.0032	0.066	0.395	0.245	0.51
Significance	0.01	0.01	0.05	NS	NS

* Atmospheric ^{14}C to the edible crop (Bg kq^{-1} in leaves / Bq m^{-3} in air)
† Coefficient of variation
‡ Average leaf ^{14}C activity at final harvest divided by the initial leaf ^{14}C activity

5.3.2 Crop dry weight and activity concentration data

The dry weights and ^{14}C activity concentrations following exposure to $^{14}CO_2$ were measured in various plant components throughout the experiment. The results reported for cabbages in the leaves, stems and roots are given in Table 24, Table 25 and Table 26, respectively.

There is a high degree of variability in both the measured dry weights and ^{14}C activity concentrations of all plant components in the cabbage crop. As an example, the measured dry weight and ^{14}C activity from the third cabbage exposure, C3, are shown in Figure 25 and Figure 26, respectively.

Table 24: Dry weight and ^{14}C activity concentration results for cabbages - leaves

		Crop replicate				
	Harvest	**C1**	**C2**	**C3**	**C4**	**C5**
Dry weight (g) per sample	**H1**	0.4 ± 0.4	4.8 ± 1.9	9.6 ± 2.2	16.3 ± 3.9	16.5 ± 13.7
	H2	0.6 ± 0.5	3.7 ± 2.7	7.3 ± 3.9	11.8 ± 6.4	7 ± 3.4
	H3	2 ± 1.4	5.2 ± 2.3	8.9 ± 6.4	16.2 ± 8.7	6.4 ± 4.4
	H4	6.9 ± 2	10.1 ± 6	7.2 ± 5.9	11.6 ± 9.9	20.9 ± 11
	H5	18.8 ± 6	32 ± 17.6	17.3 ± 11.6	18.3 ± 7.8	26.2 ± 5.2
	H6	17.2 ± 10	20.7 ± 18.7	8.6 ± 6	18.7 ± 12.1	15.4 ± 17.7
^{14}C concentration (Bq g^{-1})	**H1**	1176.1 ± 212.6	276.4 ± 117.3	146.3 ± 55.4	306.5 ± 238.7	275.5 ± 170
	H2	601.5 ± 743.3	201.6 ± 122.6	64.4 ± 43.1	116.6 ± 79.9	126.4 ± 102.8
	H3	319.2 ± 69.5	126.6 ± 101.3	92.2 ± 56	112.9 ± 90.9	249.3 ± 364.5
	H4	101.4 ± 24.5	67.9 ± 46.7	90.7 ± 68.9	81.4 ± 54.9	209.2 ± 195.1
	H5	35.4 ± 13.1	19.4 ± 24.7	71.6 ± 20.6	70.1 ± 44.7	175.7 ± 133.2
	H6	3.7 ± 0.8	18.4 ± 13.8	57.8 ± 31.4	75.1 ± 52.4	142.9 ± 38.3

Table 25: Dry weight and ^{14}C activity concentration results for cabbages - stems

		Crop replicate				
	Harvest	**C1**	**C2**	**C3**	**C4**	**C5**
Dry weight (g) per sample	**H1**	0.1 ± 0.1	1.5 ± 0.6	6 ± 1.3	9.7 ± 1.9	11.1 ± 5
	H2	0.5 ± 0.3	1.2 ± 0.8	3.4 ± 1.6	8 ± 3.5	7.1 ± 4.4
	H3	0.5 ± 0.3	3.5 ± 0.6	4.8 ± 3.5	12.1 ± 5.1	6.3 ± 3
	H4	1.9 ± 0.6	5.9 ± 0.6	4.8 ± 3.4	8 ± 5.2	10.9 ± 4.8
	H5	8 ± 1.5	15.6 ± 6.3	8.6 ± 3.9	12.5 ± 3.2	12.4 ± 1
	H6	12.6 ± 6.8	15.6 ± 7.1	7.9 ± 5.5	14.4 ± 9.8	11.1 ± 10.5
^{14}C concentration (Bq g^{-1})	**H1**	689 ± 203.6	364.2 ± 165.4	169.1 ± 59.8	213.3 ± 116.2	76.1 ± 75.5
	H2	333.8 ± 64.8	229.2 ± 142.5	72.3 ± 53.9	142.2 ± 32.6	45.3 ± 25.2
	H3	253 ± 20.3	69.2 ± 35.6	111.9 ± 96.9	126.2 ± 80.2	111.2 ± 139.4
	H4	55.5 ± 19.2	62.6 ± 36.7	93.2 ± 86.8	60.1 ± 42.1	101.5 ± 101.9
	H5	16.4 ± 5.5	11.6 ± 10.5	81.4 ± 15.9	77 ± 37.5	103.3 ± 85.2
	H6	12.2 ± 3	27.7 ± 20.7	32.3 ± 15.9	73.1 ± 37.4	72.4 ± 15.8

Table 26: Dry weight and ^{14}C activity concentration results for cabbages - roots

		Crop replicate				
	Harvest	**C1**	**C2**	**C3**	**C4**	**C5**
Dry weight (g) per sample	**H1**	0.2 ± 0.1	0.6 ± 0.3	2 ± 0.2	3.2 ± 1	3.5 ± 1
	H2	0.2 ± 0.1	0.4 ± 0.4	1.3 ± 0.7	2.8 ± 2.6	1.5 ± 1.2
	H3	0.2 ± 0.2	1 ± 0.2	2 ± 0.9	3.2 ± 2.2	0.7 ± 0.5
	H4	1 ± 0.3	1.3 ± 0.5	1.4 ± 0.8	2.7 ± 2.2	4.4 ± 3.3
	H5	3.8 ± 1.5	5.2 ± 2.7	3.9 ± 2.6	3.9 ± 1.6	8.9 ± 3.4
	H6	1.9 ± 1.2	6.4 ± 5.5	2.1 ± 2.1	4 ± 2.3	1.8 ± 2
^{14}C concentration (Bq g^{-1})	**H1**	354.4 ± 96.1	270.1 ± 132.5	160 ± 61.1	244.6 ± 141.7	53 ± 52.4
	H2	376.3 ± 84	227 ± 126.1	61.8 ± 49	115.3 ± 55.7	33.5 ± 16.2
	H3	306.2 ± 15.1	48.7 ± 36.5	153.3 ± 139.7	124.4 ± 76.9	134.1 ± 199.7
	H4	82.6 ± 36.3	38.2 ± 33.7	109.1 ± 103	56.7 ± 42.2	90.1 ± 102.3
	H5	30.1 ± 10.9	14.8 ± 16.8	112.1 ± 31.8	90.2 ± 51.7	128.2 ± 93.8
	H6	23.8 ± 8.8	26.2 ± 26.4	62.4 ± 25.6	99.9 ± 68.7	93.7 ± 23

Figure 25: Measured dry weight (per sample) of cabbage in C3 exposure (g) of the plant components. (a) Leaves, (b) Stems and (c) Roots. The data points are the means, with the vertical lines representing one standard deviation.

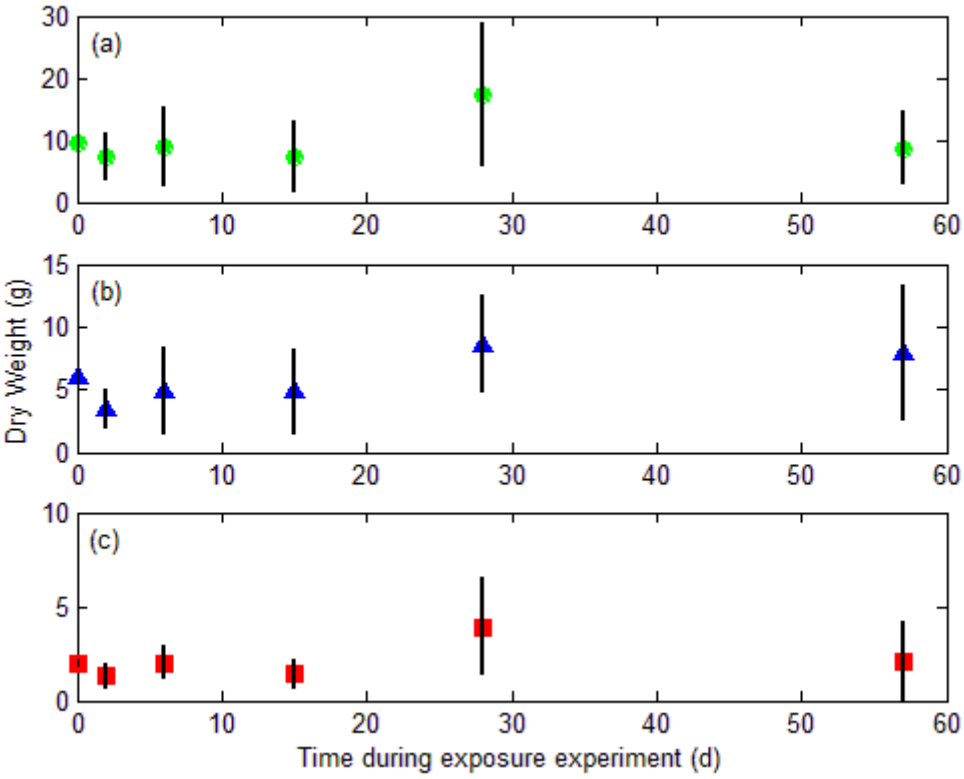

Figure 26: Measured ^{14}C activity concentration of cabbage in C3 exposure (Bq g^{-1}) of the plant components. (a) Leaves, (b) Stems and (c) Roots. The data points are the means, with the vertical lines representing one standard deviation.

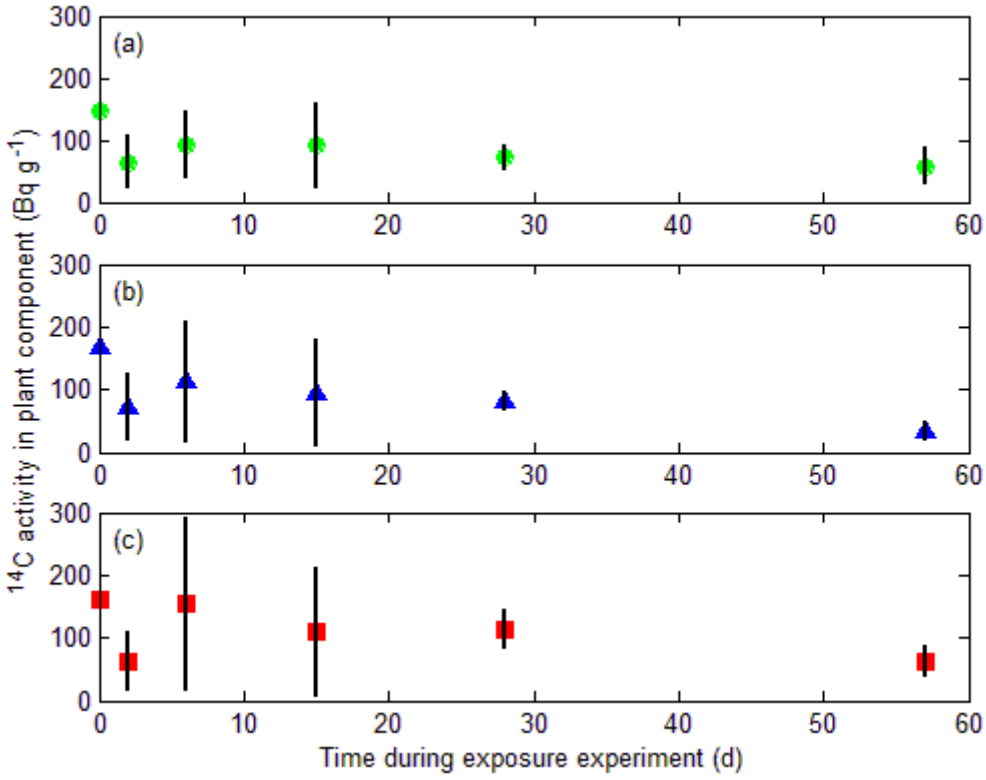

6 Application of SSPAM^{14}C to Imperial College experimental data

6.1 Interpretation of the model for experimental conditions

The paramterisation of the model for use with the experimental wind tunnel is described in Appendix A (there denoted as SSPAM^{14}C_C3). There are numerous differences relative to the prototype model described in Section 3, and these are described in the subsections below. There are four main reasons for these differences:

1. The source term in the wind tunnel experiment is based on a spike release of 14CO2 to the atmosphere above the plants which then circulates around the system. There is an active purging system which gradually removes CO2 over time. The standard interpretation of wind speed through the atmosphere compartments cannot therefore be applied and an alternative must be formulated.
2. Interpretation of crop specific data.
3. In the conceptual model discussed in Section 3, the aboveground atmosphere is split into two layers, with one sitting above the other, and the lower layer experiencing little or no turbulent mixing. For application to the Imperial College data, consideration is given to whether the non-turbulent air (DATM), could equally well be considered as a diffusive layer restricted to a small volume around the leaf surfaces (cf. Monteith & Unsworth, 2007, and their discussion of the microclimate of leaves). The connectivity of the model compartments remains unchanged, but the parameterisation of some of the exchanges may require updating.
4. Parameter optimisation: Thorne (2005) noted that many of the parameters in the Enhanced-RIMERS model were not well constrained. With an updated SSPAM14C model available, a process of optimisation against the experimental results was carried out for some of the less well characterised transfers.

As noted in the preceding section, the application of SSPAM^{14}C to results of the Imperial College experiments focuses on the cabbage data. The details of the Imperial College cabbage experiment are described in Section 5, with the other crops described in Appendix B.

6.2 Interpretation of the source term

The source terms can be taken from the Tucker (1998) study, given as integrated air concentrations (IAC, see Table 21). As these concentrations vary between crops, for the model application, separate runs would be required for each crop, and for each replicate experiment. Thus, in this study there are five cabbage runs that need to be considered separately.

In the application of the model to these experiments, the IAC's have been treated as an impulse, or initial inventory, to the turbulent atmosphere (TATM) compartment. This means that the values given in Table 21 (in MBq m^{-3} min) need to be converted to the total amount of activity in the volume of the test chamber. Tucker and Shaw (1994) report that the volume of the recirculating wind tunnel is V_{TATM} = 55 m^3.

However, unlike the situation in a free field environment it is not the wind speed that is responsible for the depletion of the atmosphere, since there is recirculation of the TATM layer. Instead there is an active purging system. Tucker and Shaw (1997) note that

> *"The tunnel was started running at a wind speed of 1 ms^{-1}. The gas was injected at 10.30am for each experiment to minimise differences in uptake caused by diurnal rhythms of stomatal conductance.* ***Immediately after injection a CO_2 purging system was activated and the exposure of the crop was allowed to continue for 10 hours before sampling the plants****. Therefore the crops were exposed to exponentially declining $^{14}CO_2$ concentrations in the wind tunnel airstream."*

As a result of the active purging of $^{14}CO_2$ from the wind tunnel atmosphere an exponential loss curve can be fitted to the data in Figure 24 for each of the exposures and a purging parameter obtained: λ_{purge} (y^{-1}). The results for the fitting procedure are given in Appendix C.

The source term is therefore modelled as in initial injection followed by exponential loss. The procedure to determine the initial ^{14}C activity concentration in the TATM layer is as follows. The decline of the concentration (Bq m^{-3}) is given by

$$C(t) = C_0 \cdot e^{-\lambda_{purge} \cdot t} \quad \text{(Equation 44)}$$

The IAC is this quantity integrated over 600 minutes so that the initial inventory injected into the wind tunnel at time $t = 0$ is

$$N_0 = \frac{\lambda_{purge} \cdot IAC \cdot V}{1 - e^{-600\lambda_{purge}}} \quad \text{(Equation 45)}$$

In the third cabbage experiment the initial inventory in the TATM compartment is therefore N_0 = 3.09E+6 Bq, with λ_{purge} = 4600 y^{-1} (Appendix C). Using these values, the half-life of ^{14}C in the TATM is approximately 79 min (~ 5000 seconds). With a wind speed of 1m s^{-1} over the same 6 m fetch, the half-life would be only 4.3 s, falling to 1.3 s for a wind speed of 5 m s^{-1}. However these values are misleading since they do not reflect the experimental conditions, being appropriate to transient 'puff' of $^{14}CO_2$ such as would be expected in the case of a spike of activity released to the atmosphere from a NPP as envisaged in the construction of the model. In order to represent the wind tunnel scenario as an 'exponentially decaying cloud' of $^{14}CO_2$ a purging loss rate is required which matches the experimental conditions.

Turnover in the wind tunnel is therefore slower by a factor of around 1000 as compared with a transient release case. However, the loss is given by Equation 10, so for a larger field (e.g. 10^4 m^2) the half times are 7.91E-03 y for a wind speed of 1 m s^{-1} wind speed and 1.58E-03 y for a wind speed of 5 ms^{-1}. Retention is therefore longer in the experiment as compare to "real world" conditions, by approximately a factor of ten in the case of a 5 m s^{-1} wind speed. Only if the field were 10^8 m^2, or larger, would the loss rates be similar for differing wind speeds.

Each of the experimental crop exposures was carried out using different sets of plants of different ages. Coupled to the fact of significantly different exposures via a range of inputs it is not possible to use the combined dataset with a single model of the release and subsequent uptake. Each experiment must be simulated using the unique source term and conditions representing the crop must then be tailored to fit. For developmental purposes, therefore, the third cabbage dataset (C3) has been taken as the basis for modelling since it has the best fit to the exponential form (see Appendix C).

6.3 Identification and interactions of atmosphere compartments

The conceptualisation of the atmosphere compartments in Section 0 is not appropriate for the experimental set up described here. The interpretation required is that turbulent mixing occurs in the bulk of the fetch, within the canopy and that the diffusive layer is limited to a small volume of still air around the foliage. The thickness of this boundary layer is typically around 1 mm (cf. Monteith & Unsworth, 2007). Modified parameter values are required, so that the parameterisation of the volume of the DATM compartment (m^3) now uses the leaf area index (LAI):

$$V_{DATM} = 2 \cdot LAI \cdot l_b \cdot A_f \quad \text{(Equation 46)}$$

Here $l_b \sim 10^{-3}$ m is the boundary layer thickness and the LAI is obtained from the data on LAI in the EMRAS potato report (IAEA, 2008)[14], which also used data from the Tucker and Shaw database. As a first approximation the mean value of LAI measured by Tucker and Shaw for all crop types over the growth period was used, 2.25 m^2 m^{-2} (see Figure 27).

[14] The data are presented in this report are not readily found in Tucker and Shaw (1997).

The volume of TATM is reduced by the confines of the experimental wind tunnel and the height of the TATM is now 1.5 m, with an overall volume of 55 m^3.

As the DATM layer is restricted to a small volume around the leaves, the exchanges in the original model between it and the soil are replaced by the equivalent to the TATM layer. Therefore the model now uses the rate parameter for transfer to SATM to represent transfers from the TATM:

$$\lambda_{\substack{SATM \\ DATM}} = \lambda_{\substack{DATM \\ SATM}} = 0$$

$$\lambda_{\substack{SATM \\ TATM}} = \kappa_{\substack{SATM \\ DATM}} \qquad \text{(Equation 47)}$$

$$\lambda_{\substack{TATM \\ SATM}} = (\varepsilon - \theta) \cdot f_{SATM} \cdot \frac{l}{l_{TATM}} \cdot \kappa_{\substack{SATM \\ DATM}}$$

However, the nature and magnitude of the fluxes as represented in Equations 6 and 36 are open to question. While there will be outgassing from the soil to the ambient atmosphere, the assumption of a rapid equilibrium in Enhanced RIMERS is thought to be unlikely: Sheppard et al. (2006b) suggest a volatilisation rate of 0.04 day^{-1} (14.6 y^{-1}) and an argument based on measurements of CO_2 fluxes from soil columns (Atkinson et al., 2011) makes the value potentially much higher, of the order of 0.5 $hour^{-1}$ or 4.4 10^3 y^{-1}. The return would be expected to be zero[15] though there might be some pumping due to pressure fluctuations. The options here are taken to be either to set the transfer between TATM and SATM to be zero[16], or to use Equation 47.

6.4 Derivation of crop specific parameters

6.4.1 Growth curves

The Tucker and Shaw data summarised in Section 5 provide a wealth of valuable information. The sets of observed growth data for each crop can be combined to give growth curves for the crop and, these can then be fitted to the logistic equation for manipulation into data suitable for the model.

Since the experimental results give the dry mass of plant tissue in grams as a function of the time (days) since the start of growth the fitted curves for the evolution of the biomass of both AGP and BGP ($m_p(t)$, g dw) take the form (albeit with different coefficients):

$$m_p(t) = \frac{a}{1 + b \cdot e^{-c \cdot (t - t0)}} = \frac{a}{1 + b \cdot d \cdot e^{-c \cdot t}} \qquad \text{(Equation 48)}$$

There is an offset of t_0 days before the start of the exposure, so that d (= e^{ct0}) is a constant. The other parameters of the logistic function (a, b and c) have been fitted to the crop data using the Solver function in Excel. The results are shown in Figure 28, for AGP and BGP compartments; the fitted parameters are given in Table 27.

[15] This assumption is based on expert opinion that there is no transfer of atmospheric carbon with the soil atmosphere (except via the plant).

[16] This transfer can be set to be zero, or non-zero, within the software implementation of the mathematical model.

Figure 27: Leaf area index (LAI) as a function of canopy age for beans, potatoes and cabbage in the Tucker and Shaw (1997) database (from IAEA, 2008).

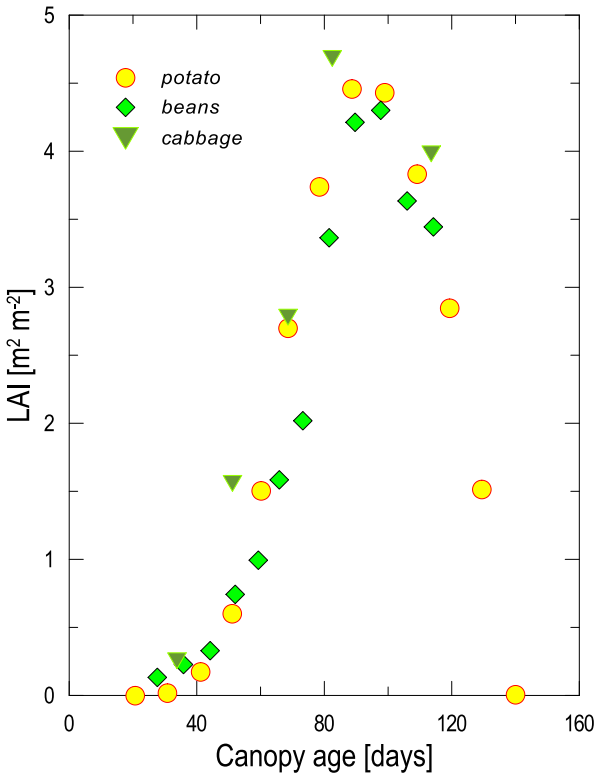

Table 27: Data used for plant dry mass as a function of time fitted by logistic equations for above and below ground plant (AGP, BGP)

Plant component	AGP	BGP
$m_p(t) = \frac{a}{1 + b \cdot d \cdot e^{-c \cdot t}}$ calculated using	a = 29.57 [g dw] b = 262.22 [-] c = 0.08 [day^{-1}]	a = 4.36 [g dw] b = 293.31 [-] c = 0.08 [day^{-1}]
t_0 = 70 days	d = 0.003157 [-]	

The advantage of using a growth curve is that it can be differentiated to give the growth rate of the various plant components, and these in turn can be linked to the photosynthesis and respiration rates. Furthermore, the translocation factor can be estimated by assuming that the growth rate of the BGP is due to fixation of carbon through the AGP. This is the basis for the parameterisation of the plant sub-model carried out in the following section.

Figure 28: Plant dry mass as a function of time fitted by logistic equations for above and below ground plant (AGP, BGP)

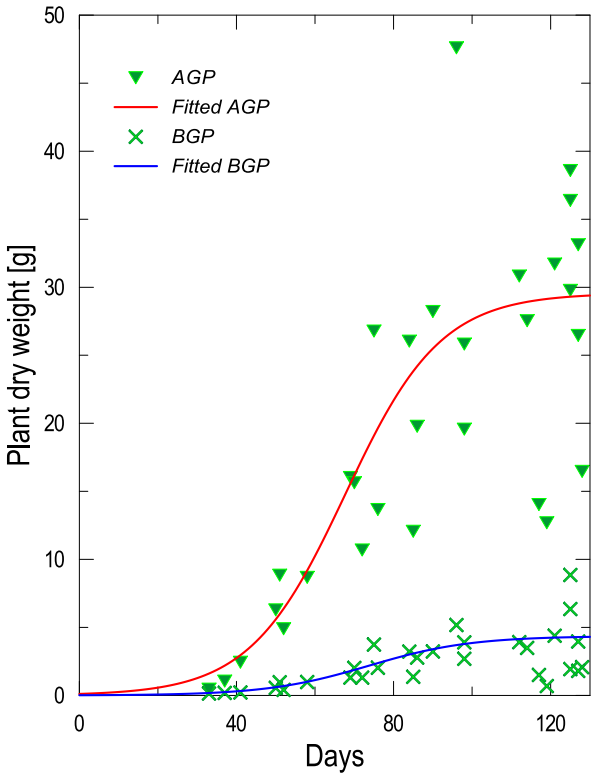

6.4.2 Translocation, photosynthesis and respiration

Using the logistic curves for the two plant components, an estimate of the translocation rate between AGP and BGP can be made assuming that all the growth of the roots comes from carbon fixation by the AGP. The only non-zero element of the translocation matrix is then

$$\kappa_{\substack{AGP \\ BGP}} = n_{spy} \cdot \frac{1}{m_{AGP}(t)} \cdot \frac{d\, m_{BGP}(t)}{dt} \qquad \text{(Equation 49)}$$

Taking the average over the 70 days after exposure, this gives $\kappa_{\substack{AGP \\ BGP}} = 0.65\ y^{-1}$.

As reported in Section 5.3.1 the net crop assimilation rates are reported from the experiment. These could be used to derive the photosynthesis and respiration rates used in the model. However, the balance between the two processes is required. Schnoor (1996) gives the global balance for a simple model of global carbon fluxes as 110 GT y^{-1} from atmosphere to land biota and 50 GT y^{-1} in the opposite direction. This ratio of 11:5 is used to determine the rates[17]. To determine the photosynthesis and respiration rates there are two alternatives, either the assimilation rates quoted by Shaw and Tucker (Table 23) can be used or the values from the growth curves.

In the first approach the quoted assimilation rates are converted into photosynthesis rates, as shown in Table 28. The values quoted assume different atmospheric carbon concentrations – one for ambient conditions and a higher rate for the measured CO_2 concentration in the wind tunnel itself. This higher rate

[17] It is assumed that this does not include soil microbial respiration, and therefore does not overestimate plant respiration.

is used here, as it better reflects the experimental conditions. The C3 release is used as the basis for the modelling, as described previously.

Table 28: Plant parameters for the SSPAM^{14}C model derived for the cabbage experimental data from the assimilation rates in Table 20 using the balance for terrestrial biota cited by Schnoor (2008). N.B. Atmospheric C concentration was found to be higher in the Tucker and Shaw (1997) wind tunnel experiment than the ambient concentration.

		Experimental replicate				
Data set	**Parameter**	**C1**	**C2**	**C3**	**C4**	**C5**
Ambient CO_2	Atmospheric carbon concentration (g C m^{-3})	0.16				
	$\dot{m}_{phot}$ (kg C m^{-2} y^{-1})	4.56E-1	2.32E-1	1.67E-1	7.00E-2	1.05E-1
	$\dot{m}_{plantResp}$ (kg C m^{-2} y^{-1})	2.07E-1	1.05E-1	7.61E-2	3.18E-2	4.76E-2
Experimental CO_2	Atmospheric carbon concentration (g C m^{-3})	2.40E-1				
	$\dot{m}_{phot}$ (kg C m^{-2} y^{-1})	6.83E-1	3.47E-1	**2.53E-1**	1.05E-1	1.57E-1
	$\dot{m}_{plantResp}$ (kg C m^{-2} y^{-1})	3.11E-1	1.58E-1	**1.15E-1**	4.78E-2	7.14E-2
(Independent)	m_{SB} (kg dw m^{-2})	2.41	4.16	**3.28**	5.47	5.25
	f_{AGP} (-)	6.59E-1	6.39E-1	**6.23E-1**	5.89E-1	6.10E-1
	f_{BGP} (-)	3.34E-1	3.54E-1	**3.71E-1**	4.05E-1	3.84E-1

The second alternative uses the details from the fitted growth curves. From the Schnoor (2008) partitioning the total net assimilation rate (kg C d^{-1}) is:

$$\begin{aligned} a_{net} &= \frac{d\,m_{AGP}}{dt} + \frac{d\,m_{BGP}}{dt} \\ &= a_{AGP} + r_{AGP} + a_{BGP} + r_{BGP} \\ &= \left(\frac{11}{6} - \frac{5}{6}\right)\frac{d\,m_{AGP}}{dt} + \left(\frac{11}{6} - \frac{5}{6}\right)\frac{d\,m_{BGP}}{dt} \end{aligned} \qquad \text{(Equation 50)}$$

The assimilation rate for total plant and total respiration (both kg C d^{-1}) are then given by:

$$\begin{aligned} a_{assim} &= \frac{11}{6}\cdot\frac{d\,m_{AGP}}{dt} + \frac{11}{6}\cdot\frac{d\,m_{BGP}}{dt} \\ a_{resp} &= \frac{5}{6}\cdot\frac{d\,m_{AGP}}{dt} + \frac{5}{6}\cdot\frac{d\,m_{BGP}}{dt} \end{aligned} \qquad \text{(Equation 51)}$$

The photosynthesis and respiration rates (kg m^{-2} y^{-1}) are then:

$$\dot{m}_{phot} = 1.95 \qquad \dot{m}_{plantResp} = 0.89 \qquad \text{(Equation 52)}$$

These values are somewhat higher than those evaluated in Table 28. In the following section the best estimate dataset for the model is optimised for experiment C3.

6.5 Model application results

Recall that the measured variables from the experiment are air concentration activity (C_{DATM}) and activity concentrations in the above ground and below ground plant (C_{AGP} and C_{BGP} respectively). There was no "FRUIT" in this experiment; had the bean data been used then the beans and pods would have comprised the fruit component of the plant.

6.5.1 Application to C3 experiment and parameter optimisation

Figure 29 shows the results of the initial application of SSPAM^{14}C to the Imperial College C3 experimental data. Clearly the configuration in the prototype model does not fit the experimental data very well.

Figure 29: Initial application of SSPAM^{14}C to the Imperial College C3 experiment..

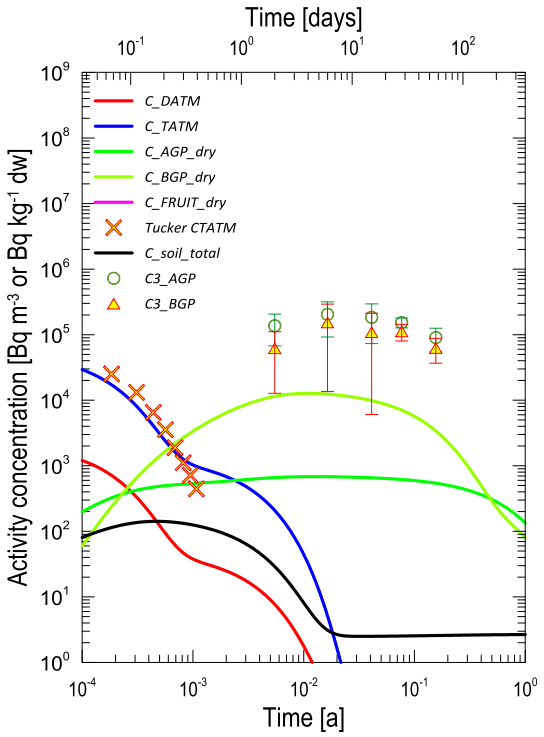

Following on from this application of the model to the experiment with minimal parameter optimisation, a series of three variant calculations were performed. The details of the parameterisation of these three variant cases, along with that of the initial model application, are set out in Table 29. The purpose of each of these variant calculations was to optimise the fit of the model to the C3 experimental data. Plots for each of these model variants are shown in Figure 30, with the results discussed below.

Exchange rate between diffusive and turbulent mixing regions of the atmosphere: During the sensitivity analysis the rate of transfer from diffusive layer to turbulent layer was found to be a key parameter. In the formulation presented in Section 3.3.1, the TATM→DATM and DATM→TATM fluxes are assumed to be in equilibrium and the rate is determined by the model parameter $\kappa_{\substack{DATM \\ TATM}}$ y^{-1}.

Increasing the transfer rate between these compartments by a factor of 1000 improves the fit of the model to the measured ^{14}C concentrations in the AGP compartment. Beyond a value of around 10^6 y^{-1} effects on the atmospheric activity concentration were seen.

Exchange rate between the soil and turbulent atmosphere compartments: It was found that decreasing the value of the loss rate from soil atmosphere (SATM) to the turbulent atmosphere (TATM) to the value recommended by Sheppard et al. (2006b) (see Section 6.3) further optimised the behaviour of the AGP activity concentration to the state shown in Figure 30a. Nevertheless there remains a significant difference between the measured and predicted above ground plant concentrations.

Revision of assimilation rates: A revision of the assimilation rates, i.e. a change in $\dot{m}_{phot}$ and $\dot{m}_{plantResp}$, as described in Section 6.4.2 led to a further improvement in the fit of the model to the experimental data since the overall net flux of carbon to the plants is increased (Figure 30b). However, it is the revision to the transfers through the diffusive layer that are the key to achieving reasonable agreement with the above ground crop activity concentration.

Looking at how the crop is modelled, the sole source of carbon for the AGP is the diffusive layer and both photosynthesis and respiration are required. The inflow of ^{14}C from DATM is then the sum of these processes since before the respired carbon can be returned to the atmosphere (DATM) it must first be obtained from the atmosphere.

$$\lambda_{\substack{DATM \\ AGP}} = (1 - f_{ru}) \cdot \frac{(\dot{m}_{phot} + \dot{m}_{plantResp}) \cdot A_f}{M_{DATM}} \qquad \text{(Equation 53)}$$

Of course, the DATM layer is thin and must import the carbon from the external TATM, so that:

$$\lambda_{\substack{TATM \\ DATM}} = \frac{(\dot{m}_{phot} + \dot{m}_{plantResp}) \cdot A_f}{M_{TATM}} \qquad \text{(Equation 54)}$$

For mass balance the return to DATM from AGP by respiration returns to TATM:

$$\lambda_{\substack{DATM \\ TATM}} = \frac{\dot{m}_{plantResp} \cdot A_f}{M_{TATM}} \qquad \text{(Equation 55)}$$

These modifications require a change to the transfer from soil atmosphere to TATM:

$$\lambda_{\substack{SATM \\ TATM}} = f_{SATM} \cdot \frac{(\varepsilon - \theta) \cdot l}{l_{TATM}} \cdot \kappa_{\substack{SATM \\ DATM}} \qquad \text{(Equation 56)}$$

This defines the preferred option – preferred in that it gives the closest fit to the AGP concentration. However, even with these modifications the modelled BGP concentration does not agree with the measured values.

Table 29: Variants for the model used to simulate the Cabbage 3 exposure

Parameter	units	First translation (Figure 29)	Optimised (Figure 30a)	Revised accumulation, optimised – preferred option (Figure 30b)	Revised accumulation, optimised, pumped TATM → SATM (Figure 30c)
$\kappa_{\substack{DATM \\ TATM}}$	y^{-1}	1000	10^6	10^6	10^6
$\lambda_{\substack{DATM \\ AGP}}$	y^{-1}	$(1-f_{ru})\frac{\dot{m}_{phot}A_f}{M_{DATM}}$	$(1-f_{ru})\frac{\dot{m}_{phot}A_f}{M_{DATM}}$	$(1-f_{ru})\frac{(\dot{m}_{phot}+\dot{m}_{resp})A_f}{M_{DATM}}$	$(1-f_{ru})\frac{(\dot{m}_{phot}+\dot{m}_{resp})A_f}{M_{DATM}}$
$\lambda_{\substack{DATM \\ TATM}}$	y^{-1}	$\kappa_{\substack{DATM \\ TATM}}$	$\kappa_{\substack{DATM \\ TATM}}$	$\frac{\dot{m}_{resp}A_f}{M_{DATM}}$	$\frac{\dot{m}_{resp}A_f}{M_{DATM}}$
$\lambda_{\substack{TATM \\ DATM}}$	y^{-1}	$f_{DATM}\frac{l_{DATM}}{l_{TATM}}\kappa_{\substack{DATM \\ TATM}}$	$f_{DATM}\frac{l_{DATM}}{l_{TATM}}\kappa_{\substack{DATM \\ TATM}}$	$\frac{(\dot{m}_{phot}+\dot{m}_{resp})A_f}{M_{TATM}}$	$\frac{(\dot{m}_{phot}+\dot{m}_{resp})A_f}{M_{TATM}}$
$\dot{m}_{phot}$	$kg\ m^{-2}\ y^{-1}$	0.253	0.253	1.95	1.95
$\dot{m}_{plantResp}$	$kg\ m^{-2}\ y^{-1}$	0.115	0.115	0.89	0.89
$\kappa_{\substack{SATM \\ xATM}}$	y^{-1}	1000	14.6	14.6	14.6
$\kappa_{\substack{SATM \\ SOL}}$	y^{-1}	10000	1000	1000	1000
$\lambda_{\substack{SATM \\ TATM}}$	y^{-1}	$\kappa_{\substack{SATM \\ DATM}}$	$\kappa_{\substack{SATM \\ DATM}}$	$f_{SATM}\frac{(\varepsilon-\theta)l}{l_{TATM}}\kappa_{\substack{SATM \\ DATM}}$	$\kappa_{\substack{SATM \\ DATM}}+\kappa_{pump}$

Figure 30: Optimising the SSPAM^{14}C model to the Imperial College C3 experiment. Here a series of parameter and process modifications are used to improve the fit of the model to the C3 experimental results. The details of these variant model parameterisations are set out in Table 29.

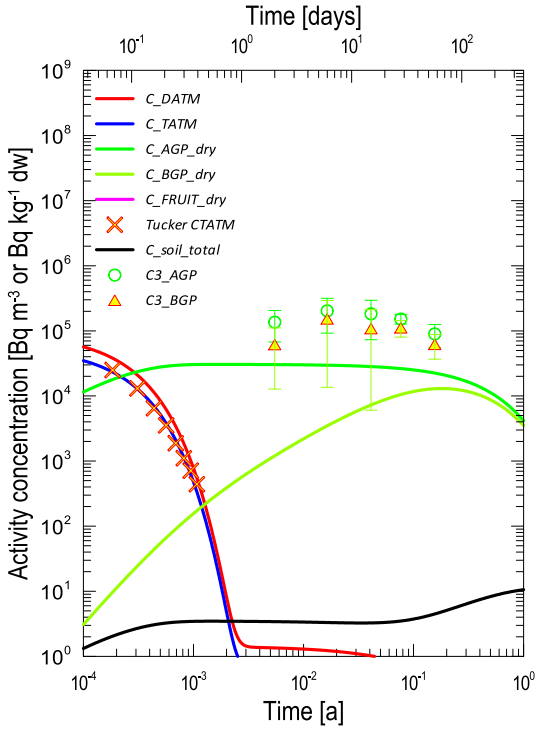

(a) Optimised

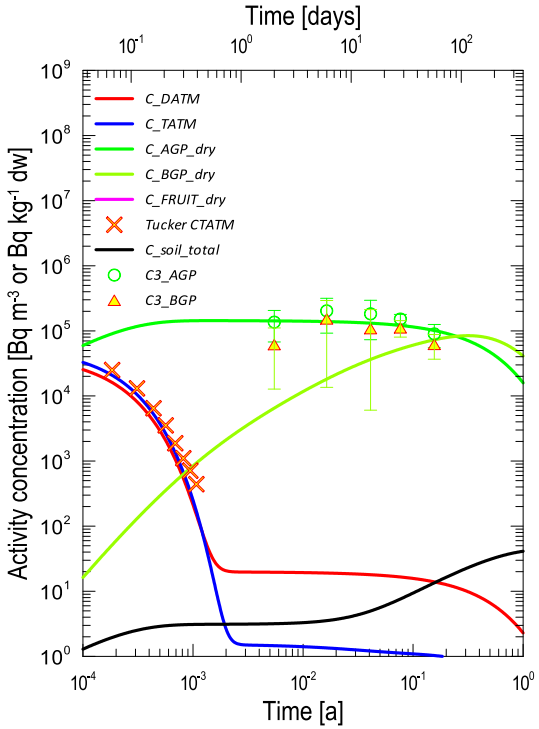

(b) Revised accumulation, optimised – "preferred option"

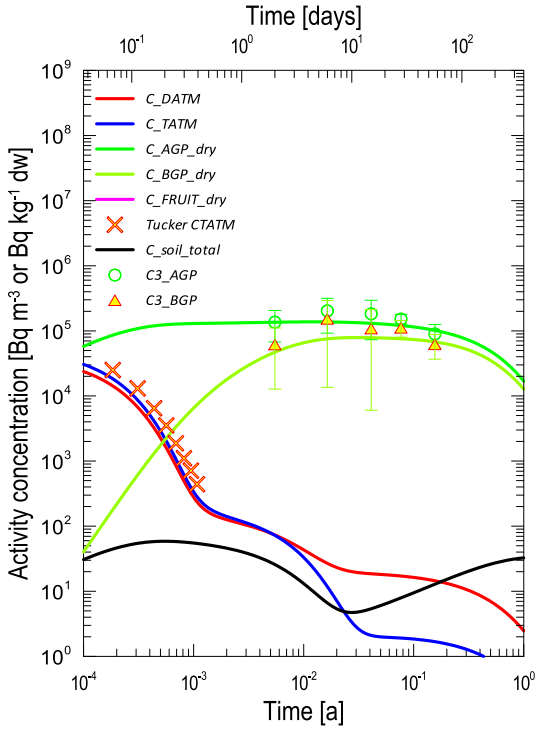

(c) Optimised, revised assimilation and atmospheric pumping

Revision of assimilation rates, with forced transfer of gas between TATM and SATM: The only way to get activity into the plant without destroying the balance of the model is for significant quantities of ^{14}C to enter the soil atmosphere. The addition of an atmospheric pumping term of 0.1 day^{-1} increases soil ^{14}C concentration, and thus the AGP and BGP concentrations – via root uptake – to levels closer to those seen in the experimental data (Figure 30c). It is not suggested that this mechanism is real but is included as the only method by which the model can reproduce the measured atmospheric, AGP and BGP concentrations from the C3 experiment.

It may be noticed that the TATM concentration in the preferred option is not as well matched to the experimental results as the initial model optimisation (Figure 30a). This is because of the greater extraction from TATM in the preferred model. It is plausible that the results stand because the TATM concentration is based on the experiment results with a fitted decay term. The calculated TATM concentration is lower than measured in the preferred option by a small amount. It is conceivable that there is some variation within the wind tunnel, e.g. small difference between what the plants see and wherever the measurement is taken.

There is a reasonable fit for the three measured components of the model system (atmosphere, above and below ground plants). The plots have shown total soil inventory since there are no measurements of soil content

The optimisation process has been useful. The assimilation model is now less dependent on *poorly constrained* rate coefficients than is the case in the Enhanced RIMERS model of Thorne (2005). The rates are now modelled in terms of measured parameters in the experimental dataset.

There is little that can be said about the soil compartments of the model and the way that they behave in the real systems. Whilst there is a recognised need to improve the understanding of processes in the soil, this is not possible with the experimental datasets used in this study.

6.5.2 Application of optimised model to other cabbage experiments

In the previous sub-section SSPAM^{14}C was optimised to fit the C3 experimental data, with the optimisation of certain atmospheric transfers and the assimilation rates being determined as the preferred model configuration (Figure 30b).

This version of SSPAM^{14}C was then applied to the other four cabbage replicate experiments, using the associated source terms, as derived in Appendix C. The results of this are shown in Figure 31.

Results for AGP are reasonable, with the exception of C1 and C2 for which there is a clear decreasing time-dependence. The reason for this is the time dependence of the uptake, as can be seen in the growth curves for the five cabbage experiments (Figure 32). Exposures C1 and C2 were sampled throughout the range from 40 to 130 days. C3, C4 and C5 were sampled from 70 to 130 days.

It is therefore hypothesised that there is a crucial, rapid, growth phase (Figure 32) in the cabbages between 40 and 70 days, for which the processes are not accounted for appropriately within SSPAM^{14}C[18]. During this period there is a higher uptake of ^{14}C (Figure 31a,b). This might be expected. As the model has been initially developed with application to long-term assessments and is here been applied to short-term data, there are potentially processes that are not represented. If the model were reconfigured to include more short-term processes, such as variable plant mass and time dependent uptake and respiration rates rather than the average values employed currently, the model performance with short-term data might be improved. However, this would in itself have implications for the computation of potential impacts associated long-term assessments.

[18] The parameterisation of plant assimilation was based upon the experimental wind tunnel data, rather than the model described in Section 6.4.2.

Also apparent in the plots for all the experiments is the close equilibrium between the AGP and BGP components, such that $C_{BGP} = a \cdot C_{AGP}$, where a is a constant, could feasibly replace the dynamic relationship modelled here.

Figure 31: Application of the SSPAM^{14}C model, as optimised to fit the Imperial College C3 experiment, to the other four cabbage experiments.

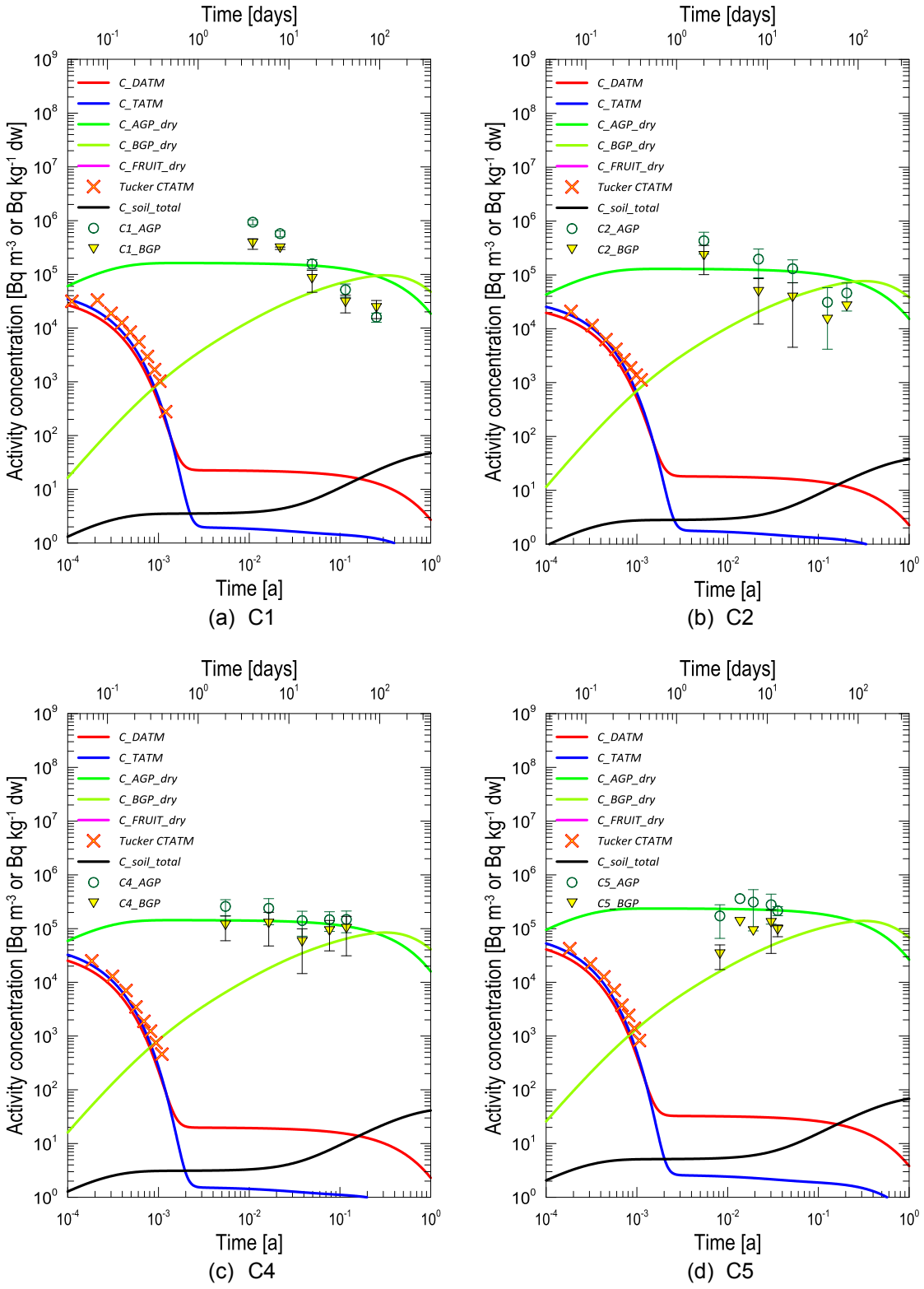

Figure 32: Growth curves from the five cabbage experiments

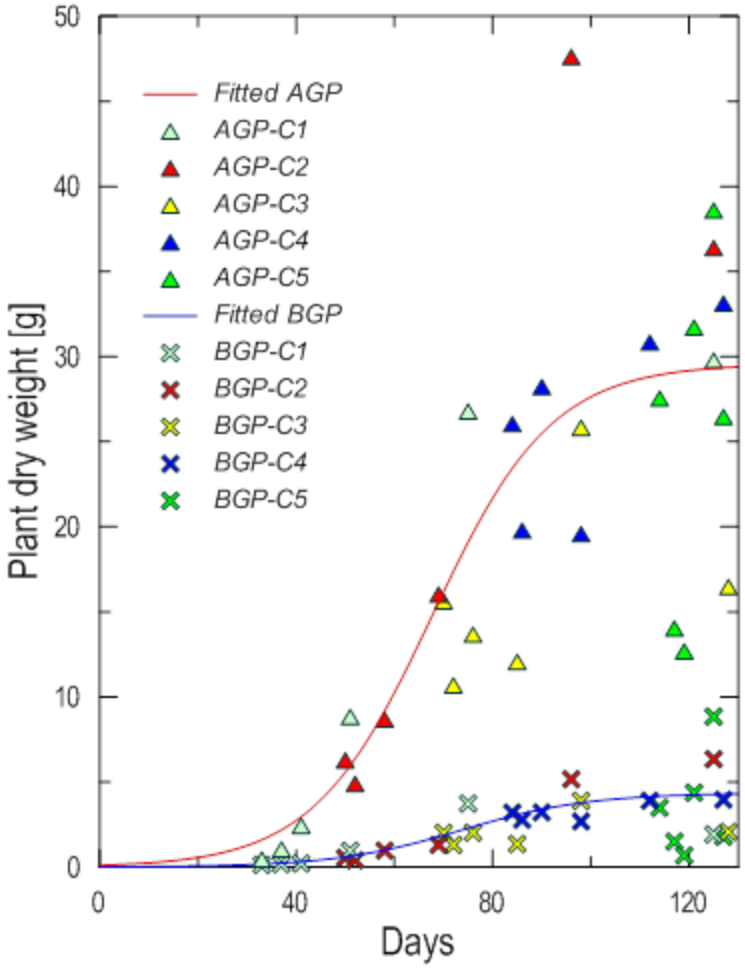

7 Conclusions and discussion

7.1 Model development

One of the aims of this project was to develop a prototype model for the behaviour of ^{14}C in a soil-plant-atmosphere system. This has been achieved via a review of existing ^{14}C soil-plant-atmosphere models and the identification of the key model compartments and interactions.

The division of the atmosphere into turbulent and diffusive layers is a conceptual model assumption common to many of the models developed in the UK (Thorne, 2005; Limer et al., 2011a,b; LLWR, 2012). The division of the plant into multiple compartments, with a separate compartment for edible plant tissues, is something that SSPAM^{14}C shares in common with models developed in Asia, and also PRISM (see Sections 2.2.3, 2.6 and 0). The most detailed aspect of SSPAM^{14}C is the soil sub-model, which draws much of its design from that of Enhanced RIMERS (Section 2.9) and the RothC model (Coleman and Jenkinson, 2005).

The initial parameterisation of SSPAM^{14}C is based upon literature recommended values for transfers.

7.2 Application to experimental data

In this study, SSPAM^{14}C has been applied to the cabbage data from the Imperial College wind tunnel experiments. An alternative conceptual and mathematical model for the atmosphere sub-model has been developed, which together with an iterative process of parameter optimisation of particular atmosphere and plant sub-model processes lead to an improved fit of the model to the experimental data. For this application, the model has been denoted SSPAM^{14}C_C3 (see Appendix A for the parameter values).

In particular, the optimisation of certain parameters within realistic constraints, lead to improved agreement between the model and the measured ^{14}C concentrations in the above-ground plant and the atmosphere. The revised parameter values were based on evidence in the literature and, where appropriate, translocation factors and the assimilation rates based on plant growth curves fitted to the experimental data. Perhaps unsurprisingly, it was the modification of the translocation and assimilation factors using the experimental data which most improved the model fit. The application of SSPAM^{14}C to the full set of cabbage experiments highlighted the need for the model to be reconfigured to account for dynamic plant masses should it be applied to assess the implications of short-term releases in the future (either operational or accidental). However, such a model development would not be required in instances where a constant plant biomass was an appropriate assumption (e.g. pasture).

The inability of the model to satisfactorily address the activity concentration in the below ground crop suggests some failing in the theoretical understanding of the system's behaviour.

It should be noted that the data used did not contain any measured soil ^{14}C concentrations, so it has not been possible to assess the suitability of the model for the soil sub-system or its parameterisation. The existence of a data set which comprised measured soil, plant and atmosphere ^{14}C concentrations would be beneficial in gaining a deeper understanding of the relevant processes.

7.3 Areas requiring attention for chronic subterranean releases

One of the model application areas considered in this study has been that of releases of ^{14}C to the biosphere associated with the disposal of ^{14}C-bearing radioactive materials. With respect to releases of ^{14}C-bearing gases, upon reaching the soil surface environment, any $^{14}CH_4$ would not automatically interact with plants. Either the gas would be released direct to the atmosphere and, as such, be lost from the system, or else it would be oxidised (to some extent) by soil microorganisms to $^{14}CO_2$ which may then be available for fixation by the plant canopy as it diffuses from the soil into the atmosphere above (e.g. Le

Mer and Roger, 2001). The recent report by Atkinson et al. (2011) provides initial data on these processes, which should be taken into account when developing models of sub-surface ^{14}C source terms.

The nature of such releases to the soil surface zone, rather than necessarily direct to the atmosphere, highlights the need to have an appropriate soil system sub-model. Within this study, the application of SSPAM^{14}C to the Imperial College data based on an atmospheric source term provides little information regarding the appropriateness of the relatively detailed soil sub-model for representing gaseous or aqueous releases of ^{14}C to the soil. There is therefore a need for appropriate validation data. The model currently used by SKB, does neither models soil processes nor the soil concentration of ^{14}C (Avila and Pröhl, 2008). It is not yet known whether a model that is currently under development for SKB will or will not explicitly model soil (Tagesson, 2012). If future experimental data shows the need for detailed soil sub-models, then any terrestrial ^{14}C soil-plant-atmosphere model used by SKB will need to incorporate explicit representation of the soil. If, however, future experimental data demonstrates that a detailed soil sub-model is not required for assessments on the timescales associated with the assessment of releases to the biosphere associated with the disposal of radioactive waste, then SSPAM^{14}C might reasonably be further developed with a simpler soil sub-model for use in such assessments.

Their extensive ecosystem database should help in this respect.

7.4 Areas requiring attention for acute atmospheric releases

In this study, SSPAM^{14}C has been applied to a scenario of acute atmospheric release of ^{14}C-bearing gas (Section 6). In doing so, a number of areas requiring further attention have been identified. These relate primarily to the rates of exchange of gas between atmospheric compartments, and between the soil atmosphere and aboveground atmosphere. It is anticipated that the data coming from the series of experiments funded by the UK's NDA RWMD (e.g. Atkinson et al., 2011) will provide further understanding and justification for some of these transfer rates. Additional data on the wider exchange of air may be available from the enhanced CO_2 experiments that were carried out in the 1990s and early 21st century (e.g. Leakey et al., 2009; Xie et al., 2005), along with micrometeorological studies from a range of agricultural and natural ecosystems (e.g. Hill et al., 2011, 2012; Sus et al., 2010).

For short term releases of ^{14}C, consideration also needs to be given to time dependent plant growth and transfer parameters, such as rates of photosynthesis (e.g. Le Dizès et al., 2012; Ota et al., 2012). This can be achieved to some extent by the use of fitted plant growth curves (Tani et al., 2011, Maul et al., 2005).

7.5 Summary

In this study a review of existing ^{14}C soil-plant-atmosphere models has been used to formulate a new model, SSPAM^{14}C. This model contains relatively detailed sub-models for the soil, plant and atmosphere systems making it, in principle, suited to modelling both long term and acute releases to the soil-atmosphere environment. The application of this model to a set of experimental data relating to a short term atmospheric release of ^{14}C-bearing gas has highlighted a number of areas requiring further development, as discussed above, both in terms of the model parameterisation, and also missing experimental data to further the empirical understanding of such systems and for model validation. Equivalent data are not yet available for assessing the performance of the model for the soil sub-system.

8 References

Albrecht A (2010). Les équations du modèle de transfert du carbone-14 (^{14}C) dans la biosphère (AquaC_14) et leur intégration dans le code "Modèle Management, MoM"; Note technique. Report number: C.NT.ASTR.10.0052.A, ANDRA, Châtenay-Malabry.

Albrecht A and Miquel S (2010). Extension of sensitivity and uncertainty analysis for long term dose assessment of high level nuclear waste disposal sites to uncertainties in the human behaviour, Journal of Environmental Radioactivity, 101, 55-67.

Allen R G, Pereira L S, Raes D and Smith M (1998). Crop evapotranspiration: Guidelines for computing crop water requirements. Food and Agriculture Organization (FAO) of the United Nations, Irrigation and Drainage Paper 56, Rome.

Amiro B D, Zhuang Y and Sheppard S C (1991). Relative importance of atmospheric and root uptake pathways for $^{14}CO_2$ transfer from contaminated soil to plants. Health Physics 61 (6), 825-829.

Andoh M A and Amano H (2003). Development of dynamic compartment model for estimation of C-14 behavior in paddy field. In: Proceedings of the International Symposium on Modelling and Radioecology, Rokkasho, Aomori, Japan, October 22-24, 2002. Institute for Environmental Sciences, Japan, 484-487.

Anten N P R (1997). Modelling canopy photosynthesis using parameters determined from simple non-destructive measurements. Ecological Research, 12, 77-88.

Aquilonius, K (2001). Dose assessment factors for releases during normal operation. D. C-14 model. In Swedish: Dosomräkningsfaktorer för normaldriftsutsläpp. D. C-14 modell. Report STUDSVIK/ES-01/36. Studsvik Eco & Safety AB, Sweden.

Aquilonius K and Hallberg B (2005). Process-oriented dose assessment model for ^{14}C due to releases during normal operation of a nuclear power plant. Journal of Environmental Radioactivity, 82, 267-283.

Atkinson B, Meredith W, Snape C, Steven M and Shaw G (2011). Experimental and Modelling Studies of Carbon-14 Behaviour in the Biosphere: Diffusion and oxidation of isotopically labelled methane ($^{13}CH_4$) in laboratory soil column experiments. NDA Radioactive Waste Management Directorate, report no. Serco/Nott/e.4041/002 Issue 1.

Aulagnier C, Le Dizès S, Maro D, Hérbert D, Lardy R, Martin R and Gonze M-A (2012). Modelling the transfer of ^{14}C from the atmosphere to grass: A case study in a grass field near AREVA-NC La Hague. Journal of Environmental Radioactivity, 112, 52-59.

Avila R and Pröhl G (2008). Models used in the SFR 1 SAR-08 and KBS-3H safety assessments for calculation of C-14 doses, SKB Rapport R-08-16.

Baes C F, Sharp R D, Sjoreen A J and Shore R W (1984). A review and analysis of parameters for assessing transport of environmentally released radionuclides through agriculture. Oak Ridge National Laboratory report ORNL-5786.

Bergström U and Barkefors C (2004). Irrigation in dose assessments models. SKB R-04-26, Svensk Kärnbränslehantering AB.

Bergström U, Nordlinder S and Appelgren A (1991). Methodology for calculation of reference release factors for airborne releases. In Swedish: Metodik förberäkning av referensutsläppsfaktorer för luftutsläpp. Report STUDSVIK/NS-91/96. Studsvik AB, Sweden.

BIOPROTA (2005). Model Review and Comparison for C-14 Dose Assessment, Theme 2 Task 3 Report. Main Contributors: S Sheppard (Task Leader) and M C Thorne.

Bush R P, White I F and Smith G M (1984). Carbon-14 Waste Management. CEC, Euratom Report EUR-8749.

Cannell M G R and Thornley J H M (2000). Modelling the Components of Plant Respiration: Some Guiding Principles. Annals of Botany, 85, pp. 45–54, 2000.

Ciffroy P,Siclet F, Damois C, Luck M and Duboudin C (2005). A dynamic model for assessing radiological consequences of routing releases in the Loire river: Parameterisation and uncertainty/sensitivity analysis. Journal of Environmental Radioactivity, 83, 9-48.

Clarke R H (1979). The First Report of a Working Group on Atmospheric Dispersion, A Model for Short and Medium Range Dispersion of Radionuclides Released to the Atmosphere. National Radiological Protection Board, NRPB-R91.

Cock J H and Yoshida S (1972). Accumulation of ^{14}C-labeled carbohydrate before flowering and its subsequent redistribution and respiration in the rice plant. Proceedings of the Crop Science Society of Japan, 41, 226-234.

Coleman K and Jenkinson D S (2005). ROTHC-26.3 A Model for the Turnover of Carbon in Soil. IACR – Rothamsted, Harpenden, Herts., November 1999 issue (modified April 2005).

CSA (2008). Guidelines for Calculating Derived Release Limits for Radioactive Material in Airborne and Liquid Effluents for Normal Operations of Nuclear Facilities. Canadian Standards Association (CSA) Standard N288.1-08. Toronto, Canada.

Ekdahl C A, Bacastow R and Keeling D C (1972). Atmospheric Carbon Dioxide and Radiocarbon in the natural carbon cycle. In Proc. Symposium on Carbon in the Biosphere. CONF-720510.

Facilia (2011). Ecolego v.5.0.195, Information, and software, available at http://ecolego.facilia.se/ecolego/show/HomePage, Facilia AB, Stockholm, Sweden.

Foken T (2008). Micrometeorology. Springer, ISBN 978-3-540-74665-2.

Garnier-Laplace J, Roussel-Debet S and Calmon P (1998). Modélisation des transferts du carbone 14 émis par les réacteurs à eau pressurisée en fonctionnement normal, dans l'environnement proche du site, dans les milieux aquatique d'eau douce et terrestre, Report IPSN/SERE n°98-07.

Hansen S. Jensen H E, Nielsen N E and Svendsen H (1993). Description of the soil plant system model DAISY, Basic principles and modelling approach. Simulation model for transformation and transport of energy and matter in the soil plant atmosphere system. Jordbrugsforlaget, The Royal Veterinary and Agricultural University, Copenhagen, Denmark.

Hill T C, Williams M, Woodward F I and Moncrieff J B (2011). Constraining ecosystem processes from tower fluxes and atmospheric profiles. Ecological Applications, 21,1474-1489.

Hill T C, Ryan E and Williams M (2012). The use of CO_2 flux time series for parameter and carbon stock estimation in carbon cycle research. Global Change Biology, 18, 179-193.

IAEA (1994). Handbook of Parameter Values for Prediction of Radionuclide Transfer in Temperate Environments. Technical Reports Series No 364, International Atomic Energy Agency, Vienna.

IAEA (2008). The Potato Scenario, Final Report. EMRAS Tritium/C14 Working Group, September 2008.

IUR (2006). Recommendations for improving predictions of the long-term environmental behaviour of ^{14}C, ^{36}Cl, ^{99}Tc, ^{237}Np and ^{238}U, Findings of the IUR "Radioecology and Waste" Task Force. IUR Report 6.

Jenkinson D S and Rayner J H (1977). The turnover of soil organic matter in some of the Rothamsted classical experiments. Soil Science, 123, 298-305.

Jenkinson D S, Hart P B S, Rayner J H and Parry L C (1987). Modelling the turnover of organic matter in long-term experiments at Rothamsted. INTECOL Bulletin, 15, 1-8.

Jenkinson D S, Harkness D D, Vance E D, Adams D E and Harrison A F (1992). Calculating net primary production and annual input of organic matter to soil from the amount and radiocarbon content of soil organic matter. Soil Biology Biochemistry, 24, 295-308.

Jouven M, Carrère P and Baumont R (2006a). Model predicting dynamics of biomass, structure and digestibility of herbage in managed permanent pastures: 1. Model description. Grass and Forage Science, 61, 112-124.

Jouven M, Carrère P and Baumont R (2006b). Model predicting dynamics of biomass, structure and digestibility of herbage in managed permanent pastures: 2. Model evaluation. Grass and Forage Science, 61, 125-133.

Keeling C D and Whorf T P (2001). http://cdiac.esd.ornl.gov/ftp/ndp001/manualoa.co2. The Carbon Dioxide Research group Scripps Institution of Oceanography (SIO), University of California La Jolla, California, USA.

Keum D-K, Jun I, Lim K-M, Choi Y-H and Lee C-W (2008). Predictive model for the ^{14}C radioactivity in a plant following an exposure to airborne $^{14}CO_2$ gas. Journal of Environmental Radioactivity, 99, 1756-1763.

Killough G G (1980). A dynamic model for estimating radiation dose to the world population from releases of ^{14}C to the atmosphere. Health Physics 38: 269–300.

Kłos R A and Shaw G (2008). Review of biosphere modelling in SAR-08. Aleksandria Sciences Project Report to SSM, ASN 08-02, Aleksandria Sciences, United Kingdom.

Kluczewski S M, Nair S and Stehr P (1986). A field study of the uptake of S-35 and C-14 into crops characteristic of the UK diet. Central Electricity Generating (TPRD/B/R86).

Koarashi J, Davis P A, Galeriu D, Melintescu A, Saito M, Siclet F and Uchida S (2008). Carbon-14 transfer into rice plants from a continuous atmospheric source: observations and model predictions. Journal of Environmental Radioactivity, 99, 1671-1679.

Leakey A D B, Ainsworth E A, Bernacchi C J, Rogers A, Long S P and Ort D R (2009). Elevated CO2 effects on plant carbon, nitrogen, and water relations: six important lessons from FACE. Journal of Experimental Botany, 60(10), 2859-2876.

Le Dizès S, Maro D, Aulagnier C, Martin R, Lardy R and Mourlon C (2011). Modelling and validating carbon-14 transfer in terrestrial environments in response to ^{14}C releases. In Proceedings of the International Conference of Radioecology and Environmental Radioactivity, Hamilton, Canada, 19-24 June 2011.

Le Dizès S, Maro D, Hébert D, Gonze M-A and Aulagnier (2012). TOCATTA: A dynamic transfer model of ^{14}C from the atmosphere to soil-plant systems. Journal of Environmental Radioactivity, 105(1), 48-59.

Le Mer J and Roger P (2001). Production, oxidation, emission and consumption of methane by soils: A review. European Journal of Soil Biology, 37, 25-50.

Lide DR (editor) (2006). CRC Handbook of Chemistry and Physics, 87th Edition. CRC Press.

Limer L, Smith G and Thorne M (2010). Disposal of Graphite: A Modelling Exercise to Determine Acceptable Release Rates to the Biosphere. A Study for the Nuclear Decommissioning Authority, Radioactive Waste Management Division, QRS-1454A-1, Version 2.2.

Limer L M C and Thorne M C (2011). NDA RWMD Biosphere Assessment Studies FY2010-2011: The Biosphere Transport, Distribution and Radiological Impact of C-14 released from a Geological Disposal Facility. Quintessa Report to the Nuclear Decommissioning Authority (NDA) Radioactive Waste Management Directorate (RWMD) QRS-1378ZM-1, Version 1.1.

Limer L M C, Thorne M C and Towler G H (2011a). Assessment Calculations for C-14 Labelled Gas for the LLWR 2011 ESC. Quintessa Limited report to LLWR Limited QRS-1443Z-1, Version 4.0, April 2011.

Limer L M C, Thorne M C and Cummings R (2011b). Consideration of Canopy Structure in Modelling ^{14}C-Labelled Gas Behaviour in the Biosphere for Human Dose Assessments. Radioprotection 46 (6), S409-S415.

Limer L M C, Smith K, Albrecht A, Marang L, Norris S, Smith G M, Thorne M C and Xu S (2012). C-14 Long-Term Dose Assessment: Data Review, Scenario Development, and Model Comparison. Final Report, Version 3.0. A report prepared within the BIOPROTA international cooperation programme and published by the Swedish Radiation Safety Authority: 2012:47.

Lindborg T (ed.) (2005). Description of surface systems. Preliminary site description Forsmark area – version 1.2. SKB R-05-03, Svensk Kärnbränslehantering AB.

Lindsay W L (1979). Chemical Equilibria in Soils. John Wiley & Sons, New York.

Löfgren A (ed.) (2008). The terrestrial ecosystems at Forsmark and Laxemar-Simpevarp, Site Descriptive Modelling SDM site. SKB Report R-08-01.

Magnusson Å, Strenström K and Aronsson P-O (2008). C-14 in spent ion-exchange resins and process water from nuclear reactors – A method for quantitative determination of organic and inorganic fractions, Journal of Radioanalytical and Nuclear Chemistry 275 (2), 261-273.

Marschner H (1995). Mineral nutrition of higher plants. Academic Press, London, 889 pp.

Maul P R, Watson C E and Thorne M C (2005). Probabilistic Modelling of C-14 and H-3 Uptake by Crops and Animals. Quintessa report to the Food Standards Agency QRS-1264A-1, Version 3.0, Henley-on-Thames, UK.

Mayall A (2003). Modelling the dispersion of radionuclides in the atmosphere. In Scott M (ed.) Modelling of Radioactivity in the Environment, Elsevier.

Mobbs S, Shaw G, Norris S, Marang L, Sumerling T, Albrecht A, Xu S, Thorne M, Limer L, Smith K and Smith G (2012). Developments in modelling of C-14 in the biosphere for solid radioactive waste disposal. 21st Radiocarbon conference, Paris, July 9-13 2012.

Mölder M (1997). Parameterization of exchange processes over a barley field. Boundary-Layer Meteorology, 84 (3), 341-361.

Monsi M and Saeki T (1953). Über den Lichtfaktor in den Pflanzengesellschäften und seine Bedeutung für die Stoffproduktion. Japanese Journal of Botany, 14, 22–52.

Monteith J L and Unsworth M H (2007). Principles of Environmental Physics, 3rd Edition, Academic Press, Amsterdam, The Netherlands.

Murthy K S (1976). Growth and development. In: Jaiswal, P.L., Wadhwani, A.M. (Eds.), Rice Production Manual. Indian Council of Agricultural Research, New Delhi, pp. 48-55.

NCRP (1985). Carbon-14 in the environment. National Council on Radiation Protection and Measurements. NCRP report no 81, USA.

Norris S N, Albrecht, A, Limer L, Marang L, Smith K, Smith G, Thorne T, Wiebert A and Xu S (2011). Consideration of Canopy Structure in Modelling ^{14}C Labelled Gas Behaviour in the Biosphere for Human Dose Assessments. Paper presented at the International Conference on Radioecology and Environmental Radioactivity (ICRER), Hamilton, Ontario 19-24 June 2011.

Okano K, Tatsumi J, Yoneyama T, Kono Y and Totsuka T (1983). Investigation on the carbon and nitrogen transfer from a terminal leaf to the root system of rice plant by a double tracer method with ^{13}C and ^{15}N. Japanese Journal of Crop Science, 52, 331-341.

Okawa S, Makino A and Mae T (2002). Shift of the major sink from the culm to the panicle at the early stage of grain filling in rice (*Oryza sativa L. cv. Sasanishiki*). Soil Science and Plant Nutrition, 48, 237-242.

Ota M, Nagai H and Koarashi J (2012). A land surface ^{14}C transfer model and numerical experiments on belowground ^{14}C accumulation and its impact on vegetation ^{14}C level. Journal of Environmental Radioactivity, 107, 13-22.

Parshotam A, Saggar S, Tate K and Parfitt R (2001). Modelling organic matter dynamics in New Zealand soils. Environment International, 27, 111-119.

Penfold J P and Watkins B (1998). Transfer of C-14 in the Biosphere Bibliography and Modelling. Rapport QuantiSci n° C NT OQUA 98-001.

Pinner A V and Maple J P (1987). Radiological impact of shallow land burial: sensitivity to site characteristics and engineered features of burial facilities. CEC Report EUR 10816 EN (NRPB-M137), Luxembourg.

Press W H, Flannery, B P, Teukolsky S A & Vetterling W T, (1992). Numerical Recipes in FORTRAN 77: Volume 1, Volume 1 of Fortran Numerical Recipes: The Art of Scientific Computing: Fortran Numerical Recipes v.1, Cambridge University Press, Cambridge UK.

Reido M, Grub A, Rosset M and Fuhrer J (1998). A pasture simulation model for dry matter production, and fluxes of carbon, nitrogen, water and energy. Ecological Modelling, 105, 141-183.

Roussel-Debet S (2001). CARBONE 14. Participation IPSN au contrat CPB ANDRA « Rôle des microorganismes sur le comportement de divers éléments dans le système sol-plante ». IRSN. Report DEI/SERLAB n° 01-009.

Schnoor J L (1996). Environmental Modeling: Fate and Transport of Pollutants in Water, Air, and Soil, John Wiley & Sons, New York, USA

Scurlock J M O, Asner G P and Gower S T (2001). Worldwide Historical Estimates and Bibliography of Leaf Area Index, 1932-2000. ORNL Technical Memorandum TM-2001/268, Oak Ridge National Laboratory, Oak Ridge, Tennessee, U.S.A.

Seinfeld J (1986). Atmospheric chemistry and physics of air pollution. Wiley Interscience Publication, New York.

Sheppard M I, Sheppard S C and Amiro B D (1991). Mobility and plant uptake of inorganic ^{14}C and ^{14}C-labelled PCB in soils of high and low retention, Health Physics 61 (4), 481-492.

Sheppard S C and Evenden W G (1996a). Retention of inorganic carbon^{-14} by isotopic exchange in soils. Journal of Environmental Quality 25 (5), 1153^{-1}161.

Sheppard S C and Evenden W G (1996b). Progressive extraction method applied to isotopic exchange of carbon^{-1}4. Communications in Soil Science Plant Analysis 27, 3059-3071.

Sheppard S C, Ciffroy P, Siclet F, Damois C, Sheppard M I and Stephenson M (2006a). Conceptual approaches for the development of dynamic specific activity models of ^{14}C transfer from surface water to humans. Journal of Environmental Radioactivity 87, 32-51.

Sheppard S C, Sheppard M I and Siclet F (2006b). Parameterization of a dynamic specific activity model of ^{14}C transfer from surface water to humans. Journal of Environmental Radioactivity 87, 15-31.

SKB (2010). Biosphere analyses for the safety assessment SR-Site – synthesis and summary of results. SKB Technical Report TR-10-09, December 2010.

Smith G M, Robinson P C and Stenhouse M J (1994). C-14 Food chain Modelling Following Release to Atmosphere. Intera report to the Ministry of Agriculture, Fisheries and Foods IE3725-1, Version 3, Henley-on-Thames, UK.

Stolp H (1977). Microbial Ecology: Organisms, Habits, Activities. Cambridge Studies in Ecology, Cambridge University Press.

Sumerling T (2012). Scoping Assessment of Carbon-14 Bearing Gas. A LLW Repository Limited Report, LLWR/ESC/R(12) 10046 Issue 1, February 2012.

Sus O, Williams M, Bernhofer C, Beziat P, Buchmann N, Ceschia E, Doherty R, Eugster W, Gruenwald T, Kutsch W, Smith P and Wattenbach M (2010). A linked carbon cycle and crop developmental model: description and evaluation against measurements of carbon fluxes and carbon stocks at several European agricultural sites. Agriculture, Ecosystems and Environment, 139, 402-418.

Tagesson T (2012). Turbulent transport in the atmospheric surface layer. SKB Technical Report TR-12-05, April 2012.

Takahashi T, Yamamoto K, Tagami K, Takeda H and Uchida S (2008). Development of a dynamic compartment model for prediction of transfer of carbon-14 to rice grains from the atmosphere. In: Proceedings of the International Symposium on Application of a Closed Experimental System to Modeling of ^{14}C Transfer in the Environment, Rokkasho, Aomori, Japan, November 15-16, 2007. Institute for Environmental Sciences, Japan, 15-20.

Tako Y, Abe K and Nitta K (1997). The Initial Tests for Performance Evaluation of Closed Plant Experiment Facility (CPEF) of Closed Ecology Experiment Facilities (CEEF). SAE technical paper series, 972517.

Tako Y, Ara, R, Otsubo K and Nitta K (2001). Sequential cultivation experiment with main crops using CEEF. In: Proceedings of the International Meeting for Advanced Technology of Environmental Control

and Life Support, Rokkasho, Aomori, Japan, September 26-28, 2001. Institute for Environmental Sciences, Japan, pp. 209e221.

Tani T, Arai R, Nozoe S, Tako Y, Takahashi T and Nakamura Y (2011). Development of a dynamic transfer model of ^{14}C from the atmosphere to rice plants. Journal of Environmental Radioactivity, 102 (4), 340-347.

Thomson G, Miller A, Smith G and Jackson D (2008). Radionuclide Release Calculations for SAR-08. Swedish Nuclear Fuel and Waste Management Company, SKB Report R-08-14. Stockholm.

Thorne M C (2005). Development of Increased Understanding of Potential Radiological Impacts of Radioactive Gases from a Deep Geological Repository: Review of FSA and Nirex Models and Associated Scoping Calculations. Mike Thorne and Associates Limited report to UK Nirex Limited MTA/P0011b/2005-5: Issue 2, November 2005.

Thorne M C (2006). Development of Increased Understanding of Potential Radiological Impacts of Radioactive Gases from a Deep Geological Repository: Sensitivity Studies with the Enhanced RIMERS Model, Mike Thorne and Associates Limited Report to Nirex, Report No. MTA/P0011b/2005-10: Issue 2.

Thorne M C, Khursheed A and Stansby S J (2003a). Assessing the Radiological Impact of Radionuclides in Sewage Sludge when Applied to Agricultural Land: Final Report. Mike Thorne and Associates report to the Food Standards Agency MTA/P0023/2003-1: Issue 1, Ripponden, UK.

Thorne M C, Kelly M and Stansby S J (2003b). Expert Elicitation of Modelling Parameters Explicitly Relevant to UK Environmental and Agricultural Conditions. Serco Assurance Report SA/ENV-0579 to the Food Standards Agency, Aviation House, 125 Kingsway, London, WC2B 6NH.

Thorne M C and MacKenzie J (2005). The Treatment of Waste-Derived Gas in the Biosphere in Nirex Safety and Performance Assessments. Quintessa Limited report to UK Nirex Limited QRS-1248A-1, Version 2.0, February 2005.

Troen R and Lundtang Petersen E (1991). European Wind Atlas. Risoe National Laboratory, Risoe, Denmark, 1991, ISBN 87-550-1482-8.

Tucker S M (1998). ^{14}C dynamics in crops following short-term exposure to atmospheric $^{14}CO_2$. PhD thesis, Imperial College London, UK.

Tucker S and Shaw G (1997). Quality Assured Modelling Data for $^{14}CO_2$ Fixation by Crops. IC.CARE/MAFF/REP/C-14/4.0, Imperial College report to the Ministry of Agriculture, Fisheries and Foods, London, UK.

Tucker S M and Shaw G (1994). Modification of the MAFF/CARE wind tunnel to allow recirculation of $^{14}CO_2$: a report on tunnel performance, IC.CARE/MAFF/REP/C-14/1.0, Imperial College at Silwood Park, Ascot, Berks, SL5 7TE.

van Hecke W (2001). Intégration du modèle C14 développé par Quantisci au code de calcul Aquabios et comparaison avec le modèle utilisé précédemment. Report ANDRA N° C NT ABSE 00-032/A, Châtenay-Malabry.

van Veen J A and Paul E A (1981). Organic carbon dynamics in grassland soils.1. Background information and computer simulation. Canadian Journal of Soil Science, 61(2), 185-201.

Vuichard N, Ciais P, Viovy N, Ammann C, Calanca P, Clifton-Brown J, Fuhrer J, Jones M, Martin C and Soussana J-F (2007). Estimating the greenhouse gas fluxes of European grasslands with a process driven model: Part 1. Model evaluation from in-situ measurements. Global Biogeochemical Cycles, 21, GB1004, doi:10.1029/2005GB002611.

Walker A J and Otlet R L (1999). Studies on gaseous species of tritium and carbon-14 in environmental air around nuclear establishments. From: Environmental Radiochemical Analysis. Special Publication of the Royal Society of Chemistry, 234, Cambridge, UK, pp. 159-169, ISBN 0-85404-734-4.

Watkins B M, Robinson P C and Smith G M (1998). Update of Models for Assessing Short-Term Atmospheric Releases of C-14 and Tritium in the Light of New Information and Experimental Data. QuantiSci report to Ministry of Agriculture, Fisheries and Foods MAFF-5044-1, London, UK.

Xie Z, Cadisch G, Edwards G, Baggs E M and Blum H (2005). Carbon dynamics in a temperate grassland soil after 9 years exposure to elevated CO_2 (Swiss FACE). Soil Biology and Biochemistry, 37(7), 1387-1395.

Xu S, Nordén M, Lager C, Hägg A-C and Andersson P (2011a). A review of a ^{14}C model used for dose assessment due to releases of normal operation in Sweden. Presented at the Nordic Society for Radiation Protection (NSFS) Conference, Reykjavik, 22-25 August 2011.

Xu X, Liu W and Kiely G (2011b). Modeling the change in soil organic carbon of grassland in response to climate change: effects of measured versus modelled carbon pools for initializing the Rothamsted Carbon model. Agriculture, Ecosystems and Environment, 140, 372-381.

Yoshida S (1981). Fundamentals of Rice Crop Science. The International Rice Research Institute, Manila, Philippines.

Zach R and Sheppard S C (1992). The Food-Chain and Dose Submodel, CALDOS, for the Assessment of Canada's Nuclear Fuel Waste Management Concept. Atomic Energy of Canada Limited, Report No. AECL-10165, COG-91-195.

Zhang Y, Ma J and Cao Z (2008). The Von Karman Constant Retrieved From CASES-97 Dataset Using a Variational Method. Atmospheric Chemistry and Physics, 8(23), 7045-7053.

Parameterisation of the transport model: SSPAM^{14}C, SSPAM^{14}C_C3

The two models constructed in the project are summarised in the data tables below. The parameterisation given is taken directly from the Ecolego implementation of the models.

Numerical data and some expressions are derived from literature values. Some are assumed on the basis of the literature values and the reasons discussed in the main text. Other values are derived from parameters used in the model, again, with justification detailed in the main report.

A few of the parameters are chosen because they give the best approximation of the SSPAM^{14}C results to those of Enhanced RIMERS (Thorne 2005).

For the SSPAM^{14}C_C3 model used to represent the Imperial College experimental data, many of the data are based on the experimental configuration described in Section 6.

Use is made in this appendix of the abbreviated names for the models' compartments:

Atmosphere sub-model

TATM	turbulent mixing layer
DATM	diffusive mixing layer

Plant sub-model

AGP	above ground plant
BGP	below ground plant
FRUIT	the parts of the plant produced as part of the reproductive cycle, including seeds, grain, tubers and taproots

Soil sub-model

SATM	soil atmosphere
SOL	soil solution
INORG	soil inorganic material
HUM	humus (non- or slowly decomposing plant material)
DPM	decomposable plant material
BIO	microbial biomass

A.1 SSPAM^{14}C – Enhanced RIMERS comparison

Global parameters

Parameter		Expression	Value	Units	Notes
Model area	A_f	10000	1.00E+04	m^2	Derived
Atmospheric carbon conc.	mC_ATM	12.0/44.0*7.17E-4	1.96E-04	kg C m^{-3}	Aquilonius & Hallberg (2005)
Seconds per year	n_spy	60.0*60.0*24.0*365.252	3.16E+07	sec y^{-1}	Derived

Atmosphere sub-model

Parameter		Expression	Value	Units	Notes
enhancement factor for DATM	f_DATM	1	1.00E+00	-	Thorne (2005)
Transfer rate	kappa_DATM_TATM	1000	1.00E+03	y^{-1}	Thorne (2005)
diffusive layer thickness	l_DATM	0.5	5.00E-01	m	Assumed
turbulent layer thickness	l_TATM	5	5.00E+00	m	Assumed
mean annual windspeed	v_wind	5	5.00E+00	m sec^{-1}	Thorne (2005)
carbon conc. DATM	mC_DATM	f_DATM*mC_ATM	1.96E-04	kg C m^{-3}	Derived
carbon conc. TATM	mC_TATM	mC_ATM	1.96E-04	kg C m^{-3}	Derived
volume DATM	V_DATM	l_DATM*A_f	5.00E+03	m^3	Derived
volume TATM	V_TATM	l_TATM*A_f	5.00E+04	m^3	Derived
Mass carbon DATM	M_DATM	mC_DATM*V_DATM	9.78E-01	kg C	Derived
Mass carbon TATM	M_TATM	mC_TATM*V_TATM	9.78E+00	kg C	Derived
Transfer coefficients from compartments in the atmosphere sub-model	lam_DATM_AGP	(1.0-f_ru)*mdot_phot*A_f/M_DATM	2.03E+03	y^{-1}	Derived
	lam_DATM_SATM	(epsilon-theta)*f_SATM*l / l_DATM*kappa_SATM_DATM	6.00E+03	y^{-1}	Derived from Thorne (2005)
	lam_DATM_TATM	kappa_DATM_TATM	1.00E+03	y^{-1}	Thorne (2005)
	lam_TATM_DATM	f_DATM*l_DATM/l_TATM*kappa_DATM_TATM	1.00E+02	y^{-1}	Thorne (2005)
external loss term	lam_TATM_E	v_wind/sqrt(A_f)*n_spy	1.58E+06	y^{-1}	Thorne (2005)

Plant sub-model

Parameter		Expression	Value	Units	Notes
fraction biomass in AGP	f_AGP	0.49	4.90E-01	-	Assumed
fraction biomass in BGP	f_BGP	0.5	5.00E-01	-	Assumed
fraction of biomass lost from model	f_export	0	0.00E+00	-	Assumed
Transfer rate	kappa_AGP_BGP	0.2	2.00E-01	y^{-1}	Assumed
Transfer rate	kappa_AGP_FRUIT	0	0.00E+00	y^{-1}	Assumed
Transfer rate	kappa_BGP_AGP	0	0.00E+00	y^{-1}	Assumed
Transfer rate	kappa_BGP_FRUIT	0	0.00E+00	y^{-1}	Assumed
Transfer rate	kappa_exd	0.001	1.00E-03	y^{-1}	Assumed, small value
Transfer rate	kappa_FRUIT_AGP	0	0.00E+00	y^{-1}	Assumed
Transfer rate	kappa_FRUIT_BGP	0	0.00E+00	y^{-1}	Assumed
Transfer rate	kappa_plantDeath	1	1.00E+00	y^{-1}	Assumed
standing biomass	m_SB	1	1.00E+00	kg fw m^{-2}	Assumed
C accumulation by photosynthesis	mdot_phot	0.2	2.00E-01	kg C m^{-2} y^{-1}	Thorne (2005)
C respiration rate	mdot_plantResp	0.12	1.20E-01	kg C m^{-2} y^{-1}	Thorne (2005)
wet / dry conversion factor	Z	5	5.00E+00	kg fw (kg dw)$^{-1}$	Assumed
fraction biomass in FRUIT	f_FRUIT	1.0-f_AGP-f_BGP	1.00E-02	-	Derived
Carbon content of plants	f_pC	6.0*12.0/(10.0+5.0*16.0+6.0*12.0)/Z	8.89E-02	-	Derived
Mass C AGP	M_AGP	f_AGP*f_pC*m_SB*A_f	4.36E+02	kg C	Derived
Mass C BGP	M_BGP	f_BGP*f_pC*m_SB*A_f	4.44E+02	kg C	Derived
Mass C FRUIT	M_FRUIT	f_fruit*f_pC*m_SB*A_f	8.89E+00	kg C	Derived
Mass C standing biomass	M_p	f_pC*m_SB*A_f	8.89E+02	kg C	Derived

Plant sub-model continued

Parameter		Expression	Value	Units	Notes
Transfer coefficients from compartments in the plant sub-model	lam_AGP_BGP	kappa_AGP_BGP	2.00E-01	y^{-1}	Assumed
	lam_AGP_DATM	mdot_plantResp*A_f/M_AGP	2.76E+00	y^{-1}	Derived
	lam_AGP_DPM	p_D*(1.0-f_export)*kappa_plantDeath	8.37E-01	y^{-1}	Derived
	lam_AGP_FRUIT	kappa_AGP_FRUIT	0.00E+00	y^{-1}	Assumed
	lam_AGP_HUM	(1.0-p_D)*(1.0-f_export)*kappa_plantDeath	1.63E-01	y^{-1}	Derived
	lam_BGP_AGP	kappa_BGP_AGP	0.00E+00	y^{-1}	Assumed
	lam_BGP_DPM	p_D*(1.0-f_export)*kappa_plantDeath	8.37E-01	y^{-1}	Derived
	lam_BGP_FRUIT	kappa_BGP_FRUIT	0.00E+00	y^{-1}	Assumed
	lam_BGP_HUM	(1.0-p_D)*(1.0-f_export)*kappa_plantDeath	1.63E-01	y^{-1}	Derived
	lam_BGP_SATM	(1.0-f_bio)*mdot_soilResp*A_f/M_BGP	5.18E+00	y^{-1}	Derived
	lam_BGP_SOL	kappa_exd	1.00E-03	y^{-1}	Assumed
	lam_FRUIT_AGP	kappa_FRUIT_AGP	0.00E+00	y^{-1}	Assumed
	lam_FRUIT_BGP	kappa_FRUIT_BGP	0.00E+00	y^{-1}	Assumed
	lam_FRUIT_DPM	p_D*(1.0-f_export)*kappa_plantDeath	8.37E-01	y^{-1}	Derived
	lam_FRUIT_HUM	(1.0-p_D)*(1.0-f_export)*kappa_plantDeath	1.63E-01	y^{-1}	Derived
Loss terms by export of plant material	lam_AGP_Elsewhere	f_export*kappa_plantDeath	0.00E+00	y^{-1}	Assumed
	lam_BGP_Elsewhere	f_export*kappa_plantDeath	0.00E+00	y^{-1}	Assumed
	lam_FRUIT_Elsewhere	f_export*kappa_plantDeath	0.00E+00	y^{-1}	Assumed

Soil sub-model

Parameter		Expression	Value	Units	Notes
soil porosity	epsilon	0.6	6.00E-01	-	Kłos et al, (2011)
Fraction total soil resp. from BIO	f_bio	0.54	5.40E-01	-	R-08-01, p152
root uptake fraction	f_ru	0.01	1.00E-02	-	1% Assumed
Enhancement factor C in SATM	f_SATM	20	2.00E+01	-	Thorne (2005)
kd for C in soil	k_d	0.1	1.00E-01	$m^3\ kg^{-1}$	Optimised
overall loss rate from BIO	kappa_BIO	0.108	1.08E-01	y^{-1}	Thorne (2005)
overall loss rate from DPM	kappa_DPM	33.4	3.34E+01	y^{-1}	Thorne (2005)
overall loss rate from HUM	kappa_HUM	0.138	1.38E-01	y^{-1}	Thorne (2005)
overall loss rate from SOL	kappa_SOL	0.409	4.09E-01	y^{-1}	Jenkinson & Rayner (1977)
sorption rate to inorganic material	kappa_s	10	1.00E+01	y^{-1}	Optimised
Transfer rate	kappa_SATM_DATM	1000	1.00E+03	y^{-1}	Thorne (2005)
Transfer rate	kappa_SATM_SOL	10000	1.00E+04	y^{-1}	Thorne (2005)
thickness of top soil	l	0.3	3.00E-01	m	Kłos et al, (2011)
density C in BIO	mC_BIO	0.065	6.50E-02	kg C m^{-2}	R-08-01, p152
density C in DPM	mC_DPM	0.464	4.64E-01	kg C m^{-2}	R-08-01, p152
density C in HUM	mC_HUM	0.203	2.03E-01	kg C m^{-2}	R-08-01, p152
density C in INORG	mC_INORG	1125	1.13E+03	kg C m^{-2}	R-08-01 Tab 6-9
respiration rate for agricultural soil	mdot_soilResp	0.5	5.00E-01	kg C m^{-2} y^{-1}	R-08-01 p177
partitioning of decay DPM → BIO	p_BIO	0.0076	7.60E-03	-	Jenkinson & Rayner (1977)
partitioning of decay HUM → DPM	p_D	0.837	8.37E-01	-	Jenkinson & Rayner (1977)
partitioning of decay DPM → SOL	p_SOL	0.1285	1.29E-01	-	Jenkinson & Rayner (1977)
volumetric fraction BIO	phi_BIO	0.1	1.00E-01	-	Assumed
volumetric fraction DPM	phi_DPM	0.2	2.00E-01	-	Assumed
volumetric fraction DPM	phi_HUM	0.3	3.00E-01	-	Assumed
mineral density	rho_inorg	2650	2.65E+03	kg m^{-3}	Kłos et al, (2011)
water density	rho_W	1000	1.00E+03	kg m^{-3}	Kłos et al, (2011)
volumetric moisture content	theta	0.1	1.00E-01	-	Kłos et al, (2011)

Soil sub-model continued

Parameter		Expression	Value	Units	Notes
density C in SATM	mC_SATM	f_SATM*mC_ATM	3.91E-03	kg C m^{-3}	Thorne (2005)
density C in SOL	mC_SOL	(epsilon-theta)/theta*mC_SATM	1.96E-02	kg C m^{-3}	Based on Thorne (2005)
partitioning of decay DPM → HUM	p_slow	1.0-p_BIO-p_SOL	8.64E-01	-	Derived
Volume SATM	V_SATM	(epsilon-theta)*l*A_f	1.50E+03	m^3	Derived
Volume SOL	V_SOL	theta*l*A_f	3.00E+02	m^3	Derived
Mass C BIO	M_BIO	mC_BIO*A_f	6.50E+02	kg C	Derived
Mass C DPM	M_DPM	mC_DPM*A_f	4.64E+03	kg C	Derived
Mass C HUM	M_HUM	mC_HUM*A_f	2.03E+03	kg C	Derived
Mass C INORG	M_INORG	mC_INORG*A_f	1.13E+07	kg C	Derived
Mass C SATM	M_SATM	mC_SATM*V_SATM	5.87E+00	kg C	Derived
Mass C SOL	M_SOL	mC_SOL*l*A_f*theta	5.87E+00	kg C	Derived
Transfer coefficients from compartments in the soil sub-model	lam_BIO_SOL	kappa_SOL	4.09E-01	y^{-1}	Thorne (2005)
	lam_DPM_BIO	p_BIO*kappa_DPM	2.54E-01	y^{-1}	Thorne (2005)
	lam_DPM_HUM	p_slow*kappa_DPM	2.89E+01	y^{-1}	Derived
	lam_DPM_SOL	p_SOL*kappa_DPM	4.29E+00	y^{-1}	Thorne (2005)
	lam_HUM_BIO	kappa_HUM	1.38E-01	y^{-1}	Thorne (2005)
	lam_HUM_SOL	(1.0-p_BIO)*kappa_HUM	1.37E-01	y^{-1}	Thorne (2005)
	lam_INORG_SOL	theta / ((1.0-epsilon)*(1.0-phi_BIO-phi_HUM-phi_DPM)*k_d*rho_inorg)*kappa_s	2.36E-02	y^{-1}	Thorne (2005)
	lam_SATM_BIO	0	0.00E+00	y^{-1}	Thorne (2005)
	lam_SATM_DATM	kappa_SATM_DATM	1.00E+03	y^{-1}	Thorne (2005)
	lam_SATM_SOL	kappa_SATM_SOL	1.00E+04	y^{-1}	Thorne (2005)
	lam_SOL_BGP	f_ru*mdot_phot*A_f/M_SOL	3.41E+00	y^{-1}	Thorne (2005)
	lam_SOL_INORG	kappa_s	1.00E+01	y^{-1}	Thorne (2005)
	lam_SOL_SATM	kappa_SATM_SOL	1.00E+04	y^{-1}	Thorne (2005)

A.2 SSPAM^{14}C_C3 – Modelling the cabbage experiments

New FEPs shown in red, modified FEPs in blue. Black denotes unchanged FEPs compared to the Enhanced-RIMERS comparison version.

Global parameters

Parameter		Expression	Value	Units	Notes
model area	A_f	4.8	4.8	m^2	experiment
atmospheric carbon conc.	mC_ATM	0.00024	2.40E-04	kg C m^{-3}	experiment
seconds per year	n_spy	60.0*60.0*24.0*365.252	3.16E+07	sec y^{-1}	Derived

A.3 References

BIOPROTA (2005). Model Review and Comparison for C-14 Dose Assessment, Theme 2 Task 3 Report. Main Contributors: S Sheppard (Task Leader) and M C Thorne.

Thorne M C (2005). Development of Increased Understanding of Potential Radiological Impacts of Radioactive Gases from a Deep Geological Repository: Review of FSA and Nirex Models and Associated Scoping Calculations. Mike Thorne and Associates Limited report to UK Nirex Limited MTA/P0011b/2005-5: Issue 2, November 2005.

Atmosphere sub-model

Parameter		Expression	Value	Units	Notes
CO_2 purging rate	lam_purge	4600	4.60E+03	y^{-1}	experiment
enhancement factor for DATM	f_DATM	1	1.00E+00	-	Thorne (2005)
Transfer rate	kappa_DATM_TATM	1000000	1.00E+06	y^{-1}	optimised
diffusive layer thickness	l_DATM	0.005	5.00E-03	m	optimised
turbulent layer thickness	l_TATM	1.5	1.50E+00	m	experiment
mean annual windspeed	v_wind	1	1.00E+00	m sec^{-1}	not used
carbon conc. DATM	mC_DATM	f_DATM*mC_ATM	2.40E-04	kg C m^{-3}	Derived
carbon conc. TATM	mC_TATM	mC_ATM	2.40E-04	kg C m^{-3}	Derived
volume DATM	V_DATM	l_DATM*A_f*(lam_purge==0.0)+2.0*LAI*l_DATM*A_f*(lam_purge>0.0)	1.08E-01	m^3	Derived
volume TATM	V_TATM	l_TATM*A_f*(lam_purge==0.0)+55.0*(lam_purge>0.0)	5.50E+01	m^3	Derived
Mass carbon DATM	M_DATM	mC_DATM*V_DATM	2.59E-05	kg C	Derived
Mass carbon TATM	M_TATM	mC_TATM*V_TATM	1.32E-02	kg C	Derived
Transfer coefficients from compartments in the atmosphere sub-model	lam_DATM_AGP	(1.0-f_ru)*(mdot_phot+mdot_plantResp) * A_f / M_DATM	5.19E+05	y^{-1}	Derived
	lam_DATM_SATM	0	0.00E+00	y^{-1}	Derived
	lam_DATM_TATM	mdot_plantResp*A_f/M_DATM	1.64E+05	y^{-1}	Derived
	lam_TATM_DATM	(mdot_phot+mdot_plantResp)*A_f/M_TATM	1.03E+03	y^{-1}	Derived
	lam_TATM_SATM	(epsilon-theta)*f_SATM*l / l_TATM*kappa_SATM_DATM	2.92E+01	y^{-1}	Derived
external loss term	lam_TATM_E	v_wind/sqrt(A_f)*n_spy*(lam_purge==0.0)+lam_purge	4.60E+03	y^{-1}	Derived

Plant sub-model

Parameter		Expression	Value	Units	Notes
fraction biomass in AGP	f_AGP	0.879019173	8.79E-01	-	experiment
fraction biomass in BGP	f_BGP	0.12	1.20E-01	-	experiment
fraction of biomass lost from model	f_export	0	0.00E+00	-	Assumed
Transfer rate	kappa_AGP_BGP	0.652	6.52E-01	y^{-1}	
Transfer rate	kappa_AGP_FRUIT	0	0.00E+00	y^{-1}	Derived from experiment
Transfer rate	kappa_BGP_AGP	0	0.00E+00	y^{-1}	
Transfer rate	kappa_BGP_FRUIT	0	0.00E+00	y^{-1}	
Transfer rate	kappa_exd	0.001	1.00E-03	y^{-1}	asumed
Transfer rate	kappa_FRUIT_AGP	0	0.00E+00	y^{-1}	Derived from experiment
Transfer rate	kappa_FRUIT_BGP	0	0.00E+00	y^{-1}	
Transfer rate	kappa_plantDeath	1	1.00E+00	y^{-1}	Assumed
Leaf area index	LAI	2.25	2.25E+00	$m^2\ m^{-2}$	Bioprota Potato Scenario
standing biomass	m_SB	0.73771	7.38E-01	kg dw m^{-2}	experiment
C acc. by photosynthesis	mdot_phot	1.951161164	1.95E+00	kg C $m^{-2}\ y^{-1}$	Derived from experiment
C respiration rate	mdot_plantResp	0.886891438	8.87E-01	kg C $m^{-2}\ y^{-1}$	
wet / dry conversion factor	Z	100.0/12.0	8.33E+00	kg fw $(kg\ dw)^{-1}$	IAEA (1994)
fraction biomass in FRUIT	f_FRUIT	1.0-f_AGP-f_BGP	9.81E-04	-	Assumed
Carbon content of plants	f_pC	6.0*12.0/(10.0+5.0*16.0+6.0*12.0)	4.44E-01	-	Derived from experiment
Mass C AGP	M_AGP	f_AGP*f_pC*m_SB*A_f	1.38E+00	kg C	Derived
Mass C BGP	M_BGP	f_BGP*f_pC*m_SB*A_f	1.89E-01	kg C	Derived
Mass C FRUIT	M_FRUIT	f_fruit*f_pC*m_SB*A_f	1.54E-03	kg C	Derived
Mass C standing biomass	M_p	f_pC*m_SB*A_f	1.57E+00	kg C	Derived

Plant sub-model continued

Parameter		Expression	Value	Units	Notes
Transfer coefficients from compartments in the plant sub-model	lam_AGP_BGP	kappa_AGP_BGP	6.52E-01	y^{-1}	Assumed
	lam_AGP_DATM	mdot_plantResp*A_f/M_AGP	3.08E+00	y^{-1}	Derived
	lam_AGP_DPM	p_D*(1.0-f_export)*kappa_plantDeath	8.37E-01	y^{-1}	Derived
	lam_AGP_FRUIT	kappa_AGP_FRUIT	0.00E+00	y^{-1}	Assumed
	lam_AGP_HUM	(1.0-p_D)*(1.0-f_export)*kappa_plantDeath	1.63E-01	y^{-1}	Derived
	lam_BGP_AGP	kappa_BGP_AGP	0.00E+00	y^{-1}	Assumed
	lam_BGP_DPM	p_D*(1.0-f_export)*kappa_plantDeath	8.37E-01	y^{-1}	Derived
	lam_BGP_FRUIT	kappa_BGP_FRUIT	0.00E+00	y^{-1}	Assumed
	lam_BGP_HUM	(1.0-p_D)*(1.0-f_export)*kappa_plantDeath	1.63E-01	y^{-1}	Derived
	lam_BGP_SATM	(1.0-f_bio)*mdot_soilResp*A_f/M_BGP	8.84E+00	y^{-1}	Derived
	lam_BGP_SOL	kappa_exd	1.00E-03	y^{-1}	Assumed
	lam_FRUIT_AGP	kappa_FRUIT_AGP	0.00E+00	y^{-1}	Assumed
	lam_FRUIT_BGP	kappa_FRUIT_BGP	0.00E+00	y^{-1}	Assumed
	lam_FRUIT_DPM	p_D*(1.0-f_export)*kappa_plantDeath	8.37E-01	y^{-1}	Derived
	lam_FRUIT_HUM	(1.0-p_D)*(1.0-f_export)*kappa_plantDeath	1.63E-01	y^{-1}	Derived
Loss terms by export of plant material	lam_AGP_Elsewhere	f_export*kappa_plantDeath	0.00E+00	y^{-1}	Assumed
	lam_BGP_Elsewhere	f_export*kappa_plantDeath	0.00E+00	y^{-1}	Assumed
	lam_FRUIT_Elsewhere	f_export*kappa_plantDeath	0.00E+00	y^{-1}	Assumed

Soil sub-model

Parameter		Expression	Value	Units	Notes
soil porosity	epsilon	0.6	6.00E-01	-	Kłos et al, (2011)
Fraction total soil resp. from BIO	f_bio	0.54	5.40E-01	-	Löfgren (2008), p152
root uptake fraction	f_ru	0.013	1.30E-02	-	Optimised
Enhancement factor C in SATM	f_SATM	20	2.00E+01	-	Thorne (2005)
kd for C in soil	k_d	0.1	1.00E-01	$m^3\ kg^{-1}$	Optimised
overall loss rate from BIO	kappa_BIO	0.108	1.08E-01	y^{-1}	Thorne (2005)
overall loss rate from DPM	kappa_DPM	33.4	3.34E+01	y^{-1}	Thorne (2005)
overall loss rate from HUM	kappa_HUM	0.138	1.38E-01	y^{-1}	Thorne (2005)
overall loss rate from SOL	kappa_SOL	0.409	4.09E-01	y^{-1}	Jenkinson & Rayner (1977)
sorption rate to inorganic material	kappa_s	10	1.00E+01	y^{-1}	Optimised
transfer rate	kappa_SATM_DATM	14.6	1.46E+01	y^{-1}	Optimised
transfer rate	kappa_SATM_SOL	1000	1.00E+03	y^{-1}	Optimised
thickness of top soil	l	0.3	3.00E-01	m	Kłos et al, (2011)
density C in BIO	mC_BIO	0.065	0.065	kg C m^{-2}	Löfgren (2008), p152
density C in DPM	mC_DPM	0.464	0.464	kg C m^{-2}	Löfgren (2008), p152
density C in HUM	mC_HUM	0.203	0.203	kg C m^{-2}	Löfgren (2008), p152
density C in INORG	mC_INORG	1125	1125	kg C m^{-2}	Löfgren (2008), Tab 6-9
respiration rate for agricultural soil	mdot_soilResp	0.756	0.756	kg C m^{-2} y^{-1}	Upper limit Löfgren (2008)
partitioning of decay DPM → BIO	p_BIO	0.0076	0.0076	-	Jenkinson & Rayner (1977)
partitioning of decay HUM → DPM	p_D	0.837	0.837	-	Jenkinson & Rayner (1977)
partitioning of decay DPM → SOL	p_SOL	0.1285	0.1285	-	Jenkinson & Rayner (1977)
volumetric fraction BIO	phi_BIO	0.1	0.1	-	Assumed
volumetric fraction DPM	phi_DPM	0.2	0.2	-	Assumed
volumetric fraction DPM	phi_HUM	0.3	0.3	-	Assumed
mineral density	rho_inorg	2650	2650	kg m^{-3}	Kłos et al, (2011)
water density	rho_W	1000	1000	kg m^{-3}	Kłos et al, (2011)
volumetric moisture content	theta	0.1	0.1	-	Kłos et al, (2011)

Soil sub-model continued

Parameter		Expression	Value	Units	Notes
density C in SATM	mC_SATM	f_SATM*mC_ATM	0.0048	kg C m^{-3}	Derived from experiment
density C in SOL	mC_SOL	(epsilon-theta)/theta*mC_SATM	0.024	kg C m^{-3}	Derived from experiment
partitioning of decay DPM → HUM	p_slow	1.0-p_BIO-p_SOL	0.8639	-	Derived
Volume SATM	V_SATM	(epsilon-theta)*l*A_f	0.72	m^3	Derived
Volume SOL	V_SOL	theta*l*A_f	0.144	m^3	Derived
Mass C BIO	M_BIO	mC_BIO*A_f	3.12E-01	kg C	Derived
Mass C DPM	M_DPM	mC_DPM*A_f	2.23E+00	kg C	Derived
Mass C HUM	M_HUM	mC_HUM*A_f	9.74E-01	kg C	Derived
Mass C INORG	M_INORG	mC_INORG*A_f	5.40E+03	kg C	Derived
Mass C SATM	M_SATM	mC_SATM*V_SATM	3.46E-03	kg C	Derived
Mass C SOL	M_SOL	mC_SOL*l*A_f*theta	3.46E-03	kg C	Derived
Transfer coefficients from compartments in the soil sub-model	lam_BIO_SOL	kappa_SOL	4.09E-01	y^{-1}	Thorne (2005)
	lam_DPM_BIO	p_BIO*kappa_DPM	2.54E-01	y^{-1}	Thorne (2005)
	lam_DPM_HUM	p_slow*kappa_DPM	2.89E+01	y^{-1}	Derived
	lam_DPM_SOL	p_SOL*kappa_DPM	4.29E+00	y^{-1}	Thorne (2005)
	lam_HUM_BIO	kappa_HUM	1.38E-01	y^{-1}	Thorne (2005)
	lam_HUM_SOL	(1.0-p_BIO)*kappa_HUM	1.37E-01	y^{-1}	Thorne (2005)
	lam_INORG_SOL	theta / ((1.0-epsilon)*(1.0-phi_BIO-phi_HUM-phi_DPM)*k_d*rho_inorg)*kappa_s	2.36E-02	y^{-1}	Thorne (2005)
	lam_SATM_BIO	0	0.00E+00	y^{-1}	Thorne (2005)
	lam_SATM_DATM	kappa_SATM_DATM*(lam_purge==0.0)	0.00E+00	y^{-1}	Experiment
	lam_SATM_SOL	kappa_SATM_SOL	1.00E+03	y^{-1}	Modified by experiment
	lam_SATM_TATM	kappa_SATM_DATM*(lam_purge>0.0)	1.46E+01	y^{-1}	Experiment
	lam_SOL_BGP	f_ru*mdot_phot*A_f/M_SOL	3.52E+01	y^{-1}	Modified by experiment
	lam_SOL_INORG	kappa_s	1.00E+01	y^{-1}	Thorne (2005)
	lam_SOL_SATM	kappa_SATM_SOL	1.00E+03	y^{-1}	Modified by experiment

Additional data from Imperial College experiments – beans and potatoes

In this appendix the data relating to the exposure and measured dry weights and ^{14}C concentrations in the bean and potato crops from the Imperial College experiments are given. As with the cabbage experiment discussed in the main body of this report, a full description of the experiments is provided by Tucker (1998) and Tucker and Shaw (1997) and the following description is based on these documents.

B.1 Experimental setup

B.1.1 Crop production

Bunyard's Exhibition broad beans were sown at a rate of six seeds per pot on 13th April 1995. These were thinned on germination to four per pot.
Approximately two hundred Romano potatoes were transferred to a dark store on 5th July 1995 and left to chit. Some tubers were split to produce sufficient plants to transfer three to each of the one hundred plots on 14th August 1995. The plants were later thinned to two per pot.

B.1.2 Gas injection

The bean and potato crops were exposed to exponentially declining $^{14}CO_2$ concentrations in the wind tunnel airstream, as shown in **Fel! Hittar inte referenskälla.** and **Fel! Hittar inte referenskälla.**. This is the same form of exposure as experienced by the cabbages (see Section 5.2.3). The integrated air concentrations of $^{14}CO_2$ during each crop exposure are shown in **Fel! Hittar inte referenskälla.**.

Figure 33: ^{14}C concentration in air above the bean crop during exposure

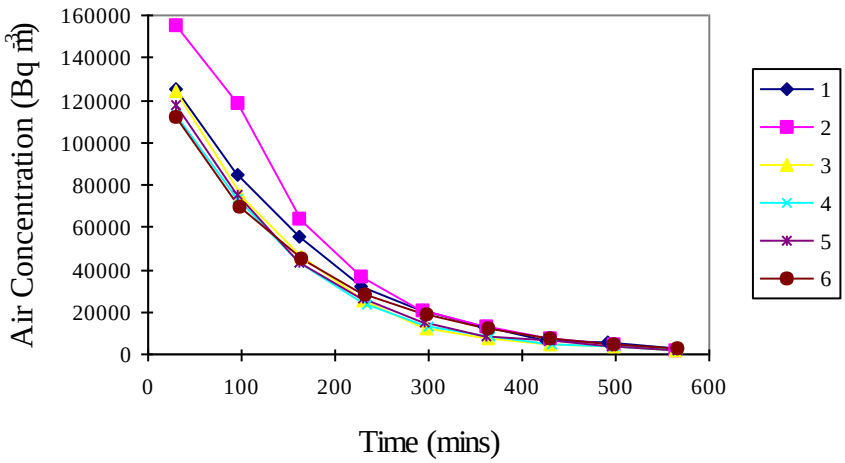

Figure 34: ^{14}C air concentration above the potato crop during exposure

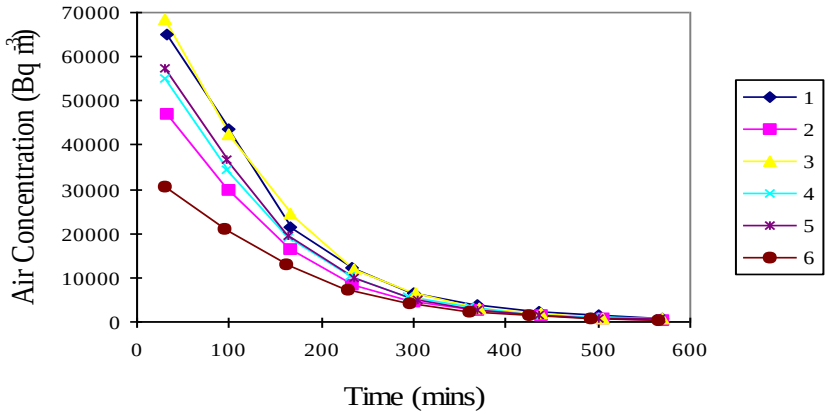

Table 30: Integrated ^{14}C air concentrations – beans and potatoes

Bean	IAC (MBq m^{-3} min)	Potato	IAC (MBq m^{-3} min)
B1	21.1	**P1**	9.8
B2	24.0	**P2**	7.0
B3	19.3	**P3**	9.6
B4	17.9	**P4**	8.1
B5	18.6	**P5**	8.3
B6	19.4	**P6**	4.8

B.1.3 Exposure and sampling codes

The sampling schedules for the beans and potatoes are given in **Fel! Hittar inte referenskälla.** and **Fel! Hittar inte referenskälla.** for respectively. The exposure code consists of a letter and number. B or P is used to identify crop (beans and potato, respectively) and the number denotes whether it was the first exposure, second etc.

Each harvest is identified by the exposure code and a harvest number e.g. B3H3 refers to the third harvest taken from the third bean exposure.

Table 31: Bean sampling schedule

Beans	B1		B2		B3		B4		B5		B6	
	Age	T	Age	T	Age	T	Age	T	Age	T	Age	T
H1	28	0	48	0	62	0	76	0	90	0	103	0
H2	32	4	50	2	67	5	80	5	95	5	106	3
H3	39	11	60	12	74	12	85	9	99	9	109	6
H4	50	22	71	23	84	22	92	16	109	19	113	10
H5	71	43	95	47	99	37	106	30	113	23	116	13
H6	119	91	119	71	119	57	119	43	119	29	119	16

Table 32: Potato sampling schedule

Pot.	P1		P2		P3		P4		P5		P6	
	Age	T	Age	T	Age	T	Age	T	Age	T	Age	T
H1	21	0	33	0	47	0	61	0	74	0	89	0
H2	31	11	38	5	53	6	65	4	79	5	90	1
H3	38	18	44	11	58	11	72	11	83	9	93	4
H4	48	28	58	25	68	21	83	22	87	13	95	6
H5	72	52	79	46	83	36	90	29	93	19	97	8
H6	97	77	97	64	97	50	97	36	100	26	100	11

B.2 Experiment results

Below are details of the experimental results for the beans and potatoes. Those from the potato aspect of the experiment have previously been used within the IAEA's Environmental Modelling for RAdiation Safety (EMRAS) programme's working group that focussed upon the modelling of tritium and ^{14}C transfer to biota and man (IAEA, 2008).

B.2.1 Net assimilation rates

Table 33 and Table 35 each show two sets of estimates for net assimilation rates for $^{12}C + {}^{14}C$ expressed in g C kg wwt^{-1} d^{-1} for beans and potatoes respectively; these assimilation rates are presented here same units used in STAR C-14.

The experimental estimates of carbon assimilation rates are lower than, though similar to, the default value of 4 g C kg wwt^{-1} d^{-1} used by STAR C-14. However, given the relatively low light levels within the MAFF/CARE wind tunnel (equivalent to a cloudy day), the STAR C-14 default carbon assimilation rate would appear to be approximately correct, if slightly conservative.

Table 33: Comparison between bean experiments: B1 to B6

Bean Experiment	Leaf Assimilation Rate g C Kg $wwt^{-1}d^{-1}$ (0.16 gCm^{-3})	Leaf Assimilation Rate g C Kg $wwt^{-1}d^{-1}$ (0.24 gCm^{-3})	Plant transfer factor (TF) * (H6)	Bean TF (H6)	TF_{bean}/ TF_{plant}	Default STAR
B1	4.7 ±0.9	7.1 ±1.4	50.8	7.25	0.14	10
B2	3.8 ±0.9	5.6 ±1.3	230.3	29.45	0.13	10
B3	2.6 ±1.3	3.8 ±1.9	229.9	29.73	0.13	10
B4	4.6 ±1.8	7.0 ±2.7	541.9	170.8	0.32	10
B5	3.1 ±2.1	4.7 ±3.2	708	535.7	0.76	10
B6	3.4 ±1.7	5.0 ±2.6	79.1	52	0.66	10

* Atmospheric ^{14}C to the edible crop

Table 34: Comparison between potato experiments: P1 to P6

Potato Experiment	Leaf Assimilation Rate g C Kg $wwt^{-1}d^{-1}$ (0.16g C m^{-3})	Leaf Assimilation Rate g C Kg $wwt^{-1}d^{-1}$ (0.24g C m^{-3})	Plant TF (H6)	Tubers TF (H6)	TF_{tubs}/ TF_{plant}	CoV Tuber Inventory %	Default STAR Assimilation Rate
P1	1.9 ± 1.1	2.9 ± 1.6	414.2	113.4	0.27	109	10
P2	2.2 ± 1.0	3.1 ± 1.5	170.6	50.5	0.30	57	10
P3	1.1 ± 1.5	2.7 ± 2.2	1021.5	941.7	0.92	25	10
P4	2.2 ± 1.5	3.3 ± 2.2	1785.8	1138.3	0.64	72	10
P5	2.8 ± 1.5	4.2 ± 2.2	1575.5	1495.9	0.95	43	10
P6	1.0 ± 0.5	1.5 ± 0.7	574.3	514	0.90	129	10

Table 35: Comparison between potato experiments: P1 to P6

Potato Experiment	Leaf Assimilation Rate g C Kg $wwt^{-1}d^{-1}$ (0.16g C m^{-3})	Leaf Assimilation Rate g C Kg $wwt^{-1}d^{-1}$ (0.24g C m^{-3})	Plant TF (H6)	Tubers TF (H6)	TF_{tubs}/ TF_{plant}	CoV Tuber Inventory %	Default STAR Assimilation Rate
P1	1.9 ± 1.1	2.9 ± 1.6	414.2	113.4	0.27	109	10
P2	2.2 ± 1.0	3.1 ± 1.5	170.6	50.5	0.30	57	10
P3	1.1 ± 1.5	2.7 ± 2.2	1021.5	941.7	0.92	25	10
P4	2.2 ± 1.5	3.3 ± 2.2	1785.8	1138.3	0.64	72	10
P5	2.8 ± 1.5	4.2 ± 2.2	1575.5	1495.9	0.95	43	10
P6	1.0 ± 0.5	1.5 ± 0.7	574.3	514	0.90	129	10

B.2.2 Crop dry weight and activity concentration data

The dry weights and ^{14}C activity concentrations following exposure to $^{14}CO_2$ were measured in various plant components throughout the experiment. The results reported for beans in leaves, stems, roots, pods and beans are given in Table 36, Table 37, Table 38, Table 39 and Table 40 respectively. The results reported for potatoes in leaves, stems, roots and tubers are given in Table 41, Table 42, Table 43 and Table 44 respectively.

As was seen with the cabbage results, there is a high degree of variability in both the measured dry weights and ^{14}C activities of all plant components for each of bean and potato crops.

With respect to the potato crop, IAEA (2008) hypothesised that the large standard deviations in the measured ^{14}C activities in the leaves and tubers reflect the variability of leaf properties and illumination, as well as the variability in tuber growth rates. The variability observed with the other crops can be explained using similar arguments. For potatoes, the key part of the plant with respect to human exposure is the tuber, since that is the part consumed directly. As noted in IAEA (2008), potato tubers are composed mostly of imported carbon, meaning that it is reasonable to expect that large tubers import more ^{14}C than small ones in contaminated plants. Oparka (1985) described a linear relationship between tuber size and ^{14}C inventory. This may have some importance for radiological dose assessment because potatoes may be graded by tuber size before consumption e.g. large tubers are used for baking potatoes.

B.3 References

IAEA (2008). The Potato Scenario, Final Report. EMRAS Tritium/C14 Working Group, September 2008.

Tucker S M (1998). ^{14}C dynamics in crops following short-term exposure to atmospheric $^{14}CO_2$. PhD thesis, Imperial College London, UK.

Tucker S and Shaw G (1997). Quality Assured Modelling Data for $^{14}CO_2$ Fixation by Crops. IC.CARE/MAFF/REP/C-14/4.0, Imperial College report to the Ministry of Agriculture, Fisheries and Foods, London, UK.

Table 36: Dry weight and ^{14}C activity concentration results for beans - leaves

		Crop replicate					
	Harvest	**B1**	**B2**	**B3**	**B4**	**B5**	**B6**
Dry weight (g)	**H1**	0.3 ± 0.1	1.4 ± 0.6	2.9 ± 1.1	6.1 ± 0.7	5.1 ± 2.5	2 ± 1.7
	H2	0.5 ± 0.1	2.7 ± 0.5	4.2 ± 2.2	5.6 ± 1.3	5.2 ± 1.8	2.5 ± 1.5
	H3	0.7 ± 0.4	3.6 ± 1	6.6 ± 4.1	5.7 ± 1.4	4.3 ± 2.4	2.5 ± 2
	H4	2.8 ± 1.1	5.7 ± 1.3	8 ± 2.2	5.5 ± 2.1	0.9 ± 1	1.1 ± 0.8
	H5	7.4 ± 2.4	6.5 ± 2.5	8.1 ± 4.2	1.8 ± 1.4	1.6 ± 0.7	4.3 ± 5.8
	H6	2 ± 2.6	10.1 ± 17.3	2.9 ± 2.2	1.3 ± 1.5	0.9 ± 0.8	1.1 ± 0.8
^{14}C concentration (Bq g^{-1})	**H1**	4499.7 ± 634.6	2895.2 ± 480.9	1664.3 ± 753.5	1746.3 ± 735.2	524.5 ± 380.2	387.6 ± 229.5
	H2	2900 ± 206.8	2314.1 ± 689.7	777.1 ± 196.3	1027.3 ± 1042.4	301.3 ± 111.9	404.3 ± 139.2
	H3	1371.3 ± 230.2	945.2 ± 278.1	611 ± 147.9	601.9 ± 349.3	268.8 ± 128	115.1 ± 85.2
	H4	276.8 ± 97.1	564.9 ± 224.5	386.7 ± 135.3	478.1 ± 264.8	331.3 ± 178.9	274.3 ± 153.7
	H5	97.6 ± 33.4	142 ± 60.8	434.4 ± 231.7	943 ± 775.6	100.7 ± 73.7	398.9 ± 371.4
	H6	33.9 ± 26.9	111.1 ± 88.1	115 ± 42.7	1664.8 ± 1723.2	86 ± 49.2	335.7 ± 168.7

Table 37: Dry weight and ^{14}C activity concentration results for beans - stems

		Crop replicate					
	Harvest	**B1**	**B2**	**B3**	**B4**	**B5**	**B6**
Dry weight (g)	**H1**	0.1 ± 0.04	1.3 ± 0.6	5.3 ± 2.5	16 ± 3.5	14.4 ± 4.8	13.2 ± 3.5
	H2	0.1 ± 0.03	1.4 ± 0.5	6.9 ± 3.6	11.4 ± 2.6	12.9 ± 3.5	14.2 ± 4.5
	H3	0.3 ± 0.1	4.2 ± 1.5	13.1 ± 7	14.5 ± 4.2	11 ± 3.5	9.1 ± 4.2
	H4	1.8 ± 0.5	10.3 ± 2.6	16.5 ± 5.3	15.7 ± 6.3	12 ± 4	9.5 ± 2.5
	H5	10.9 ± 3.6	16.2 ± 5.7	21 ± 3.9	9.4 ± 6.8	11.7 ± 3.4	11.4 ± 5.1
	H6	15.4 ± 3.1	13.6 ± 3.8	14.7 ± 7.8	10.9 ± 1.6	12.9 ± 1.4	8 ± 3.3
^{14}C concentration (Bq g^{-1})	**H1**	3576.9 ± 732.8	2739.3 ± 775.4	738.4 ± 323.8	545.9 ± 235.3	93.1 ± 96.4	42.3 ± 22.5
	H2	2942 ± 386.7	2418.1 ± 958.6	823 ± 193.5	294.3 ± 79.6	49.9 ± 24.7	23.9 ± 14.9
	H3	1321.7 ± 322	809.5 ± 191.3	517.5 ± 230.7	397.2 ± 334.6	67.6 ± 75.8	13.3 ± 9.8
	H4	194.9 ± 79.4	389.3 ± 90.1	306.1 ± 60	195.3 ± 113.6	36.7 ± 23.7	10.7 ± 3.4
	H5	43.5 ± 15	193.8 ± 44.8	249 ± 98.5	263.9 ± 153.6	47.9 ± 70	10.5 ± 9.3
	H6	26.5 ± 9.5	250.3 ± 53.6	204 ± 62.7	341.3 ± 103.3	47.9 ± 29.8	27.1 ± 54.2

Table 38: Dry weight and ^{14}C activity concentration results for beans - roots

		Crop replicate					
	Harvest	**B1**	**B2**	**B3**	**B4**	**B5**	**B6**
Dry weight (g)	**H1**	0.2 ± 0.1	0.6 ± 0.5	1.5 ± 0.5	3.1 ± 0.8	3.7 ± 1.8	4.1 ± 3.2
	H2	0.3 ± 0.1	0.8 ± 0.3	1.9 ± 0.6	2.4 ± 0.7	2.9 ± 1.2	3.1 ± 1.5
	H3	0.3 ± 0.1	4 ± 0.6	2.1 ± 1	2.3 ± 1.1	3.5 ± 1.4	2.5 ± 1.4
	H4	0.8 ± 0.3	2.6 ± 0.6	3.6 ± 1.8	3 ± 0.7	2.8 ± 0.6	1.9 ± 0.6
	H5	3 ± 0.8	3.2 ± 1.2	6.8 ± 5.6	2.1 ± 1	2.9 ± 1.1	1.9 ± 1.5
	H6	3.5 ± 0.6	2.4 ± 1.2	2.6 ± 1.4	2 ± 0.8	1.7 ± 1.1	1.7 ± 1.2
^{14}C concentration (Bq g^{-1})	**H1**	546 ± 204.3	972 ± 112.5	334.4 ± 258	370 ± 134.7	44.4 ± 43.8	10 ± 9.5
	H2	349.4 ± 124.5	815.1 ± 431.1	322.9 ± 138.2	177.5 ± 59.4	34.4 ± 30.7	8.4 ± 8.2
	H3	512.2 ± 280.3	328.3 ± 191.1	319.9 ± 186.8	253.5 ± 296.8	643 ± 78.1	4 ± 3.7
	H4	197.8 ± 111.1	181 ± 67.4	189.8 ± 75.5	136.8 ± 83.6	10.8 ± 12	4 ± 2.3
	H5	101.2 ± 42.1	153.7 ± 58.3	98.2 ± 50.3	119.1 ± 161.8	26.8 ± 49	4.5 ± 2.7
	H6	92.2 ± 22.2	203.7 ± 40.2	126.4 ± 32.1	135 ± 64.4	8.2 ± 8.8	10.4 ± 21.2

Table 39: Dry weight and ^{14}C activity concentration results for beans - pods

		Crop replicate					
	Harvest	**B1**	**B2**	**B3**	**B4**	**B5**	**B6**
Dry weight (g)	**H1**	0	0	0	0.2 ± 0.2	7.3 ± 3.1	6 ± 2.4
	H2	0	0	0	0.5 ± 0.2	2.6 ± 1.5	6 ± 1
	H3	0	0	0	3.4 ± 3.4	8.4 ± 0.5	3.6 ± 2.4
	H4	0	0	1.4 ± 1.2	5.4 ± 2.6	4.4 ± 2.4	3.7 ± 1.1
	H5	0	7.9 ± 2.8	11.7 ± 3.6	6.1 ± 3.7	3.4 ± 1.1	4.9 ± 4.5
	H6	7.6 ± 1.2	4.3 ± 2.2	6 ± 4.5	3.2 ± 1.3	3.9 ± 1.4	1.7 ± 0.9
^{14}C concentration (Bq g^{-1})	**H1**	0	0	0	3015.9 ± 995.6	728.7 ± 784.7	146.6 ± 119.9
	H2	0	0	0	704.1 ± 686.4	1116 ± 676	115.6 ± 76.9
	H3	0	0	0	1101.7 ± 1101.7	941.6 ± 487.2	31.6 ± 20.3
	H4	0	0	145.6 ± 52.1	252.7 ± 116.9	691.3 ± 290.6	61.2 ± 29.7
	H5	0	0	145.6 ± 52.1	252.7 ± 116.9	691.3 ± 290.6	61.2 ± 29.7
	H6	10 ± 6.9	53.3 ± 23.4	43.7 ± 33.1	521.8 ± 216.5	564.2 ± 440.1	54.1 ± 43.4

Table 40: Dry weight and ^{14}C activity concentration results for beans - beans

		Crop replicate					
	Harvest	**B1**	**B2**	**B3**	**B4**	**B5**	**B6**
Dry weight (g)	**H1**	0	0	0	0.2 ± 0.2	3.6 ± 2.3	9.6 ± 4.8
	H2	0	0	0	0.5 ± 0.2	6.8 ± 3	14.5 ± 4.4
	H3	0	0	0	2.8 ± 2.8	8.3 ± 3.2	11.8 ± 9.5
	H4	0	0	1.4 ± 1.2	3.3 ± 1.8	13.6 ± 5.7	11.4 ± 5.4
	H5	0	6.5 ± 3.5	9.3 ± 4	9.3 ± 3.1	13.2 ± 5	14.4 ± 15.4
	H6	21.1 ± 9.1	17.7 ± 13.1	19.4 ± 18.7	14.6 ± 3.8	12.9 ± 3.8	3.1 ± 3.3
^{14}C concentration (Bq g^{-1})	**H1**	0	0	0	30159.9 ± 995.6	1413.9 ± 1089	119.4 ± 91.7
	H2	0	0	0	704.1 ± 686.4	2316.8 ± 622.8	388.8 ± 277.4
	H3	0	0	0	918.8 ± 918.8	1125.4 ± 786.1	123.3 ± 54.6
	H4	0	0	145.6 ± 52.1	173.6 ± 61.7	875.1 ± 329	276 ± 139.7
	H5	0	54.3 ± 13	40.3 ± 24	127.4 ± 100.9	1025.4 ± 775.8	288.1 ± 372
	H6	6.9 ± 2.3	48.5 ± 17.1	35.7 ± 16.5	225.6 ± 79.3	689.4 ± 400.2	330.1 ± 465

Table 41: Dry weight and ^{14}C activity concentration results for potatoes - leaves

		Crop replicate					
	Harvest	**P1**	**P2**	**P3**	**P4**	**P5**	**P6**
Dry weight (g)	**H1**	3.2 ± 2.3	11.2 ± 5.1	7.8 ± 2.9	15.5 ± 7	6 ± 2.4	6.2 ± 6.8
	H2	10 ± 8.4	5.4 ± 2	12.8 ± 4.9	12.1 ± 8.4	4.2 ± 2.2	5.4 ± 4.9
	H3	7 ± 1.2	6.5 ± 4.6	6.7 ± 5.2	4.4 ± 2.4	2.6 ± 2.7	6.9 ± 5
	H4	15.5 ± 9.4	15.6 ± 1.6	6.3 ± 5.4	3.1 ± 2.2	4.3 ± 2.4	10.9 ± 5.5
	H5	9.4 ± 8.8	15.4 ± 15.7	5.8 ± 5.7	7.7 ± 8.1	5.1 ± 1.7	7.5 ± 8.3
	H6	6.8 ± 8.3	5 ± 4.8	2.7 ± 1.8	0.6 *	2.2 ± 1.9	3.2 ± 0.4
^{14}C concentration (Bq g^{-1})	**H1**	1126.3 ± 373.9	482.9 ± 218.9	291.4 ± 213.6	362 ± 207.1	456.6 ± 296.5	68.9 ± 37.6
	H2	312.7 ± 115.7	393.7 ± 187.2	307.3 ± 147.5	42.6 ± 13.7	119.3 ± 87.1	65.7 ± 22.3
	H3	215.5 ± 55.4	482.4 ± 138.6	196.8 ± 115.3	95.4 ± 78.9	89.7 ± 118.6	27.4 ± 9.7
	H4	224.7 ± 148.8	279.8 ± 240	322.2 ± 88.3	191.3 ± 26.7	79.3 ± 33.5	77.7 ± 51.2
	H5	106 ± 50.7	187.2 ± 119.1	177 ± 157.5	132.3 ± 43.8	46.9 ± 29.9	26.4 ± 28.5
	H6	101.4 ± 38.5	47.1 ± 27.4	107.6 ± 121.4	28.6 *	55.3 ± 17	76.1 ± 59.7

* No standard deviation reported.

Table 42: Dry weight and ^{14}C activity concentration results for potatoes - stems

		Crop replicate					
	Harvest	**P1**	**P2**	**P3**	**P4**	**P5**	**P6**
Dry weight (g)	**H1**	1.7 ± 1	11.9 ± 4.7	12.1 ± 5	22.6 ± 9.4	8.8 ± 4.7	14 ± 11.9
	H2	7.5 ± 7.1	8 ± 4.5	12 ± 5.1	9.1 ± 5.3	8.2 ± 2.6	9 ± 4
	H3	9.6 ± 2.2	10.9 ± 5.6	9.4 ± 6.1	7.9 ± 4.1	6.5 ± 1.3	17 ± 7.6
	H4	15.5 ± 8.6	18.4 ± 3	12 ± 9.8	9.5 ± 5.9	8.2 ± 2.1	17.3 ± 4
	H5	11.3 ± 6	14.7 ± 8.8	12.2 ± 2.9	16.3 ± 19	15.6 ± 11.3	17.1 ± 10.9
	H6	14.7 ± 6.1	7.1 ± 2.4	8.7 ± 0.5	47.4 ± 1.9	14.7 ± 2.6	7.2 ± 0.4
^{14}C concentration (Bq g^{-1})	**H1**	891.3 ± 296	285 ± 133.69	100.8 ± 88.4	63.9 ± 54.6	57 ± 29.9	12.3 ± 10.1
	H2	266.9 ± 50.7	207.8 ± 75.4	164.2 ± 90.1	31 ± 10.3	62.8 ± 52.2	7.3 ± 2.9
	H3	113.3 ± 33.4	273.3 ± 147.6	128.5 ± 95.7	75.6 ± 46.5	17.5 ± 16.3	8.4 ± 0.8
	H4	162.3 ± 81.3	222.9 ± 153	213.6 ± 112.9	157 ± 105.9	64.3 ± 38.1	7.7 ± 6.9
	H5	141 ± 49.7	261.6 ± 19.2	71.2 ± 54.2	122 ± 80.3	41.1 ± 46.7	3.9 ± 3
	H6	142.8 ± 36.8	84.7 ± 72.8	40.5 ± 37.1	109.5 ± 361	35.2 ± 20.7	6.6 ± 5.5

Table 43: Dry weight and ^{14}C activity concentration results for potatoes - roots

		Crop replicate					
	Harvest	**P1**	**P2**	**P3**	**P4**	**P5**	**P6**
Dry weight (g)	**H1**	7.7 ± 4.4	2.9 ± 1.5	3.4 ± 1.8	2.7 ± 1.6	1.5 ± 0.9	1 ± 0.4
	H2	1.3 ± 1.1	1.1 ± 0.6	2.8 ± 1	2.7 ± 0.6	0.7 ± 0.3	1.3 ± 0.6
	H3	1.8 ± 1.3	1.9 ± 1.1	1.4 ± 0.4	1 ± 0.8	1.1 ± 0.7	0.7 ± 0.4
	H4	2.7 ± 1.4	3.4 ± 1.7	1.6 ± 0.9	0.8 ± 0.6	1.6 ± 0.6	2.2 ± 0.3
	H5	1.4 ± 1.4	1.3 ± 1.2	2.1 ± 1.5	1.5 ± 0.4	1.3 ± 1	1.2 ± 1.5
	H6	1.3 ± 1	0.9 ± 0.4	0.7 ± 0.1	0.5 ± 0.7	1.6 ± 0.8	0.2 ± 0.05
^{14}C concentration (Bq g^{-1})	**H1**	45.7 ± 36.4	169.9 ± 112.8	54.8 ± 35.8	115.3 ± 106.7	34.4 ± 17.1	1.9 ± 1.4
	H2	67.5 ± 30.9	97.8 ± 54.9	70.8 ± 48.5	20.7 ± 15.8	34.8 ± 13.7	7.9 ± 12.1
	H3	39.3 ± 20.8	200 ± 244	29.9 ± 24.9	22.8 ± 20.3	54.2 ± 53.3	4.2 ± 2.7
	H4	60.4 ± 19.2	249 ± 188.7	85.5 ± 49.5	77.9 ± 77.6	54.3 ± 30.8	1.9 ± 1.2
	H5	119 ± 90.6	179.3 ± 127.8	22.1 ± 15.1	44.4 ± 21	18.3 ± 17.3	6.4 ± 9.1
	H6	119.3 ± 134.9	41.2 ± 27.2	11.4 ± 6.9	72.6 ± 69.8	34.6 ± 14.5	9.3 ± 0.4

Table 44: Dry weight and ^{14}C activity concentration results for potatoes - tubers

		Crop replicate					
	Harvest	**P1**	**P2**	**P3**	**P4**	**P5**	**P6**
Dry weight (g)	**H1**	0	0	9.8 ± 7.2	27.6 ± 27.8	38.1 ± 17.8	36.7 ± 14.2
	H2	0	0	13.3 ± 11.2	42.3 ± 20.1	24.3 ± 18.9	70.3 ± 25
	H3	0.3 ± 0.03	3.8 ± 0.7	13.4 ± 4	24.5 ± 12.1	49.3 ± 54.6	48.2 ± 9.4
	H4	11 ± 8.3	12.5 ± 3	16.3 ± 12.7	32.3 ± 18.7	75.8 ± 25.8	121.7 ± 52.7
	H5	40.7 ± 32.6	45.3 ± 47.5	50.3 ± 41.9	35.7 ± 10.7	49.1 ± 30.3	77.6 ± 68.4
	H6	78.3 ± 87.2	30.2 ± 8.7	46.5 ± 1.9	50 ± 2.2	76.9 ± 6	40.4 ± 35.1
^{14}C concentration (Bq g^{-1})	**H1**	0	0	605.7 ± 558.7	365 ± 301.2	119.9 ± 83.1	4.3 ± 3.9
	H2	0	0	982.2 ± 315.7	90.4 ± 67.9	91.6 ± 97.4	14.8 ± 14.2
	H3	22.5 ± 2.9	12 ± 6.6	711.4 ± 503.2	251.1 ± 249.6	5 ± 0.1	22.7 ± 27.1
	H4	18.9 ± 9	46.9 ± 27.3	549.1 ± 73.9	245.3 ± 204.2	104.4 ± 91.8	28.5 ± 38.9
	H5	18 ± 10.8	34.4 ± 36.1	389.3 ± 276.4	352.9 ± 48.3	34.8 ± 19.8	8.7 ± 6.9
	H6	15.2 ± 6.5	13 ± 9.1	224.6 ± 141.3	181.5 ± 124.5	158.7 ± 56.9	43 ± 41.2

Determination of the source terms for SSPAM ^{14}C for the cabbage crop

Fitted exponentials obtained using Grapher 8, www.goldensoftware.com.

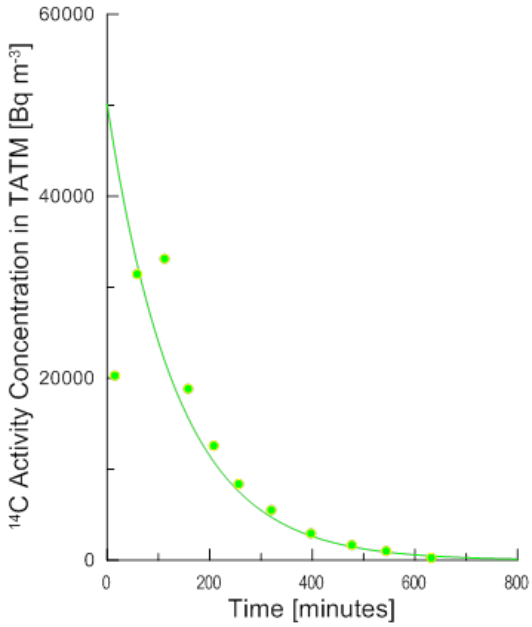

Cabbage 1

Fit 1: Exponential

Equation ln(Y) = -0.007372544384 * X + 10.82235734

Alternate Y = exp(-**0.007372544384** * X) * **50129.11935**

Number of data points used = 11

Average X = 288.955

Average ln(Y) = 8.69203

Residual sum of squares = 1.22127

Regression sum of squares = 22.5606

Coefficient of determination, R-squared = 0.948647

Residual mean square, sigma-hat-sq'd = 0.135697

Note that this is not a true initial inventory case as there is a build-up in the first 100 minutes!

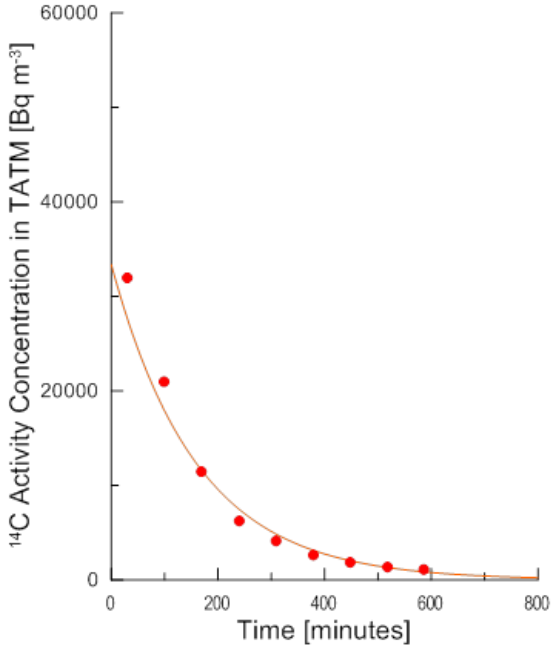

Cabbage 2

Fit 2: Exponential

Equation ln(Y) = -0.006236605797 * X + 10.41527736

Alternate Y = exp(-**0.006236605797 * X) * 33365.48815**

Number of data points used = 9

Average X = 308.667

Average ln(Y) = 8.49025

Residual sum of squares = 0.20837

Regression sum of squares = 11.3159

Coefficient of determination, R-squared = 0.981919

Residual mean square, sigma-hat-sq'd = 0.0297672

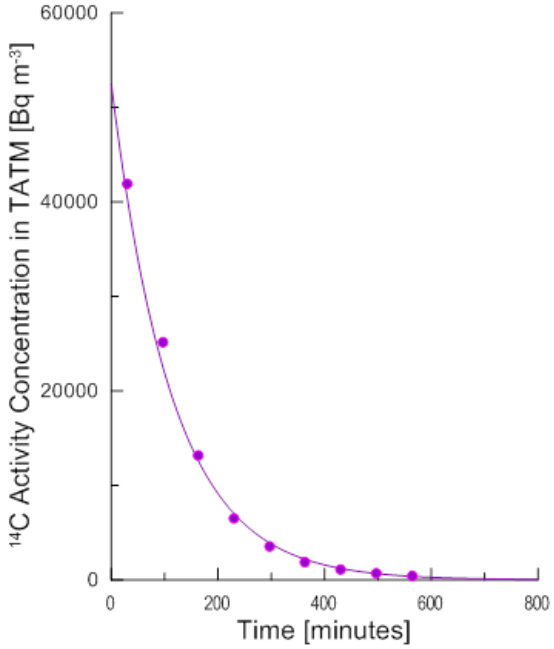

Cabbage 3 – base option

Fit 3: Exponential

Equation ln(Y) = -0.008743795633 * X + 10.86851237

Alternate Y = exp(-**0.008743795633** * X) * **52497.05607**

Number of data points used = 9

Average X = 296.833

Average ln(Y) = 8.27306

Residual sum of squares = 0.0915985

Regression sum of squares = 20.4388

Coefficient of determination, R-squared = 0.995538

Residual mean square, sigma-hat-sq'd = 0.0130855

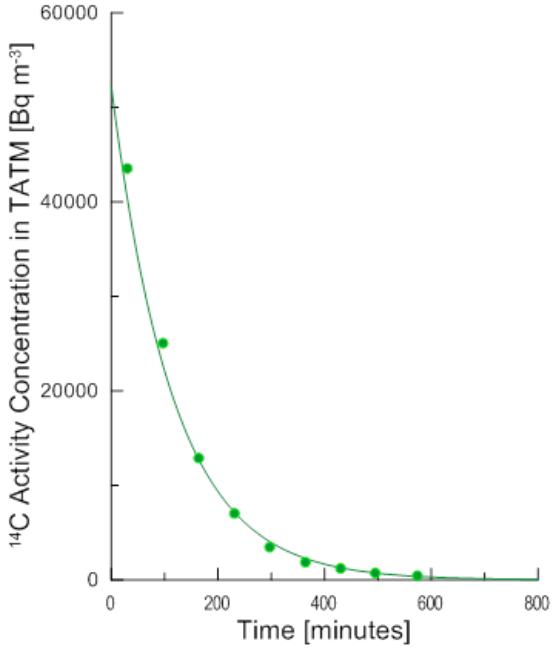

Cabbage 4

Fit 4: Exponential

Equation ln(Y) = -0.008601002339 * X + 10.86377074

Alternate Y = exp(-**0.008601002339** * X) * **52248.72346**

Number of data points used = 9

Average X = 298

Average ln(Y) = 8.30067

Residual sum of squares = 0.120707

Regression sum of squares = 20.0801

Coefficient of determination, R-squared = 0.994025

Residual mean square, sigma-hat-sq'd = 0.0172438

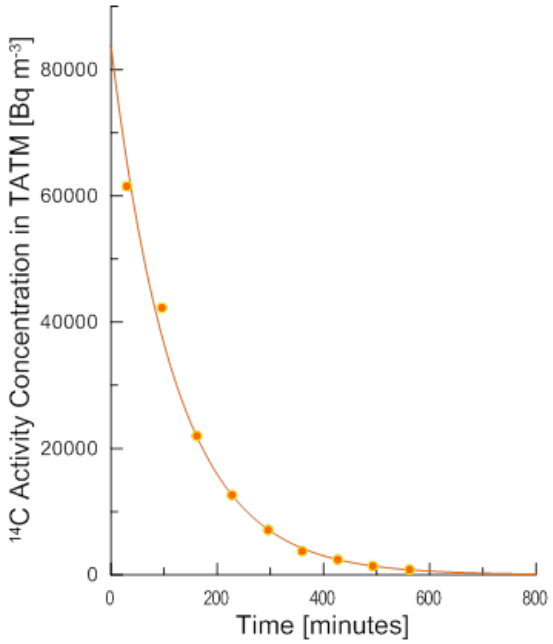

Cabbage 5

Fit 5: Exponential

Equation ln(Y) = -0.008314764739 * X + 11.33824549

Alternate Y = exp(-**0.008314764739** * X) * **83972.57137**

Number of data points used = 9

Average X = 294.889

Average ln(Y) = 8.88631

Residual sum of squares = 0.0322981

Regression sum of squares = 18.2619

Coefficient of determination, R-squared = 0.998235

Residual mean square, sigma-hat-sq'd = 0.00461402

Using the integrated air concentrations (from 0 to 600 minutes) quoted by Shaw and Tucker (1997) the initial inventory in the TATM compartment is derived by

$$N_0 = \frac{\lambda_{purge}.IAC.V}{1-e^{-\lambda_{purge}t_2}} \text{ Bq} \qquad \text{(Equation 57)}$$

Here the volume of the wind tunnel is 55 m^3 and λ_{purge} is the decay constant taken from the above plots. With the IAC taken from Shaw and Tucker (1997) the following parameters are used:

Parameter	Units	Experimental replicate				
		C1	C2	C3	C4	C5
IAC	Bq min	7.40E+6	6.00E+6	6.40E+6	6.41E+6	1.06E+7
t_2	min	6.00E+2	6.00E+2	6.00E+2	6.00E+2	6.00E+2
λ_{purge}	min^{-1}	7.37E-3	6.24E-3	8.74E-3	8.60E-3	8.32E-3
$N_0 = \frac{\lambda_{purge} \cdot IAC \cdot V}{1 - e^{-600\lambda_{purge}}}$	Bq	3.04E+6	2.11E+6	3.09E+6	3.05E+6	4.88E+6
λ_{purge}	y^{-1}	3.88E+3	3.28E+3	4.60E+3	4.52E+3	4.37E+3

2013:20

The Swedish Radiation Safety Authority has a comprehensive responsibility to ensure that society is safe from the effects of radiation. The Authority works to achieve radiation safety in a number of areas: nuclear power, medical care as well as commercial products and services. The Authority also works to achieve protection from natural radiation and to increase the level of radiation safety internationally.

The Swedish Radiation Safety Authority works proactively and preventively to protect people and the environment from the harmful effects of radiation, now and in the future. The Authority issues regulations and supervises compliance, while also supporting research, providing training and information, and issuing advice. Often, activities involving radiation require licences issued by the Authority. The Swedish Radiation Safety Authority maintains emergency preparedness around the clock with the aim of limiting the aftermath of radiation accidents and the unintentional spreading of radioactive substances. The Authority participates in international co-operation in order to promote radiation safety and finances projects aiming to raise the level of radiation safety in certain Eastern European countries.

The Authority reports to the Ministry of the Environment and has around 270 employees with competencies in the fields of engineering, natural and behavioural sciences, law, economics and communications. We have received quality, environmental and working environment certification.

Strålsäkerhetsmyndigheten
Swedish Radiation Safety Authority

SE-171 16 Stockholm
Solna strandväg 96

Tel: +46 8 799 40 00
Fax: +46 8 799 40 10

E-mail: registrator@ssm.se
Web: stralsakerhetsmyndigheten.se